The Thesis Committee for Kenechukwu Moneke
Certifies that this is the approved version of the following Thesis:

Gel Reaction and Permeability Modification for CO_2 Leakage Remediation and Flood Conformance

APPROVED BY
SUPERVISING COMMITTEE:

Matthew T. Balhoff, Supervisor

David DiCarlo, Co-Supervisor

Gel Reaction and Permeability Modification for CO_2 Leakage Remediation and Flood Conformance

by

Kenechukwu Moneke

Thesis

Presented to the Faculty of the Graduate School of

The University of Texas at Austin

in Partial Fulfillment

of the Requirements

for the Degree of

Master of Science in Engineering

The University of Texas at Austin

August 2020

Dedication

To my amazing parents for all the love, prayers and financial support which helped me in completing this project; to my siblings and to my friends, who always remind me to never give up.

Acknowledgements

I would like to acknowledge my thesis advisor, Dr Matthew T.Balhoff, for his continued support, guidance, and words of encouragement in accomplishing this work and my graduate degree

I would like to thank Dr David DiCarlo for providing his insight and time as the second reader of this thesis report and also acting as my co-supervisor.

I will always be grateful to my colleagues and researchers; Julia Jin, Peixi Zhu, Lucas Mejia and Ahmad Alfakher. They had the patience and the generosity to introduce me to everything in the labs from the first day I started and also provided valuable feedback on experimental procedures, material handling, and experimental data analysis.

I would like to acknowledge the funding and support from the CCP (CO2 Capture Project), a group of major energy companies (BP, Chevron, and Petrobras) working together to advance the technologies that will underpin the deployment of industrial-scale CO2 capture and storage (CCS) in the oil & gas industry.

I would also like to thank the staff at the Hildebrand Department of Petroleum and Geosystems Engineering, especially Glen Baum, Gary Miscoe, Daryl Nygaard, Barbara Messmore, and Amy Stewart.

Finally, I would like to acknowledge my parents: thank you for always standing by and supporting me, regardless of my career goals.

Abstract

Gel Reaction and Permeability Modification for CO_2 Leakage Remediation and Flood Conformance

Kenechukwu Moneke, MSE

The University of Texas at Austin, 2020

Supervisor: Matthew T. Balhoff, David DiCarlo

Carbon Capture and Storage (CCS) program, also known as CO2 sequestration, has been proposed as a long-term process to mitigate emissions of greenhouse gases such as CO2 in the atmosphere. One of the biggest challenges associated with the CO2 sequestration process is the migration and leakage of the CO2 due to the formation of leakage pathways which weakens the integrity of the reservoir caprock. To ensure the CO2 storage effectiveness and minimize the environmental and economic risk, it is important to monitor the subsurface CO2 migration and apply a treatment method if leakage is detected.

One of the potential treatment methods to mitigate the leakage challenge in the CCS program is the use of chemical sealants such as silicate gel. The concentrated potassium silicate solution (i.e. silicate gel) reacts with the dissolved CO2 species to form a silica gel barrier which prevents the captured CO2 from escaping into the atmosphere and reduces the reservoir permeability.

This thesis aims to evaluate the potential of silica gel as leakage prevention and remediation measure during the CO2 sequestration process. The use of the silica gel as a permeability modifier, conformance control agent and an effective cap rock sealant was also investigated. The mother solution used in these experiments is Betol K28T diluted with deionized water (50 wt.%) which acts as the silicate gel being investigated. Bulk gelation experiments were initially performed to measure the gel time at different silicate content, acid concentrations, salinities, and temperatures. The results were then fit to an existing model for gelation time and then used as a predictive tool for the core flood experiments. Core flood experiments were then performed to investigate the reaction transport of silicate gel in porous media, compare the results obtained from gelation in porous media to the gelation results from the earlier bulk experiments and finally, investigate the capability of the gel in permeability reduction and sealing of the core. These core flood experiments were conducted in two conditions: ambient condition with an acetic acid solution as a CO2 substitute and the High-Pressure High-Temperature (1500 psi, 600C, 30,000ppm) condition with CO2 saturated brine.

From the core flood experiments, it is shown that using potassium silicate reagents (Betol K28T) to form a silica gel barrier is an applicable strategy for mitigating the risk of CO2 leakage Reduction in the core permeability (up to 90%) of the Benthemier sandstone core was observed during barrier formation. However, to further validate the use of the silica gel to form a chemical barrier under CO2 storage conditions, additional modeling and experiments using micromodel chips and field-scale conditions are recommended.

Table of Contents

List of Tables

List of Figures

Chapter 1: INTRODUCTION

1.1. INTRODUCTION

In this chapter, background information on carbon storage and leakage, concerns are presented along with the motivation for the work performed in this thesis. The aims and objectives of the research, the problem statement, the justification for the research as well as its relevance in the current oil and gas industry situation, are described.

1.2. BACKGROUND AND MOTIVATION

Excessive emission of carbon dioxide (CO_2) into the atmosphere increases the "greenhouse effect" resulting in an environmental phenomenon known as "global warming" (IPCC, 2005). This phenomenon causes the earth to become warmer than it would be naturally resulting in environmental (such as climate change) and health (such as respiratory diseases) effects.

Figure 1.1. shows the percentage increase in carbon dioxide emissions in the United States between 1990 and 2018 as observed by the U.S Environmental Protection Agency.

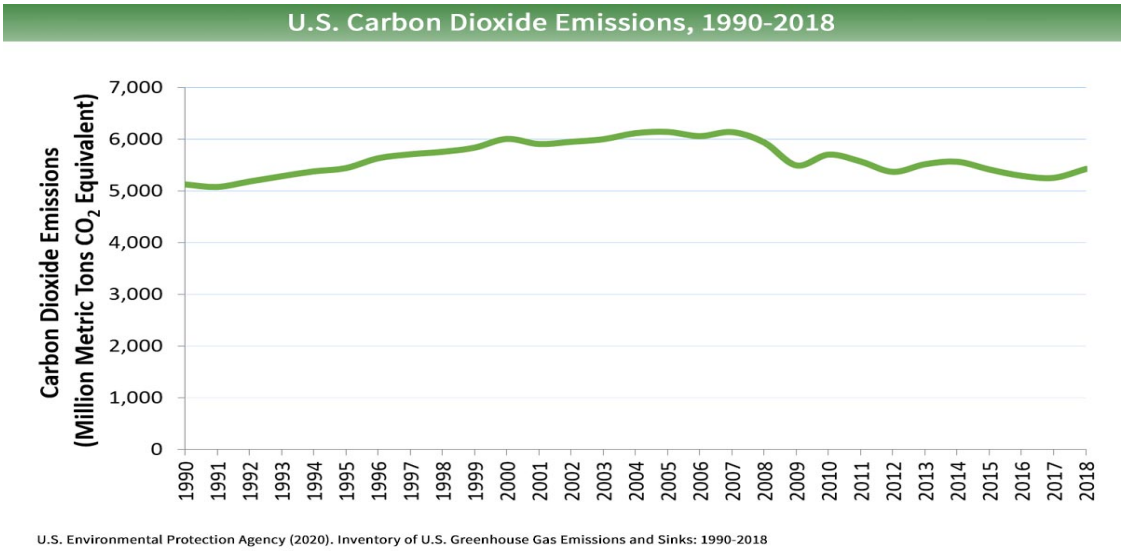

Figure 1.1: U.S. Carbon Dioxide Emissions, 1990-2018 (U.S Environmental Protection Agency, 2020)

To combat the growing challenge of global warming, the Paris Agreement in 2015 committed signatories to 'holding the increase in the global average temperature to well below 2°C above preindustrial levels and pursuing efforts to limit the temperature increase to 1.5°C above pre-industrial levels". (UNFCCC, 2015).

In 2014, Leung et al. provided the following suggestions to mitigate the increase of CO2 emissions into the atmosphere (Leung et al., 2014). They include;

a. Increasing the energy efficiency of industrial processes

b. Switching to less carbon-intensive fuels (e.g., from coal to natural gas)

c. Increasing the capacity of biological sinks (via afforestation, agriculture etc.)

d. Increasing energy production from renewables (solar, wind, hydro, etc.) and nuclear sources

e. The addition of carbon capture and storage (CCS) capability to fossil-fuel based power sources and energy-intensive industries

The first four suggestions by Leung et al. (2014) provide a long-term strategy to reduce the CO2 emissions in the atmosphere whereas the last suggestion (CCS) is a recommended short term strategy for reducing the CO2 emissions (Stangeland and Baird, 2006). The CCS option involves the capture and sequestration or storage of carbon dioxide (CO2) into depleted oil and gas fields or permeable brine-filled (saline) aquifers. Due to their massive potential storage capacity, saline aquifers have been identified as very promising geologic storage sites (IPPC, 2005). The main advantage of storing CO2 at high pressures within aquifers is that the required storage volume is substantially less than if the CO2 were at "standard" (room)-pressure conditions. To safely store the CO2, it must be trapped under an impermeable rock acting as a seal (IPPC, 2005).

Figure 1.2. shows the potential CO2 leakage pathway such as geological planar structures (e.g. faults, joints and/or fracture zones) as well as caprocks which contain variable hydraulic conductivity (e.g. facies changes or sand channels within a shale caprock)

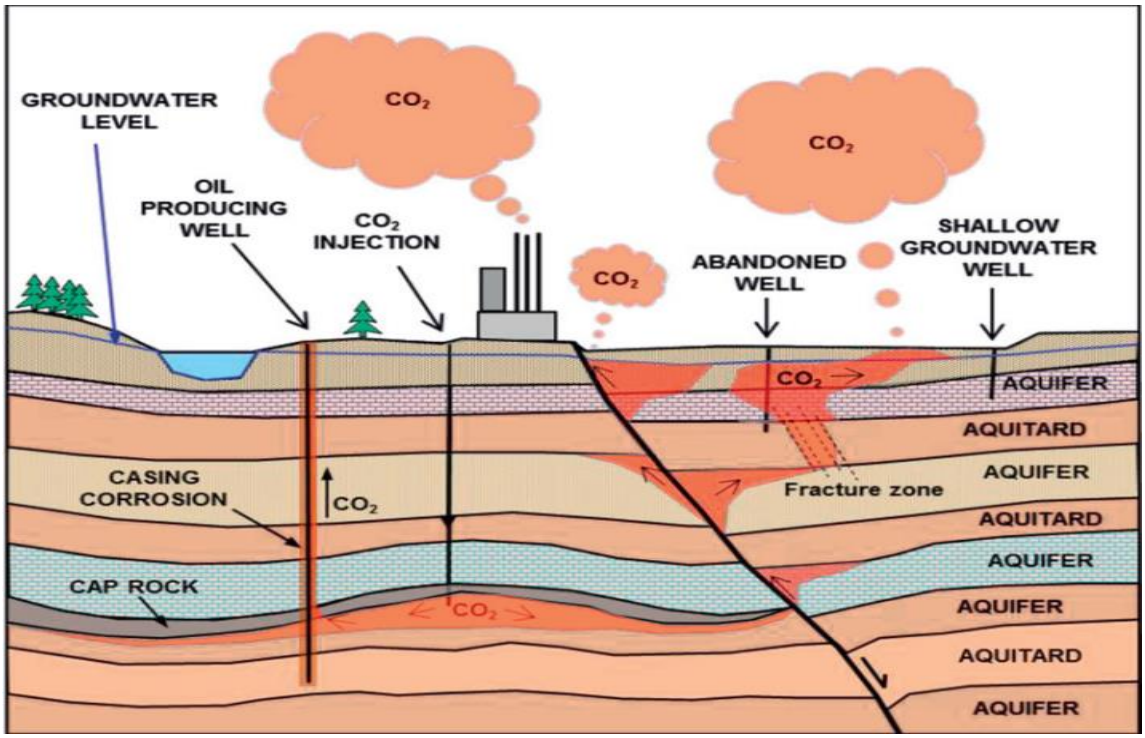

Figure 1.2: Schematic figure showing potential leakage pathways such as faults, joints and/or fracture zones as well as caprocks from a geological CO2 storage site (Modified from IPPC, 2004; Brydie et al., 2014)

CO_2 storage is thus important for limiting CO_2 emissions, but it needs to be stored securely to prevent leakage. Leakage occurs when an injected CO_2 or CO_2-brine mixture is detected outside of the intended geological storage formation (IPCC, 2005).

This project, therefore, evaluates the potential of conformance control agents such as silica gel as leakage prevention and remediation measure to improve carbon dioxide (CO_2) sequestration and storage. These conformance control or sealing agents need also to stay in place over the long term. Therefore, the long term thermo-stability of the sealing agents exposed to CO_2 has to be addressed.

1.3. PROBLEM STATEMENT

Monitoring of geologic CO_2 storage reservoirs is needed to detect possible leakage pathways or other deterioration of storage integrity (Wright et al., 2004). It is thus crucial to have engineering options to mitigate (i.e. reduction of the short-term effects of leakage) and/or remediate (i.e. long term engineered solution to prevent further leakage or impacts) further fluid leakage. A CO_2 storage project will be considered successful if more than 99% of the injected CO_2 is stored in the intended formation for more than 100 years (Brydie et al., 2014).

One potential method to seal a supercritical CO_2 and/or CO_2-rich brine leakage pathway is through the injection of a sealing agent solution (Brydie et al., 2014). The idea is that the sealing agent chemically reacts directly with the supercritical CO_2 and/or dissolved CO_2 species to form a pore-blocking precipitate which acts as a leakage barrier (Fleury, 2017). Also, the long-term thermo-stability of the sealing agents exposed to CO_2 has to be addressed as the sealing agents need also to stay in place over the long term.

1.4. AIM AND OBJECTIVES

The main aim of this thesis is to evaluate the potential of conformance control agents such as silica gel as leakage prevention and remediation measure to improve carbon dioxide (CO_2) capture and sequestration.

The following objectives were achieved by using the silica gel to conduct bulk gelation core flood experiments;

- Predict and quantify the reactive transport of silicate gel in porous media,
- Compare the results obtained from gelation in porous media to the gelation results from the bulk experiments, and

- Investigate the effectiveness of the capability of the gel for permeability reduction and sealing of the core within small- and medium-scale porous media under reservoir conditions.

1.5. THE RELEVANCE OF THE PROJECT TO THE OIL AND GAS INDUSTRY

The use of conformance control agents such as silica gel provides a solution to the leakage challenge encountered in the carbon dioxide (CO_2) capture and sequestration (CCS) process (IPCC, 2005). The CCS process is beneficial to the oil and gas industry as it curbs the CO_2 emissions in the atmosphere thus preventing global warming as well as acting as a source for CO_2 enhanced oil recovery to increase oil production (IPCC, 2005).

1.6. Chapter Descriptions

This thesis entails five chapters which will discuss the application of conformance control agents such as silica gel as leakage prevention and remediation measure to improve carbon dioxide (CO_2) capture and sequestration.

Chapter 1 highlights the background and motivation for the work performed in this thesis. It details the aims and objectives of the research, the problem statement, the justification for the research as well as its relevance in the current oil and gas industry situation. Chapter 2 describes the background information about CO_2 flooding and its control sealants as well as a literature review on CO_2-saturated brine, the use of silica gel for conformance control to mitigate CO_2 leakage and another relevant research with regards to CO_2 leakage control. Chapter 3 describes the materials and methods of the experiments that are performed. The experimental approach including materials, equipment, procedures, measurements, and calculations for conducting the core flooding experiments performed in this work is presented in this chapter. The experimental

approach is presented step by step from core preparation to silicate solution flooding. Chapter 4 discusses the results of the core flood experiments conducted in Chapter 3. The results from the bulk gelation phase and core flood experiment phase are analyzed and discussed.

Finally, Chapter 5 summarizes the conclusions from the experiments in the thesis. It also discusses the limitations of the application of the results observed in this thesis to reservoir scale phenomena as well as providing possible recommendations for future work to aid the methodology employed in this thesis.

Chapter 2: BACKGROUND AND LITERATURE REVIEW

2.1. INTRODUCTION

This chapter describes background information about CO_2 flooding and its control using sealants. On this topic, there is a literature review on the use of silica gel for conformance control to mitigate CO_2 leakage and other relevant research with regards to CO_2 leakage control.

To effectively reduce carbon emissions into the atmosphere, injected CO_2 must remain underground for an exceedingly long time (usually thousands of years) with only insignificant amounts of leakage back to the surface (Benson and Cook, 2005). The feasibility of geological carbon sequestration and storage would be strengthened if the risk of CO_2 leakage could be lessened via mitigation or remediation techniques. One potential method is to use a silica gel to seal CO_2 leakage pathways (Brydie et al., 2014). The concentrated potassium silicate solution (i.e. the sealing agent) reacts with acidic CO_2 saturated brine to form a silica gel barrier and reduces the reservoir permeability. The long-term thermo-stability of the sealing agents exposed to CO_2 has to be addressed as the sealing agents need also to remain in place over the long term.

To evaluate the potential of conformance control agents such as silica gel as leakage prevention and remediation measure to improve carbon dioxide (CO_2) capture and sequestration, background information and literature review on the mechanisms behind (CO_2) capture and sequestration process are discussed.

2.2. CARBON CAPTURE AND STORAGE (CCS)

CO_2 found in the atmosphere comes from both natural sources and anthropogenic sources. The natural sources include; animal and plant respiration, CO_2 deposits found in rock layers within the Earth's crust, emissions from volcanic eruptions, decomposition of organic matter and oceans

(IPCC, 2005). The anthropogenic or man-made sources include; human breathing, subsurface CO_2 leakage, burning of fossil fuel, industrial plants and electricity production from power plants (IPCC, 2005).

Excessive emission of carbon dioxide (CO_2) into the atmosphere increases the "greenhouse effect" resulting in an environmental phenomenon known as "Global warming" (IPCC, 2005). This phenomenon causes the earth to become warmer than it would be naturally resulting in environmental (such as climate change) and health (such as respiratory diseases) effects. In 2014, Leung et al. provided the following suggestions to mitigate the increase of CO_2 emissions into the atmosphere (Leung et al., 2014). They include;

- Increasing the energy efficiency of industrial processes
- Switching to less carbon-intensive fuels (that is, from coal to natural gas)
- Increasing the capacity of biological sinks (via afforestation, agriculture etc.)
- Increasing energy production from renewable (solar, wind, hydro) and nuclear sources
- The addition of carbon capture and storage (CCS) capability to fossil-fuel based power sources and energy-intensive industries

The first four suggestions by Leung et al. (2014) provide a long-term strategy to reduce the CO_2 emissions in the atmosphere whereas the last suggestion which is the CCS option is recommended for short term strategy for reducing the CO_2 emissions (Stangeland and Baird, 2006). The CCS option involves the capture and sequestration or storage of carbon dioxide (CO_2) into depleted oil and gas fields or porous and permeable brine filled (saline) aquifers. The idea behind the geologic carbon capture and storage (CCS) is to return the released carbon dioxide (CO_2) to geologic storage (IPCC, 2005). The main advantage of storing CO_2 in its supercritical condition (high pressure, saline environment) is that the required storage volume is substantially

less than if the CO_2 were at "standard" (room)-pressure conditions. However, to safely store the CO_2, it must be trapped under an impermeable rock acting as a seal (IPCC, 2005).

The CO_2 injected into the sedimentary rocks would be forced under pressure into the pore space which was initially occupied by saline fluids (brine) or hydrocarbon-brine mixtures in the case of Enhanced Oil Recovery (EOR) (DePaolo et al., 2013).

Figure 2.1 shows the typical conditions and rock properties encountered during the carbon sequestration process.

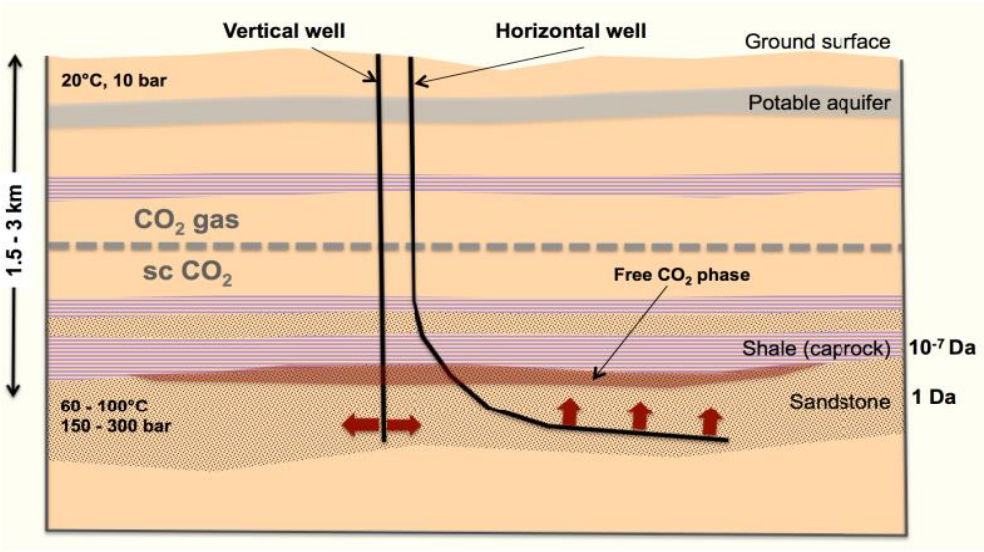

Figure 2.1. Schematic diagram of a carbon sequestration system illustrating the typical conditions and rock properties encountered (DePaolo et al., 2013).

It should be noted that the density of the supercritical CO_2 is roughly 50 to 70% that of typical brines, and its viscosity is about 15 times lower than typical brines (Benson and Cole, 2008). Injected CO_2 has a high tendency of migrating upward within the porous, permeable rock formations into which it is injected, and therefore it can only be kept underground and safely stored if the porous rocks are overlain by impermeable rock layers acting as a seal (DePaolo et al., 2013).

The CCS process must include the capture of carbon dioxide and its associated compounds from producing sources, transportation, and storage of the captured CO_2 (Brydie et al., 2014). The captured CO_2 is used in the injection processes into deep underground geological formations for permanent storage and existing oil fields as an enhanced oil recovery technique for additional recovery of hydrocarbons (Ajayi et al., 2019). The selection of a geological site for storage must be done to meet three main conditions: capacity, injectivity and containment.

2.3. RISKS AND CHALLENGES IN CO2 STORAGE

As with most technologies, carbon dioxide capture and storage (CCS) comes with its risks and challenges which must be properly addressed before implementation. It is important to perform a risk assessment analysis before embarking on any project. Some of the risks and challenges involved in CO_2 storage include CO_2 leakage and induced seismicity (Ajayi et al., 2019).

2.3.1. CO_2 leakage and leakage pathways

The biggest challenge associated with the CO_2 sequestration process is the possibility of leakage of the CO_2 due to the formation of leakage pathways during the long-term storage of the captured CO_2 (RISCS, 2014). In this context, leakage refers to a scenario where an injected CO_2 or CO_2-brine mixture is detected outside of the intended geological storage complex (RISCS, 2014). Thus, it is important to understand the reasons for the CO_2 leakage, its pathways, and its sealing methods.

For a leak to occur, a leak source, a leakage pathway, and a pressure differential between the reservoir and potential pathway must all be present (Blue,2016; Watson et al., 2009). However, factors such as a leak source and a pressure differential between the reservoir and a potential

pathway are already present and cannot be controlled or remediated. Therefore, the leakage pathway is the only factor that can be controlled or remediated during the CO_2 storage process (Blue, 2016).

Based on the research of Espie (2005), the main CO_2 leakage mechanisms include (Peng, 2017):

- Wellbore failure
- Bypassing of the trap (spillage, aquifer migration)
- Seal structure failure (capillary failure, faults, and fractures)

Figures 2.2 and 2.3 show the storage complex of CO_2 and its potential leakage pathways, respectively. RISCS is concerned primarily with the impacts of the leakage illustrated by the green arrows outlined in red and not with processes within the storage complex, outlined by the red dashed line, or with leakage which does not impact on groundwater resources or near-surface environments (RISCS, 2014)

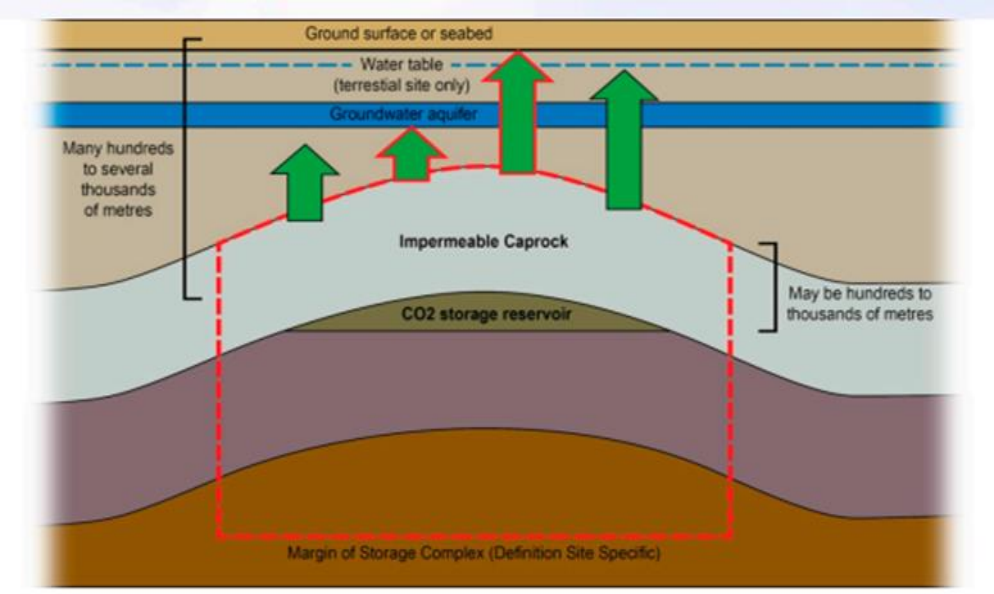

Figure 2.2: Schematic illustration of a CO_2 storage complex (RISCS, 2014)

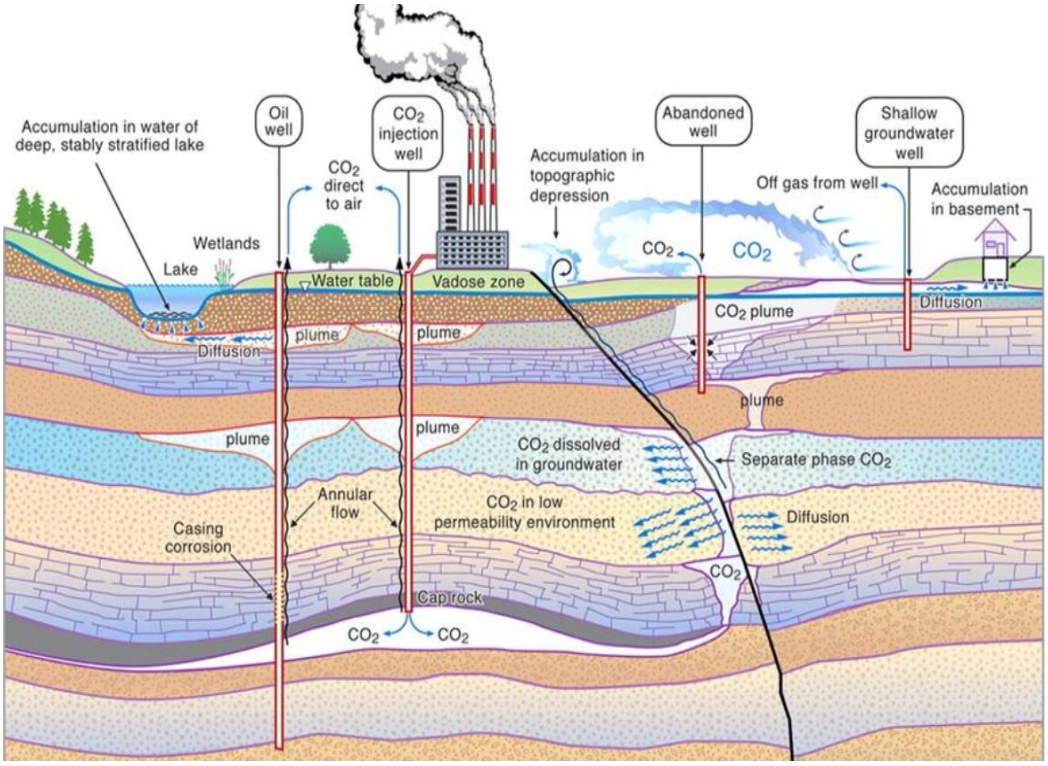

Figure 2.3: CO_2 Potential leakage pathways (Saptharishi and Makwana, 2011)

The two different types of leakage pathways are; i) geological leakage pathways and ii) engineering (human-created) leakage pathways.

i. Geological leakage pathways: this indicates that CO_2 is leaking through natural pathways and have no connection with human activities. These leakage pathways include (Peng, 2017):

- CO_2 leaks across the caprock
- CO_2 leaks through natural faults and fractures
- Unconfined lateral migration
- Volcanic and tectonic activities induced CO_2 leakage

Figure 2.4 shows several geological CO_2 leakage pathways via caprocks, natural fractures and induced fractures.

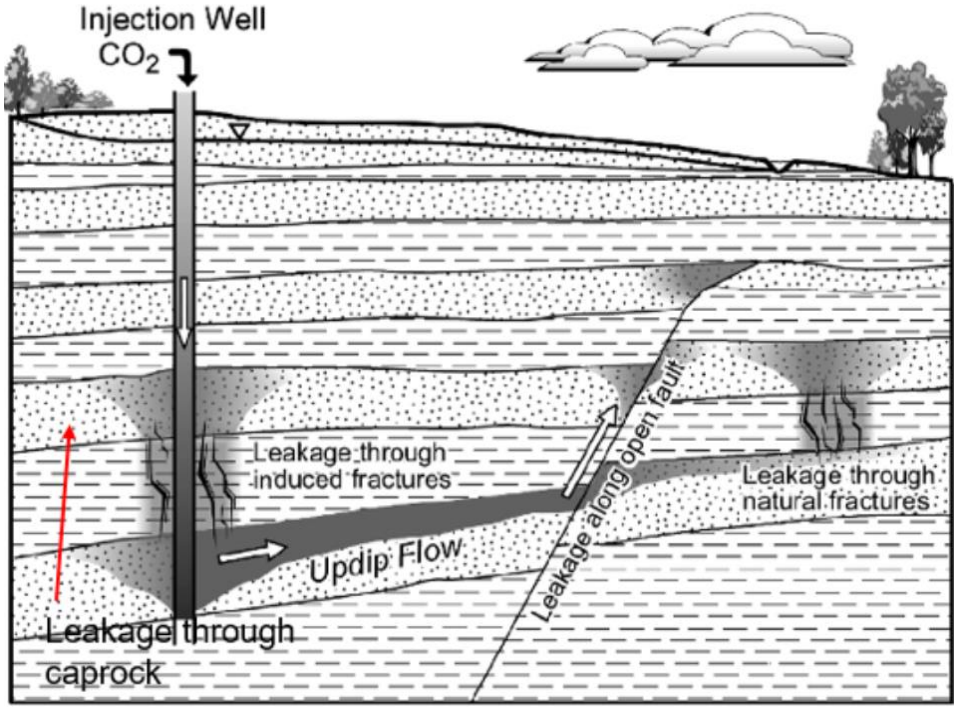

Figure 2.4. Geological CO_2 leakage pathways (Stefan and Celia, 2009)

ii. Engineering Leakage Pathways: these are created by various human activities, and there are five basic types of engineering leakage pathways (Peng, 2017).:

- CO_2 leaks through abandoned wells
- CO_2 leakage due to storage reservoir overfill
- CO_2 leaks through injection-induced fractures and faults
- CO_2 leakage due to post-storage disruption
- CO_2 leaks due to injection operations

Figure 2.5 shows the CO_2 leakage pathways in an abandoned well (a form of engineering leakage pathways).

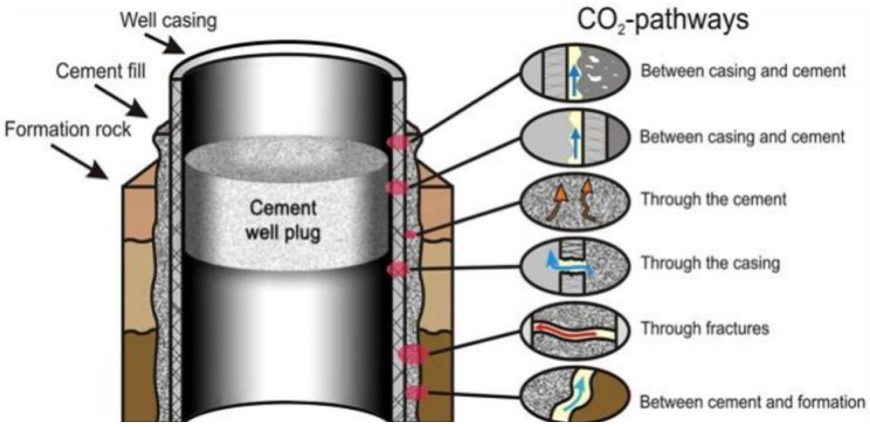

Figure 2.5. Abandoned well leakage pathways (Nordbotten and Celia, 2011; Peng, 2017)

2.4. REMEDIATION OPTIONS FOR CO_2 LEAKAGE

CO_2 sequestration into deep saline aquifers and abandoned reservoirs result in increased pore pressure of the rock. The increased rock pore pressure creates leakage pathways for the injected or stored CO_2 (IPCC,2005). Therefore, once these leakage pathways are initiated due to shear failure of the rock, it becomes critical to initiate remediation options. Monitoring of geologic CO2 storage reservoirs is needed to detect possible leakage pathways or other deterioration of storage integrity (Wright et al., 2004). It is thus crucial to have engineering options to mitigate (i.e. reduction of the short-term effects of leakage) and/or remediate (i.e. long term engineered solution to prevent further leakage or impacts) further fluid leakage. A CO_2 storage project will be considered successful if more than 99% of the injected CO_2 is stored in the intended formation for more than 100 years (IPCC, 2005).

One of the remediation options to mitigate the leakage challenge in CCS is the use of chemical sealants (Brydie et al., 2014; Fleury, 2017). To effectively seal a supercritical CO_2 and/or

CO_2-rich brine leakage pathway via injection of the sealing agent solution, the sealing agent chemically reacts directly with the supercritical CO_2 and/or dissolved CO_2 species to form a pore-blocking precipitate which acts as a leakage barrier and prevent the captured CO_2 from escaping into the atmosphere (Brydie et al., 2014; Fleury, 2017).

Chemical sealants may play a significant role in reducing or mitigating the CO_2 leakage process. The sealant materials should have these following characteristics (Peng, 2017):

a) Sealants for CO_2 leakage control usually work under relatively low pH conditions (3-6). They should also have acid resistance ability, thermal stability, and no harm to the matrix of the rock formation.
b) The pressure is a crucial factor which can influence sealant performance. Therefore, sealants need appropriate mechanical properties to tolerate high pressures.
c) Some other properties such as high-temperature stability, longer-term stability, cost-effective, high sealant integrity and environmentally friendly are also significant for sealants.

The commonly used chemical sealants are cement, geopolymers, foams, gel systems, nanoparticles, and biofilms barriers (Peng, 2017). However, in this thesis, only the gel system will be discussed.

2.5. CO_2 TRIGGERED SILICATE GELATION

CO_2 triggered gelation is necessary to control the CO_2 leakage. In the case of CO_2 leakage, conventional leakage mitigation methods, including cement injection, hydraulic barriers, and other mechanical sealing methods, can play a role in leakage control to a certain extent. To ensure the

CO_2 storage effectiveness and minimize the environmental and economic risk, it is important to monitor the subsurface CO_2 migration and apply a treatment method if leakage is detected.

A gel system approach relies on the gel to arrive at the fracture location of the caprock and seal the leakage pathway. Two gel systems, crosslinked polymer, and silica have been used for decades to improve the relative permeability of oil phase during water or CO_2 flooding recovery. The success of these gel systems as conformance control agents in improving oil recovery has inspired researchers to use them as a treatment method for leakage remediation in CO_2 sequestration (Hadi Mosleh et al., 2016; Manceau et al., 2014; Tongwa et al., 2013).

In this thesis, a silicate solution with low viscosity was applied to seal the CO_2 leakage and its sealing performance was evaluated through experimental works. The gelation process of the silicate solution is triggered by a change of pH, salinity, or temperature. The silicate solution used in this thesis was triggered for gelation by lowering the pH in the presence of CO_2 and relatively high temperature of 60^0C (reservoir temperature).

2.5.1. Gel performance of CO_2 triggered gelation

In this thesis, a silicate gel system was applied as the CO_2 triggered sealant for sealing CO_2 leakage during the geological storage process. In the CO_2 leakage paths, CO_2 dissolves in the solution and reduces its pH to an acidic environment when CO_2 confronts the injected gel system. Then the gelation can be triggered to block or control CO_2 leakage with the generation of gel.

The permeability reduction, KR is a measure of the capability of gel for water shutoff. This reflects the ability of the gel to reduce the permeability of the formation as well as blocking open fractures and features. This is defined as

$$KR = \frac{k1-k2}{k1} * 100\% \quad (2.1)$$

where k1 is the initial permeability before the gel treatment and k2 is the permeability after gel treatment.

Since the injection rate was kept constant before and after the gel treatment in this thesis, equation 2.1 above can be expressed as the flowing equation based on the relation of permeability with flow rate and pressure difference:

$$KR = \frac{\Delta P2 - \Delta P1}{\Delta P1} * 100\% \quad (2.2)$$

where ΔP1 is the pressure difference for CO_2 before gel treatment, ΔP2 is the pressure difference for CO_2 after gel treatment, and KR is also a measure of the water flow resistance with the formation of gels in the simulated leakage zone.

The apparent resistance factor, Z, is usually applied to evaluate the blocking performance of gel toward gas such as CO_2 which leaks from the storage structures. This factor can be expressed as follows:

$$Z = \frac{\Delta P2}{\Delta P1} \quad (2.3)$$

where Z represents the resistance toward CO_2 after the gel formation in the porous domain.
From equations 2.2 and 2.3, it can be seen that

$$KR = (Z-1) *100\% \quad (2.4)$$

2.6. CO_2 LEAKAGE CONTROL SEALANTS (GEL SYSTEM)

Gel systems are commonly used as conformance control agents in CO2 EOR flooding. They can seal the high permeability zones, control the profile of CO2, and improve the CO2 sweep efficiency. There are three types of gel systems used in CO_2 EOR flooding and they are;

a) Organic polymer gels
b) Inorganic gels
c) Microgels

Figure 2.6 shows the classifications of conformance control gel systems into inorganic gels, organic polymer gels and microgels.

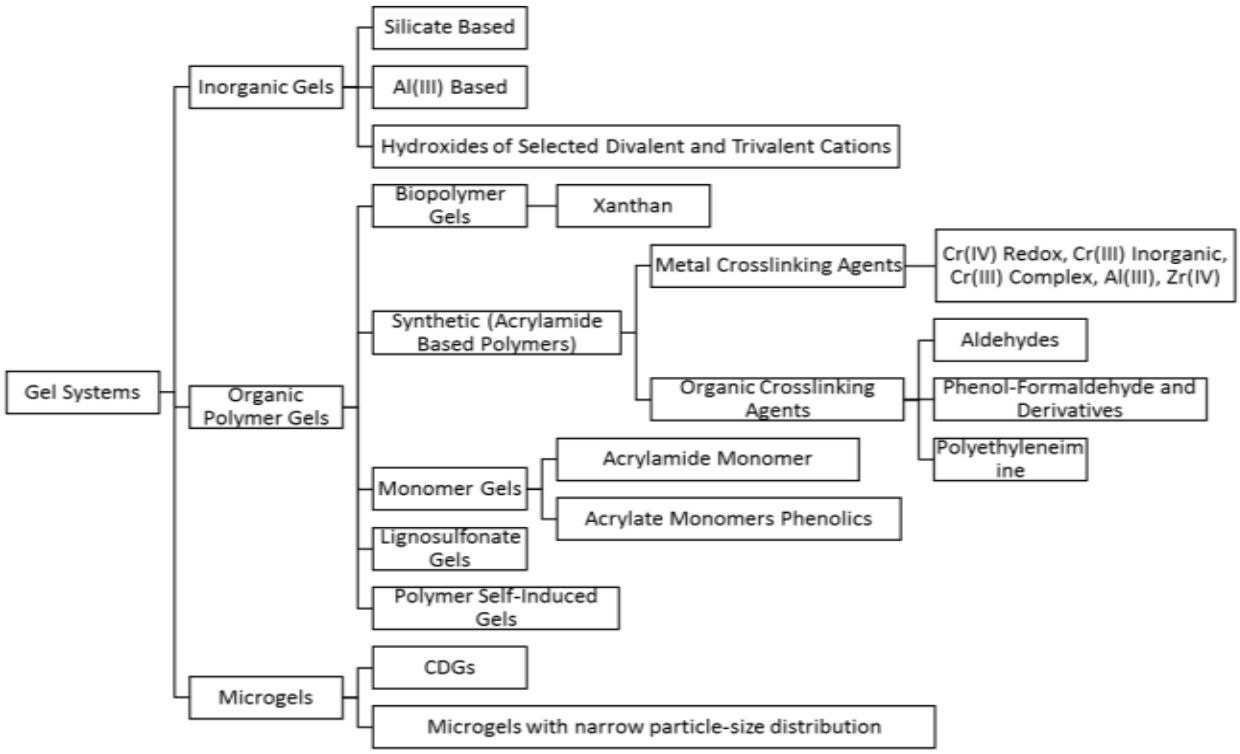

Figure 2.6: Classification of gels based on chemical composition (Peng, 2017)

In this thesis, experiments are conducted using inorganic gel (silica gel) as the conformance control agent in CO_2 EOR flooding.

2.6.1. Organic polymer gel

In CO_2 leakage control, organic polymer gels such as the organic crosslinked polymer gel (OCP) are the most widely used conformance control agent. Crosslinked polymer gel has been widely used to reduce the mobility ratio and decrease operational costs by reducing water production (Hild and Wackowski, 1999; Ricks and Portwood, 2000).

Figure 2.7 shows an organic polymer gel and the resulting crosslinked system.

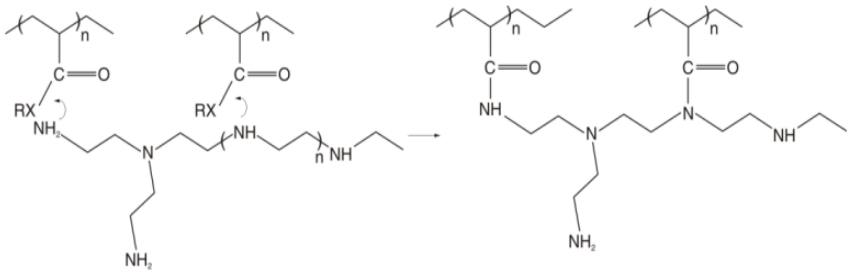

Figure 2.7: OCP system general crosslinking mechanism (Vasquez, J. E. et al., 2010)

The base polymer of this crosslinked system is usually a copolymer of acrylamide and t-butyl acrylate (PAtBA). An organic crosslinker is a material based on polyethyleneimine (PEI). The amine groups on PEI react with the amide and/or ester groups to form an amide linkage (Peng, 2017; Vasquez et al., 2010). Table 2.1 shows the several types of organic crosslinked polymer (OCP) systems and their respective properties

Table 2.1. Types of organic crosslinked polymer (OCP) systems and their properties (Peng, 2017)

OCP system			Apply condition ranges				Reference
Base material	Crosslinker	Others	Temperature, °C	Viscosity (before/after gelation), cp	Optimum pH	Formation pressure, MPa	
PAM	PEI	-	16 – 60	30/30,000	Neutral or weak-alkaline	> 17.93	Aird, T. H. (2014), Vasquez, J. E. et al (2010), Bach et al (2001)
PAtBA	PEI	-	49 – 127				
PAtBA	PEI	Water-soluble carbonate retarder	127 – 177				
PAM	Phenol-Formaldehyde	-	60 – 140	8.9-89/Not mentioned	8 – 9	-	Albonico, P. et al (1995)
PAtBA	PEI	Fluid-loss control additives and non-cement particulates	4 – 204	20-30/Not mentioned	Neutral or weak-alkaline	> 17.93	Vasquez, J., & Curtice, R. (2015)
High-molecule-weight (8~15 million Dalton) partially hydrolyzed polyacrylamide, PHPA	PEI	Non-ionic surfactant	Could reach 107.2	20/10,000	-	-	Crespo, F. et al (2014)

One of the major challenges in gel treatment is gelation time control. To solve this problem, Li et al (2015) proposed a new type of material based on the CO_2 sensitive gel system, which is a modified polyacrylamide-methenamineresorcinol gel system. From the results of Li et al. (2015), it can be seen that the CO_2 -sensitive gel could reduce 97% - 99% of the water permeability in a low permeability core (59.6 to 120.2 md) at operating conditions of 70°C and 20,000 ppm formation water salinity environments. However, at higher operating conditions such as when the temperature, water salinity and core permeability were increased to 90°C, 200,000 ppm and 1698.5md respectively, the reduction to the permeability decreased to 90% - 93% (Peng, 2017).

2.6.1.1 Benefits of Organic polymer gels

Peng (2017) gave the following benefits;

- Can be prepared with produced water
- Good stability (thermal, mechanical, and chemical)
- strength and size-controlled
- uses a simple, one-component injection process
- has no injectivity problemS as it can flow through porous media even when particles are larger than pore throat

2.6.1.2. Limitations of Organic polymer gels

Peng (2017) gave the following limitations;

- inefficient permeability reduction as it requires further testing to realize the permeability reduction efficiency to gas
- Small particle size combined with high salinity may damage formation

- Cannot be used in unfractured porous media as it can preferentially enter into a fracture or fracture-feature channels while minimizing gel penetration into low permeable hydrocarbon zones/matrix

2.6.2. Inorganic gels

Inorganic gels can either be aluminum, silicate, or hydroxide-based gels. However, the most widely used inorganic gel in the industry is the silicate-based gel.

Silicate gel is known to be environmentally friendly because no heavy metal is needed for the gelation process. The starting composition is a stable solution of sodium silicate ($(SiO_2)n: Na_2O$, $n<4$) monomers at pH > 11. A change of pH, salinity or temperature can trigger the gelation process. The silicate molecules react with each other at pH < 10 and form oligomer, and then small particles. The particles will continue to grow into larger sizes through polymerization. When pH < 7 or salt is present, colloidal aggregation can simultaneously occur between particles and lead to a 3D gel network (Axford, 1997; Iler, 1979; McIntosh, 2012). Rheological measurements show that the triggered silica solution is a low-viscosity, Newtonian fluid at an early time, which is advantageous for reservoir injection. However, the apparent viscosity increases by several orders of magnitude due to the reaction at the gel time (Jurinak and Summers, 1991a; Lakatos and Lakatos-Szabo, 2012).

Lakatoset et al. (1999) proposed that silicate gels could control unwanted fluid flow due to the following properties (a) they have low initial viscosities such as 2 cp so that they can penetrate deep formation (b) they have enough high-environmental conditions (temperature, acid) resistance, (c) they are cost-effective, (d) they are environmentally friendly, and (e) they are easily removed if an unexpected accident occurs.

Since the gel time is dependent on the gelation kinetics, it is also known to be affected by pH, temperature, salinity, silica concentration (Jurinak and Summers, 1991b) and morphology of silica (Huang et al., 2017). Prediction of gel time in bulk solution is challenging because the complicated gelation process is still not fully understood.

However, a gel model was proposed by Stavland et al. (2011) to predict gelation time with given silicate content, acid concentration, salinity, and temperature. According to Stavland et al. (2011), the gelation time for our systems in acetic acid(HAc) should have the following form:

$$\ln(t_{gel}) = M + a[\mathrm{Si}] + b[\mathrm{HAc}] + c[\mathrm{NaCl}] + E_a/RT \qquad (2.5)$$

In eq. 2.5, t_{gel} is the gelation time in minutes, [Si], [HAc], [NaCl] are silicate, acetic acid and NaCl concentration in wt.%, T is the temperature in kelvin, M, a, b, c, and Ea are fitting parameters, and R=8.314 J·mol−1·K−1. In particular, Ea is the activation energy.

It has been shown in core flood experiments that silica gel can reduce permeability in conventional core samples (permeability > 10 md) by 100-1000 times, and the produced gel can withstand 1000-4000 psi/ft of pressure gradient before failure (Jurinak and Summers, 1991b; Nasr-El-Din and Taylor, 2005). Jurinak and Summers (1991b) also measured the permeability of CO_2 before and after gel treatment. They showed that CO2 accelerated the gelation process and the gel could achieve a 99.5% permeability reduction. For field injection, the gelation process can be triggered in either a preinjection (Skrettingland et al., 2012) or post-injection manner by reservoir fluid pH, e.g., during CO_2 flooding (Oglesby et al., 2016). A pre-flush with brine may be necessary to remove Mg^{2+} or Ca^{2+} metals. Silica solution produces a base (high pH) environment, which can cause those metals to precipitate and lead to early plugging (Skrettingland et al., 2012).

Silica gel treatments are successful for flow diversion in oil recovery by reducing water-cut, gas-oil ratio and improving oil production (Jurinak and Summers, 1991a; Lakatos and

Lakatos-Szabo, 2012; Oglesby et al., 2016). Compared to oil field injection, the main goal in CO2 leakage remediation is to seal the fractured rocks, although flow diversion can be a side-benefit of the treatment (Tongwa et al., 2013).

Reservoir conditions such as pH, temperature and salinity need to be considered at the design of a silica injection, because these factors are critical to the gelling kinetics and gel time, especially for leakage remediation. Unfortunately, the gel time is difficult to control due to the complexity of the gelation process as well as the presence of dispersion in porous media.

Figure 2.8 shows the polymerization and precipitation process involved in an alkaline silica solution. It details how the polymerization of the silicate-based gel occurs.

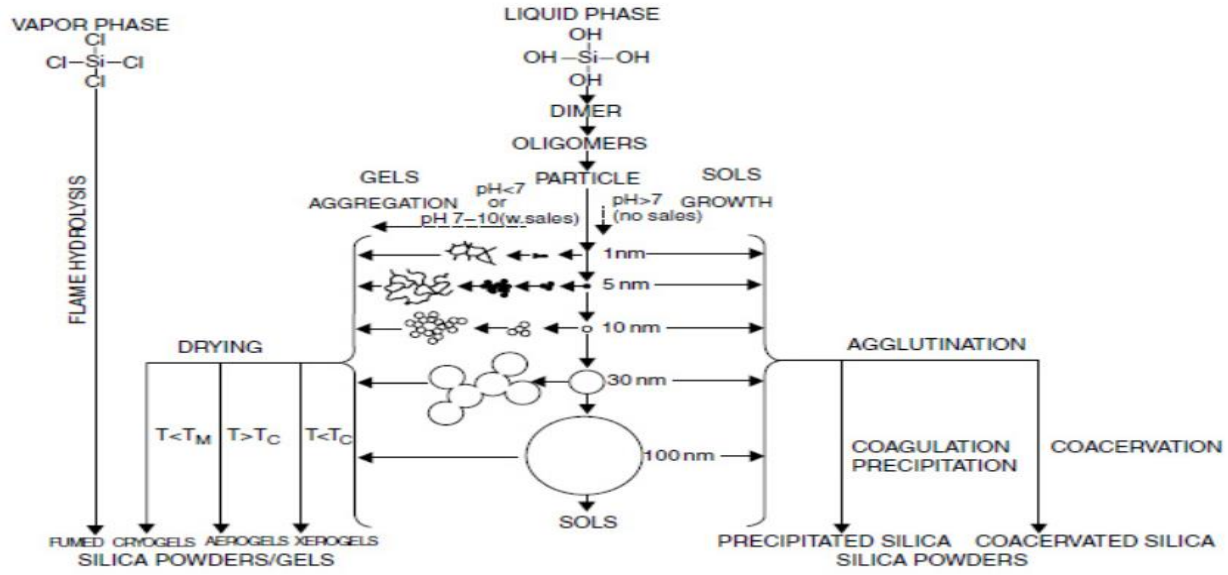

Figure 2.8: General overview of polymerization and precipitation of alkaline silica solution (Bergna et al,2006)

2.6.2.1. Silicate Gel Benefits (Fleury et al., 2016)

- Low initial viscosity which results in deep penetration
- Good stability (thermal, mechanical, and chemical)
- Low cost

- Environmentally friendly (no heavy metals)
- Not shear sensitive
- Internal initiators allow pump times of minutes to 2 weeks
- Selective setting - They will only set in direct contact with an initiator, such as CO_2. If an uninitiated mixture enters a water zone, it will be diluted and form a slush of precipitates in dilute polymer-like water. If that mix contacts crude oil, it will not set at all.

2.6.2.2 Complications/Drawbacks of Silicate Gel (Fleury et al., 2016)

- Extremely sensitive to strong acids, high brine and calcium concentration
- Syneresis effect (shrinkage and water expulsion) inducing potentially a time-dependent blocking effect
- Solution penetration may be short if the buffer capacity of the rock is high
- Setting time difficult to control and difficulty in completely sealing fractures
- Relatively weak gels do not provide good long-term fluid-shutoff performance
- Silicates are prone to form precipitates instead of gel
- Injectivity issue - Silicate solution also will clean scale and other deposit and loose coatings off of steel pipes, tanks and wellbore tubular. These solids can come loose and be pumped downhole causing injectivity issues.

Table 2.3 below shows the typical properties ranges of Organic crosslinked polymer gel(OCP) and silicate gel in terms of target temperature, pressure tolerance, pH, salinity tolerance, viscosity and gelation time.

Table 2.2: Properties ranges of Organic crosslinked polymer gel(OCP) and silicate gel (Peng, 2017)

Properties/Sealants	Properties Ranges of Sealants	
	Organic Crosslinked Polymer Gel	Silicate Gel
Target Temperature (°C)	4-204	< 200
Compressive Strength/Pressure Tolerance (Mpa	< 17.93	< 17.5
pH	Neutral or Weak Alkaline	0-4/7-10
Salinity Tolerance (ppm)	NG	< 120,000
Viscosity (cp)	30-30,000	2-10,000
Setting/Gelation Time (mins)	240-360	4 to 65

2.6.3. Microgels

Microgels are micrometer scale, fully water-soluble, stable, and non-toxic colloidal particles (Schmitz and Pich, 2016). They are commonly synthesized by emulsification method. Microgel solution formulated with a low concentration of polymer and internal crosslinker was developed to enhance the viscosity of polymer solution gels and to increase the level of polymer adsorption and Residual Resistance Factor (RRF) (Abdulbaki, 2012).

Common formulations include a polyethyleneimine organic cross-linker typically with a polyacrylate base. UT-Austin has also conducted previous research and experiments with a pH-triggered microgel using polyelectrolytes. A pH-triggered microgel uses polyelectrolytes, which is very pH sensitive and capable of retaining significant volumes of water and swelling (up to 1000 times the original volume) (Danyalov, 2012).

Figure 2.9 shows the pathway to supramolecular cross-linked microgels

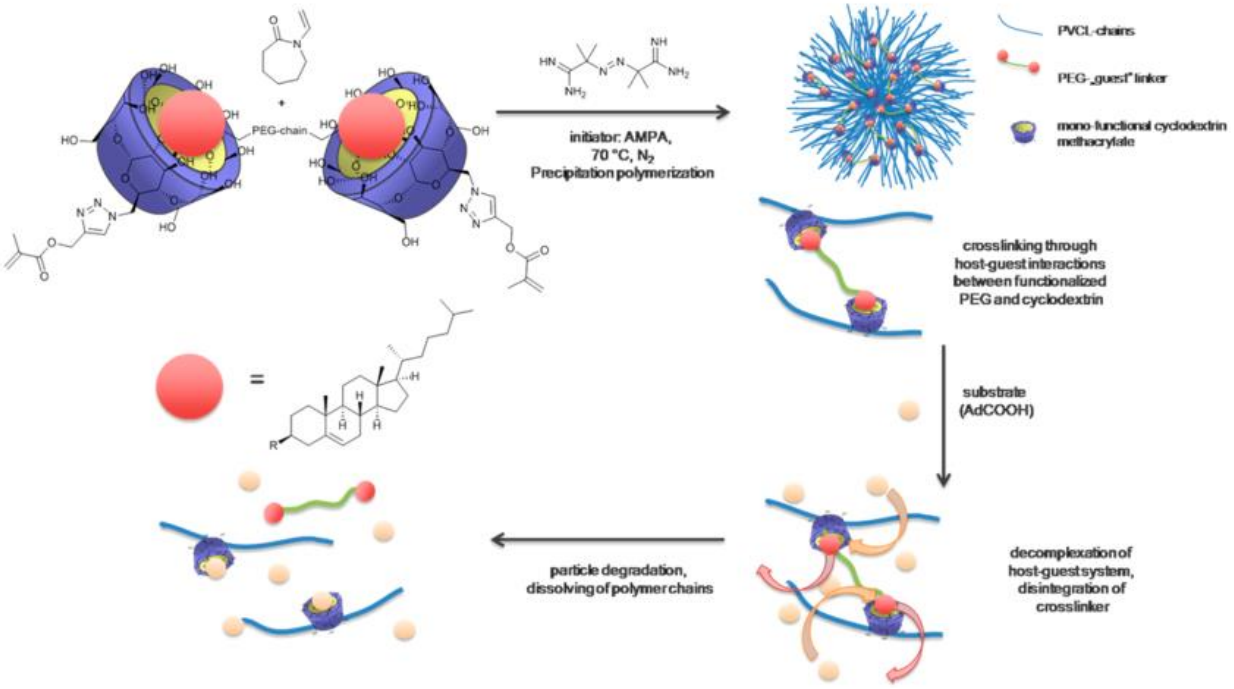

Figure 2.9: Pathway to supramolecular cross-linked microgels (Schmitz and Pich, 2016)

2.6.3.1. Benefits of Microgel (Abdulbaki, 2012; Balhoff et al., 2015; Danyalov, 2012)

- Larger, more rigid, and more stable than polymer alone
- Low concentration required
- Slower crosslinking reaction rate compared to OCP
- More economical compared to OCP
- Primarily intramolecular crosslinks
- Intramolecular bonds stronger than intermolecular bonds
- Formation of many separate polymer microgels
- DPR (disproportionate permeability reduction) OR RPM (relative permeability modification) effect

2.6.3.2. Limitations of Microgel (Abdulbaki, 2012; Balhoff et al., 2015; Danyalov, 2012)

- Possible shrinkage over long-term
- The added cost of acid pre-flush
- Gel internal permeability is velocity-dependent

Therefore, an ideal sealant for CO_2 storage and sequestration needs to be high-pressure, high-temperature, and acid-tolerant. It should be environmentally friendly and cost-effective. It should be noted that delivering the plugging materials (silica gel) into the specific geologic area in the reservoir where leakage occurs is quite challenging.

2.7. Review On Previous Leakage Control Methods During Co2 Sequestration Process

Mitchell et al. (2009) investigated the utility of biofilms directly as a barrier to reduce the permeability of CO2 leakage pathways. Biofilms are microorganism assemblages firmly attached to a surface and are capable of reducing the permeability of deep geological formations under high pressure. The experiment was conducted using a unique high pressure (8.9 MPa), moderate temperature (32 °C) flow reactor containing 40 millidarcy Berea sandstone cores in the presence of supercritical-CO_2, The flow reactor containing the sandstone core was inoculated with the biofilm-forming organism Shewanella fridgidimarina. The results of the electron microscopy revealed that the substantial biofilm growth caused >95% reduction in core permeability. Therefore, the observations showed that the engineered biofilm barrier has the potential to enhance the performance of the CO_2 geological storage.

Reveillere et al. (2012) presented and discussed key issues associated with hydraulic barrier technology for leakage control. They suggested that a hydraulic barrier can be created by increasing the pressure over the leak through brine or water injection within the overlying aquifer to counter the driving forces of the CO2 migration. This suggestion focused more on the hydraulic

barrier to block the CO_2 leakage than the permeability reduction. They evaluated the applicability for blocking the CO_2 leakage from deep saline aquifers through simulation. They also simulated a leakage scenario and three implementation cases of hydraulic barriers (brine injection 10 m away from the leak with or without delay, or 1 km away without delay) using the 3D multiphase flow transport code TOUGH2/ECO2N. Then they assessed the effectiveness of the hydraulic barrier in stopping the leakage and trapping the accumulated CO_2 in the overlying aquifer. Therefore, the results showed the suitability of a hydraulic barrier for controlling CO_2 leakage in the low transmissivity overlying aquifers.

Tongwa et al. (2013) investigated four candidate fracture-sealing materials for blocking CO_2 leakage, including paraffin wax, polymer-based gel, silica-based gel, and micro cement. They noticed that both the gel and the wax-filled fractures had wormholes which limited their effectiveness as sealant agents. Also, it was observed that the gels could not withstand large pressure differentials in a fracture whereas the micro-cement did. Their work showed that all these four materials can reduce the permeability of the leakage pathways and the micro cement exhibited the most effective sealing performance. Thus, micro-cement is recommended for sealing of fractures if the fracture width is above half a millimeter.

Ito et al. (2014) devised a method to reduce the permeability of leakage pathways of the CO_2 storage reservoir at deep depth using CO_2 reactive aqueous grout. They demonstrated the idea through laboratory experiments simulating subsurface condition at 1000 m deep, i.e. 10 MPa and 40 °C, and using a silicate solution. The results indicated that this method could lead to a 99% permeability reduction and they used a reactive transport simulator TOUGHREACT to reproduce the experimental results. The silica precipitation, which was produced from the reaction, can fill up pores of leakage paths and provide a barrier to block the CO_2 migration.

Batôt et al. (2017) investigated the use of foams for blocking CO_2 leakage pathways, by injecting water and appropriate surfactants in the direction of the leakage paths. They studied the capacity of foams to reduce gas flow for CO_2-brine systems in rock core sample with common surfactants, as a function of interstitial velocity and gas to water fraction. The performance of the generated foams was evaluated from the relative foam viscosity, the ratio of the measured pressure drop in the presence of foam to the pressure drop in single-phase condition for the same interstitial velocity. Their study showed that the use of foams in a CCS context can be adapted for emergency remediation with effective and stable properties. Whatever the pressure and permeability/porosity, the relative foam viscosity can be described as a power law versus the shear rate evaluated from an empirical law established for polymer systems in which the interstitial velocity, permeability, and porosity are the main variables.

Recently, Castaneda-Herrera et al. (2018) studied the use of amorphous silica gel to form a geochemical gel barrier in porous media, as a suitable technology for treating CO_2 leakage. Their technique is based on the in-situ reaction between the leaking CO2 and a sodium silicate solution to produce the amorphous silica gel precipitate. The concentration gradient given by the mixing front between the solutions played a crucial role in determining the effectiveness of the reaction in a column experiment. Their micro-CT imaging results showed that a strong permeability barrier can be formed if silicate solutions are acidified before injection. They observed a significant drop in permeability when CO_2 is injected which demonstrated a successful barrier formation at reservoir conditions. Also, they observed that the reduction in the permeability of a Berea Sandstone core was higher in experiments where supercritical CO_2 was injected. Therefore, they concluded that the use of sodium silicate as a reagent to form a geochemical barrier was a promising technology to abate CO2 leakage for carbon sequestration purposes.

2.8. NUMERICAL MODELING

Numerical simulations can be a useful tool to study gel transport in porous media and aid the design of silica gel treatment. Most of these simulations simplify the gelation process as one simple chemical reaction.

Kim et al. (2007) performed simulations of silica injection for gel barrier construction to control groundwater flow. The gel plugging was modelled by setting the produced gel as a very high viscosity (therefore low mobility) fluid. The concentration of silica and salinity were included in the kinetics of gel reaction. Effect of pH and temperature were not considered in the simulations.

Amiri et al. (2014) performed 2D simulations to match experimental observations of silica injection into an unconsolidated core containing oil and water. To do so, they assume very slow silica gelation at the early time of the simulation and switch to fast gelation reaction at gel time observed from core flood experiments. This approach makes upscaling of the simulations challenging.

A similar approach that relies on experimental observation to determine gel time was adopted by Hatzignatiou et al. (2014). In their work, the gel plugging was modelled as permeability reduction caused by gel adsorption on to the rock surface.

Omekeh et al. (2017) also developed a population model that incorporates nucleation, polymerization, and colloidal aggregation into the gelation process. While assumptions were made to simplify the model, it includes all the important aspects of the gel reaction. For the prediction of bulk gel time, the model matches well with experimental data. They also demonstrated large scale simulation and showed that silica gel can reach over 3000 ft from the wellbore if a pre-flush is applied to remove high valent metals. However, Omekeh et al. (2017) did not match their model with core flood experiments and did not study permeability reduction of gel in porous media.

Zhu et al. (2019) performed a reservoir simulation study to investigate the injection of gel systems such as crosslinked polymer gels and silica gels, as a leakage treatment method in a CO_2 storage reservoir. They modeled the fracture sealing capability of the gel by adopting an adsorption and permeability reduction approach. The simulation results show that selecting the appropriate operating conditions for the reservoir properties was crucial to the success of CO_2 leakage remediation. From their results, it is shown that successful treatment can reduce CO_2 leakage by 103 times over 25 years of post-treatment CO_2 injection.

Table 2.4 shows the CO_2 leakage data for the base cases whereas Figure 2.10(a) and (b). shows a plot of the gel adsorption versus composition in the aqueous phase using a crosslinked polymer gel and silica gel, respectively.

Table 2.3: CO_2 leakage data for the base cases (Zhu et al.,2019)

Cumulative CO_2	**Initial period (0-5 years) lb_m**	**Post-Treatment (6-31 years) lb_m**	**All-time lb_m**	**Leakage ratio %**		
				Initial period	**Post-treatment**	**All-time**
Injected	95.27	476.73	572.0	N/A	N/A	N/A
Leakage without treatment	0.185	35.17	35.35	0.19	7.4	6.2
Leakage (crosslinked polymer)	0.185	0.005	0.19	0.19	0.001	0.03
Leakage (Silica)	0.185	0.044	0.229	0.19	0.009	0.04

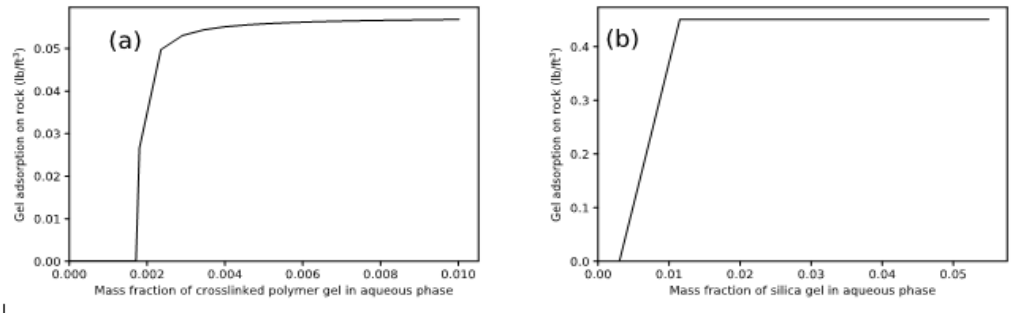

Figure 2.10: Gel adsorption versus composition in the aqueous phase (a) crosslinked polymer gel; (b) silica gel (Zhu et al.,2019)

Chapter 3: Experimental Materials and Approaches

3.1. INTRODUCTION

The experimental approach including materials, equipment, procedures, measurements, and calculations for conducting the core flooding experiments performed in this work is presented in this chapter. The experimental approach for core floods is presented step by step from core preparation to silicate solution flooding. The experimental approach is similar to that used by Fortenberry (2013), Unomah (2013), Koh (2015), Lee (2015) and Qi et al. (2017). The experimental results are presented in Chapter 4. This experiment is conducted in two major phases:

- Bulk gelation
- Core flood

The main objectives of conducting these bulk gelation and core flood experiments are as follows:

- to predict the reactive transport of silicate gel in porous media,
- to compare the results obtained from gelation in porous media to the gelation results from the bulk experiments, and
- to investigate the effectiveness of the capability of the gel for permeability reduction and sealing of the core within small- and medium-scale porous media under reservoir conditions.

In the bulk gelation phase, the reactive gelation process of the silicate solution was investigated. The time required to gel at different silicate content, acid type, acid content, salinity and temperature were measured and analysed. Acetic (HAc) and hydrochloric (HCl) acid were

used as two different gelation initiators. The purpose of this phase is to determine and quantify how the gelation process is affected by weak (i.e. HAc) and strong (i.e. HCl) acid solutions.

In the core flood experiment phase, the experiments were conducted based on the results obtained from the bulk (or batch) gelation experiments. The main objectives of conducting these core flood experiments were to understand the reactive transport of silicate gel in porous media, compare the results obtained from gelation in porous media to the gelation results from the earlier bulk experiments and, finally, investigate the capability of the gel in permeability reduction and sealing of the core. These core flood experiments were conducted in two major conditions: a) ambient temperature and pressure with an acetic acid solution as a CO_2 substitute, and b) the High-Pressure High-Temperature with CO_2 saturated brine.

3.2. FLUID PREPARATION

3.2.1. Brine solution

All the brines were prepared with laboratory-grade sodium chloride (NaCl) salts dissolved in deionized water. Salts were measured out using weight by volume. Deionized (DI) water and the appropriate salts were mixed using a magnetic stir plate and magnetic stirrer bars. Before injecting the brines in any core or batch samples, they were filtered with a 0.45-micron cellulose filter.

3.2.2. EDTA solution

Ethylenediaminetetraacetic acid (EDTA), sodium bicarbonate ($NaHCO_3$), and sodium hydrosulfate ($NaHSO_4$) salts were dissolved in deionized water to form the desired EDTA solution. The resulting solution was mixed using a magnetic stir plate and magnetic stirrer bars. Before injecting the brines in any core, they were filtered with a 0.45-micron cellulose filter.

3.2.3. Acid solution

The acid solutions were prepared with the acid reagents (either acetic (HAc) or hydrochloric (HCl) acid), sodium chloride (NaCl) and deionized water. The desired salt concentration was measured out using weight by volume. The acetic acid had an assay of 99.7% and a density of 1.05 g/cm^3. The required acid concentration was calculated using the density and the assay of the acid reagent.

Deionized (DI) water, acid solution and NaCl were thoroughly mixed using a magnetic stir plate and magnetic stirrer bars. Before injecting the desired acid solution in any core, they were filtered with a 0.45-micron cellulose filter.

3.2.4. Silicate solution

The stock silicate solution used is a 28.7 wt% potassium silicate solution (Betol K28T) purchased from Woellner. It has a density of 1.25 g/cm^3 and viscosity of 28 mPas. The chemical formula of potassium silicate is $(SiO_2)n: K_2O$ with n=3.92. Therefore, SiO_2 and K_2O content is 20.5 wt.% and 8.2 wt.%, respectively. The pH of the stock solution is 11.62.

Potassium silicate is stable at this pH and no gelation occurs. The silicate solutions used for experimental core flood injections were diluted from this stock solution with deionized water to their desired concentrations.

3.2.5 CO_2 saturated brine

CO_2 saturated brine is prepared using the isothermal expansion method developed by El-Maghraby et al.,(2010) by mixing CO_2 and brine (30,000 ppm) at 1500 psi and 60^0C until a complete equilibration of CO2 and brine is achieved.

3.3. BULK GELATION EXPERIMENTS

In the bulk gelation phase, the gelation process of the silicate solution was inspected. The gel time at different silicate content, acid type, acid content, salinity and temperature were measured and analysed. Acetic (HAc) and hydrochloric (HCl) acid were used as two different gelation initiators. The purpose of this phase is to determine and quantify how the gelation process is affected by weak (i.e. HAc) and strong (i.e. HCl) acid solutions.

3.3.1. Description of sealant material (silica gel)

The proposed sealant material is silica gel. The stock silicate solution used is a 28.7 wt% potassium silicate solution (Betol K28T) purchased from Woellner. This silicate solution has been applied on a field test in Serbia. The idea was to induce the formation of a barrier through the reaction of a potassium silicate solution with leaking CO_2 either in the form of dissolved CO_2or as supercritical CO_2 (Castañeda-Herrera et al., 2018).

The chemical formula of potassium silicate is $(SiO_2)n$: K_2O with n=3.92. Therefore, SiO_2 and K_2Ocontent is 20.5 wt.% and 8.2 wt.%, respectively. The pH of the stock solution is 11.62. Potassium silicate is stable at this pH and no gelation occurs.

3.3.2. Preparation of sealant and gelling system

The silicate solutions used for experimental core flood injections were diluted from this stock solution (Betol K28T) with deionized water to their desired concentrations. An aqueous solution with measured acid and NaCl concentration were prepared in test tubes. NaCl was chosen for the salinity study because we assume that the formation will be preflushed with NaCl brine to remove calcium and magnesium.

A predetermined amount of stock potassium silicate solution was added into the test tubes to form a gelling system that has desired concentration of each species. The test tube was well shaken to ensure a homogeneous mixture and quickly transferred into an oven that was set at a target temperature. The gelation time was determined by visual inspection of the sample and tilting the test tube constantly until a significant loss of sample fluidity was observed. The sample was inspected every 5-15 minutes at early times. For samples with long gelation, the time interval for inspection was gradually increased.

3.3.3. Gelation activated by acetic acid (HAc)

The mother solution used in these experiments is Betol K28T diluted with deionized water (50 wt.%). Following the methodology of Tognonvi (2009), we tested several mixtures of diluted Betol K28T and acetic acid (1M) with varying salinities and at different temperatures.

To investigate the effect of acid and silicate concentrations on the gelation process(i.e. gel time), precipitation was qualitatively observed at 40°C for various fractions of the diluted stock potassium silicate solution (6.12 wt%, 8.11 wt%, 10.1 wt% and 12.1 wt%) and acetic acid concentrations (0.6 wt%, 0.7 wt%, 0.8 wt% and 0.9 wt%).

To investigate the effect of salinity and temperature on the gelation process (i.e. gel time), precipitation was qualitatively observed using a constant silicate content of 8.64 wt% and acetic acid (HAc) content of 0.94 wt%. at varying salinities (500, 1000, 2500 and 5000 ppm, respectively) and temperatures (22.2°C, 40°C, 45°C, 55°C, 62.5°C, and 78°C, respectively).

3.3.4. Gelation activated by hydrochloric acid (HCl)

The mother solution used in these experiments is Betol K28T diluted with deionized water (50 wt%). Following the methodology of Tognonvi (2009), we tested several mixtures of diluted Betol K28T and hydrochloric acid (1M) with varying salinities and at different temperatures.

To investigate the effect of acid and silicate concentrations on the gelation process (i.e. gel time), precipitation was qualitatively observed at 40°C for various fractions of the diluted stock potassium silicate solution (6.12 wt%, 8.11 wt%, 10.1 wt% and 12.1 wt%) and hydrochloric acid concentrations (0.6 wt%, 0.7 wt%, 0.8 wt%, 0.9 wt% and 1 wt%).

To investigate the effect of salinity on the gelation process (i.e. gel time), precipitation was qualitatively observed using a constant silicate content of 8.11 wt% and hydrochloric acid (HCl) content of 0.7 wt%. at 40°C with varying salinities (500, 1000, 2500 and 5000 ppm, respectively).

To investigate the effect of temperature on the gelation process, precipitation was qualitatively observed for various fractions of the diluted stock potassium silicate solution (6.57 wt%, 8.57 wt%, and 10.36 wt%) and hydrochloric acid concentrations (0.6 wt% and 0.7 wt%) at varying temperatures of 40°C to 78°C.

3.3.5. Batch gel time experiments at higher salinities and acid concentrations

From the previous batch gelation experiments, the right acid reagent to be used as the CO_2 substitute is determined to be acetic acid (HAC) and a final batch experiment using the determined acid reagent at higher salinities and acid concentrations.

To mimic reservoir conditions and ensure accurate results, it is necessary to perform experiments near reservoir conditions of high salinity and a corresponding acetic acid (HAc) concentration that would be analogous to the CO_2 concentration in the reservoir.

Therefore, an additional set of batch experiments were performed using higher salinities and acetic acid concentrations. The samples in this set of experiments have HAc concentration from 0.001 to 1 wt%, 9 wt% silicate solution and salinity from 5000 to 50,000 ppm. The gelation time was measured at 60°C.

3.4. CORE FLOOD EXPERIMENTS

The main objectives of conducting these core flood experiments are to predict the reaction transport of silicate gel in porous media, compare the gelation results obtained from the porous media to the gelation results from the earlier bulk experiments and finally, investigate the capability of the gel for permeability reduction and sealing of the core.

These core flood experiments are conducted under two conditions: ambient with an acetic acid solution as a CO_2 substitute and the High-Pressure, High-Temperature condition with CO_2 saturated brine.

3.4.1. Core flood equipment

In this section, the equipment used for fluid preparation and core flood experiment is presented.

3.4.1.1. Pump

All core flood experiments were performed at constant flow rates. A Teledyne Instrument Specialties Company (ISCO) pump (Figure 3.1) was used to inject fluid at a desired flow rate. The pump has a capacity that can vary from 500 mL to 1000 mL (dependent on column size). Pumps held mineral oil that was used to displace fluids into the core and was refilled immediately when

emptied to prevent prolonged periods of inactive time during chemical floods. Effluent fractions were collected based on the set flow rate on the pump.

Figure 3.1 shows the Teledyne ISCO 5000 syringe pump and LabViewTM software used in the experiment.

Figure 3.1 a) Pump used to inject fluids in experiments b) Teledyne ISCO 5000 syringe pump and LabViewTM software

3.4.1.2. Fluid Columns

Custom polycarbonate columns, shown in Figure 3.2, were used to hold acetic acid (HAc), brine, EDTA and potassium silicate (Betol K28T) solutions that were injected into the core. These columns were custom-designed to hold different volumes of solution.

Mineral oil was injected into these fluid columns and would displace the desired fluid solution out into the core. The exact volume of mineral oil-injected was carefully determined so that only the desired fluid solution would be displaced, and no mineral oil enters the core.

Figure 3.2 shows the polycarbonate fluid columns used to hold injection solutions.

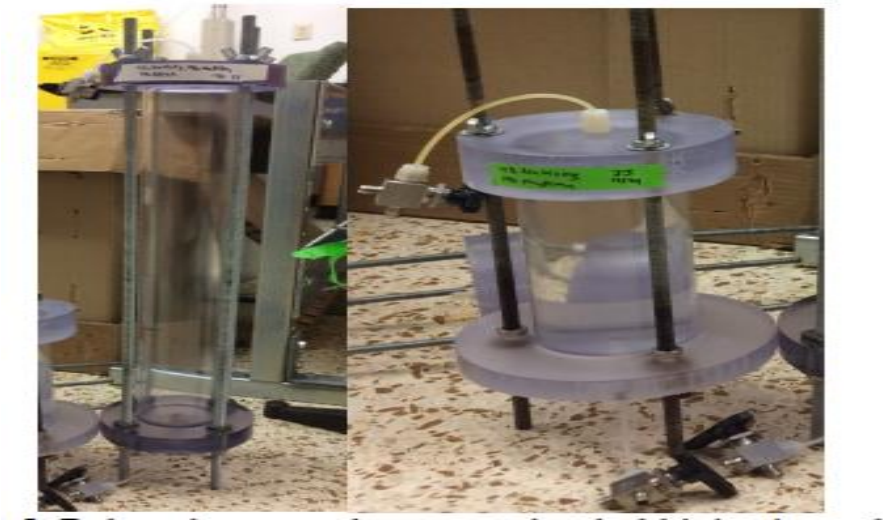

Figure 3.2: Polycarbonate columns used to hold injection solutions

Another fluid column used was the Kontes Chromaflex® glass columns (Figure 3.3) with a pressure rating of 50 psi. These were also used for brine solution injection. These columns were 0.5 to 2 feet in length and 2 inches in outer diameter. The end pieces include a Vitron O ring and washer to prevent leaking when hand tightened. These columns can withstand up to 50 psi, but usually, a maximum of 20 psi was used for additional safety precautions.

Figure 3.3. shows the Kontes Chromaflex® glass columns, which is another fluid column that was used in the experiment.

Figure 3.3: Kontes Chromaflex® glass columns

3.4.1.3. Pressure Transducers

Pressure transducers (Rosemount 3051T) were connected to the core in all experiments. Four sectional pressure transducers recorded a pressure range of 0-30 psi. Two additional whole pressure transducers were used to record pressures from 0-150 psi. The hydraulic connection between the pressure tap and the pressure transducer pressure drop was recorded by a data acquisition software (National Instruments LabViewTM).

Figure 3.4 shows a generalized set up of the pump, core, columns, and pressure transducers.

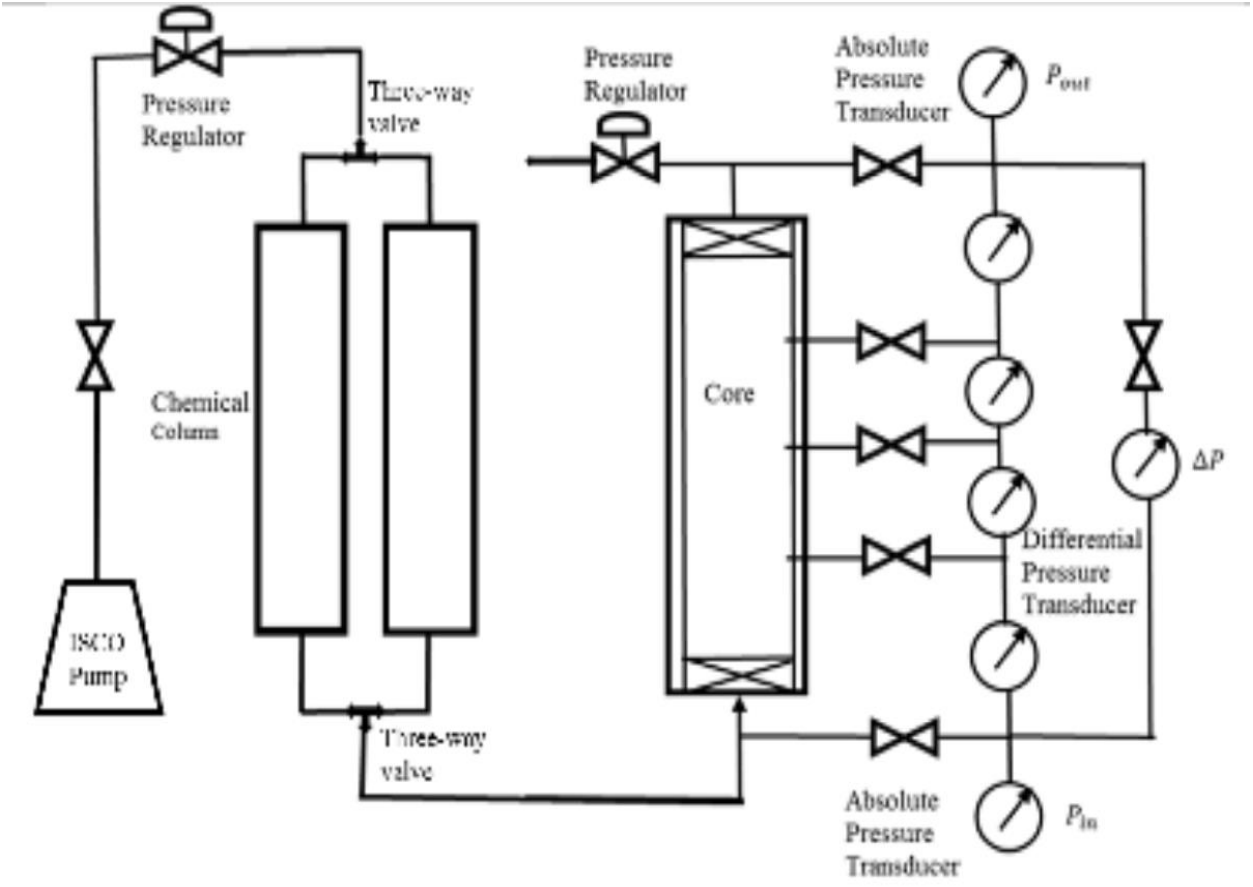

Figure 3.4: General core flood schematic showing pump, core, and pressure transducer set up (Jin, 2019)

3.4.1.4. Fractional Sample Collector

A Teledyne ISCO Retriever 500 fraction collector (Figure 3.5) was used to collect effluent samples from each experiment. The fraction collector was programmed to move every set time interval as determined by the flow rate and desired fraction size.

For example, for a flow rate of 0.5 mL/min and a fraction size of 10 mL, the appropriate time interval was calculated to be $\frac{10\ \text{mL}}{0.5\ \text{mL/min}}$ or 20 minutes. In this example, after 20 minutes, the fraction collector would move to the next tube and have collected 10 mL of effluent.

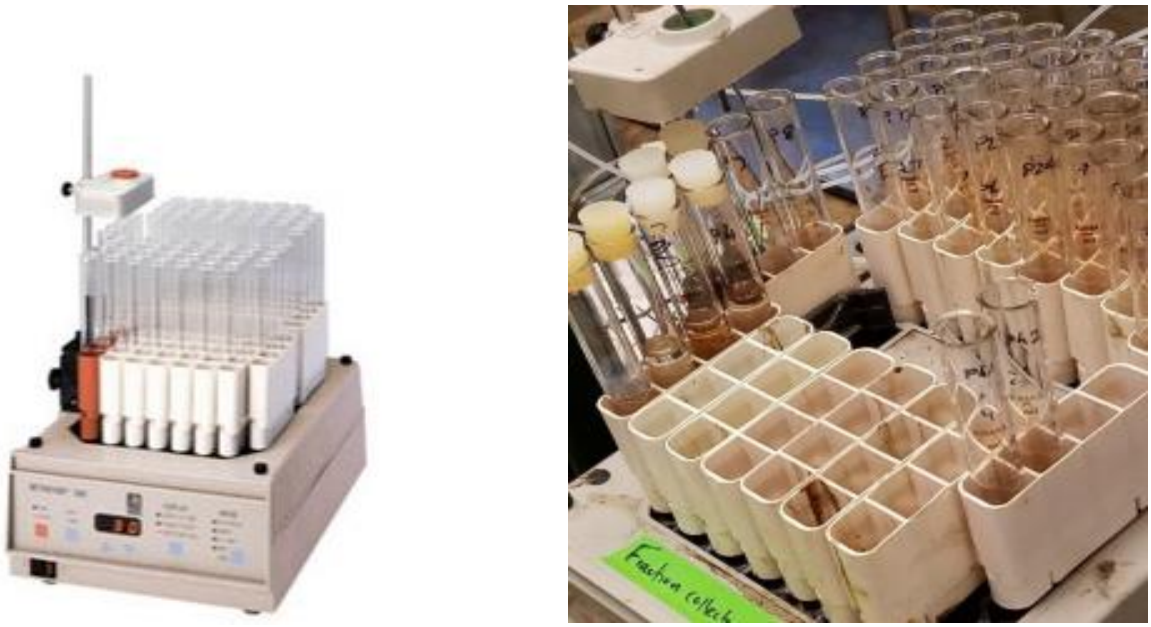

Figure 3.5: Fraction collector used to collect effluent samples in experiments.

3.4.1.5. Refractometer

A hand-held portable refractometer (Figure 3.6) was used for reading the refractive index/salinity index of solutions. The refractometer measures salinity from 0 parts per thousand (% ppt) to 100 ppt. It also measures specific gravity (d 20/20) from 1-1.070. To measure the salinity index of effluent samples, the refractometer was used to determine the salinity of the effluents in parts per thousand.

Figure 3.6 shows the refractometer which is used to measure the salinity index.

Figure 3.6: Refractometer and salinity index

3.4.1.6. Digital balance scale

A digital balance scale (Sartorius) with a 0-2 kg range and 0.01 g readability was used to measure the mass of solutions. A different balance scale (Ranger) with a 0-5 kg range and 0.0000 kg readability were used (Figure 3.7) to measure the mass of the core.

Disposable weighing boats were used for the measurement of solids such as KCl, NaCl, $NaHCO_3$, EDTA-Na^{4+} and $Na_2S_2O_4$

Figure 3.7: Digital balance scales

3.5. AMBIENT PHASE CORE FLOOD EXPERIMENT

In this section, the core flood experiments are conducted under ambient conditions using an acetic acid solution as a CO_2 substitute. Two sets of experiments were proposed. The first experiment was the initial pilot experiment run to investigate the gel's capability at sealing and permeability reduction whereas additional experiments were performed to verify the results of the first experiment and perform sensitivity analysis.

3.5.1. Materials

Based on the results from the bulk gelation experiments, acetic acid was chosen as the CO_2 substitute in conducting this ambient phase. The core used was a Benthemier Sandstone. Cores used in these experiments were all 1.5 inches in diameter and 12 inches (1 ft) in length. The core is fully saturated with acetic acid. The injecting fluid for the gelation process is a silicate solution (Betol K28T). Cores were drilled out from the original Benthemier sandstone blocks and dried in a high-temperature oven (at least 90°C) for at least 36 hrs.

3.5.2. Core flood setup and schematic representation for the ambient phase

The core is divided into four sections. The pressure tap on each section is linked to a 0-35 psi differential pressure transducer; the inlet and outlet of the core are linked to a 0-300 psi differential pressure transducer. Additionally, the inlet and outlet of the core are linked to two 0-150 psi absolute pressure transducers. The linkage/connection between the pressure taps and the pressure transducers are the Swagelok® three-way valves and the tubing filled with water.

Using this hydraulic connection and a National Instruments LabViewTM data acquisition system software, the pressure drops for each section and the entire core are measured, recorded

and displayed instantly on a computer. The core has an inlet where the fluid is injected into the core and an outlet where the displaced fluid is produced (effluent) and goes to Teledyne Isco Retriever™ 500 fraction collector.

In case the air gets in the core accidentally, a back-pressure regulator (BPR) is connected to the outlet line to remove the air from the core by setting the BPR at 50 psi and injecting the brine at 50 psi.

Figures 3.8 a,b and c show the schematic representation and a pictorial view of the core flood apparatus set up in the ambient condition

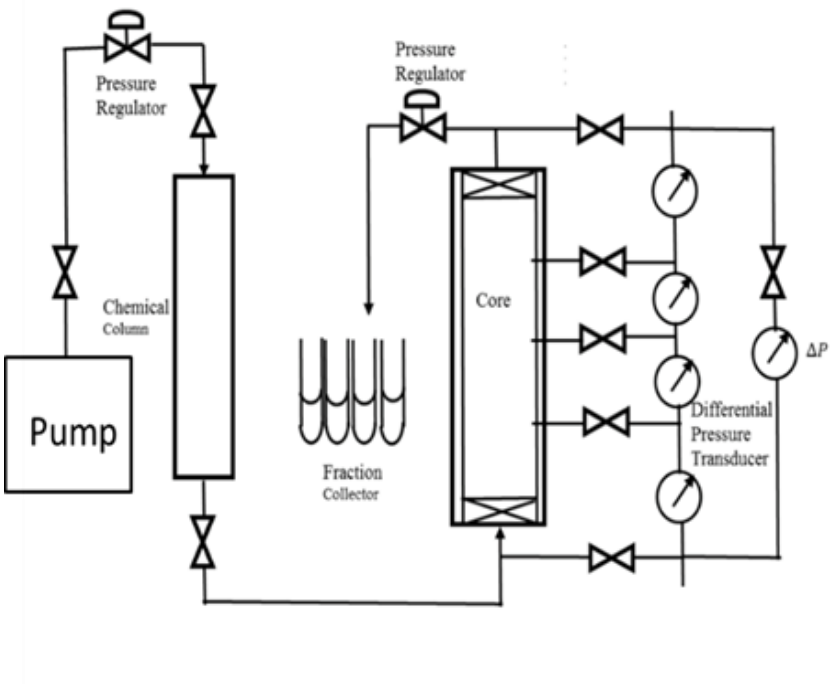

Figure 3.8. (a) Schematic representation

Figure 3.8. (b) Ambient Coreflood set up in the Lab

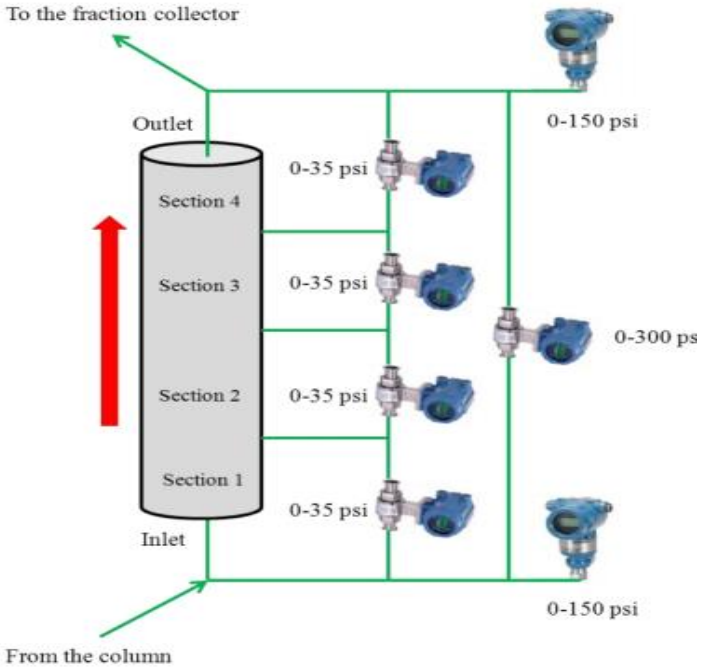

Figure 3.8. c) Coreflood apparatus showing a core with four sections connected to four 0- 35 psi differential pressure transducers; and with inlet & outlet connected to two 0-150 psi absolute pressure transducers, and a 0-300 psi differential pressure transducer.

3.5.3. Core preparation and experimental procedures

Here, the procedures for the ambient core flood experiment such as the steps for core preparation and silicate solution injection are discussed.

3.5.3.1. Core-epoxy preparation

Materials used for core preparation include a core, a 2" diameter and 15" length transparent polycarbonate cylinder tube, two 2" diameter polycarbonate endcaps, epoxy resin (EPON Resin 828), hardener (Versamid 140), silicon glue, aluminum foil, pressure taps, nylon fitting connectors, thread seal tape, 5-min epoxy, and five three-way valves were used. The equipment used here includes a drill, drill bits, air system, and a water tub used for leaking test.

The core preparation procedure is described as follows:

i. The Benthemier sandstone cores were taken from the oven after being dried and left to cool to room temperature.

ii. The dimensions (length and, mass) of the core were measured. The diameter was measured from three different spots and recorded. Bulk Volume (V_B) of the core was determined using equation 3.1 and the average of the three measurements.

$$V_B = hA = h\pi\frac{D^2}{4} \tag{3.1}$$

where h is the core length, A is the area, and D is the diameter of the core.

iii. Weigh the core and calculate the bulk density of the core using equation 3.2

$$\rho_B = \frac{m}{V_B} \tag{3.2}$$

where ρ_B is the density of the core, and m is the mass of the core.

iv. Two end caps (Figure 3.9) were placed on the ends of the core and connected to the core with quick 5-minute curing epoxy (Grainger). The epoxy was only used to secure the end

caps to the end of the core, but it was important to leave the flat end of the core clear of any epoxy to prevent any blockage.

Figure 3.9 shows the custom polycarbonate end cap pieces

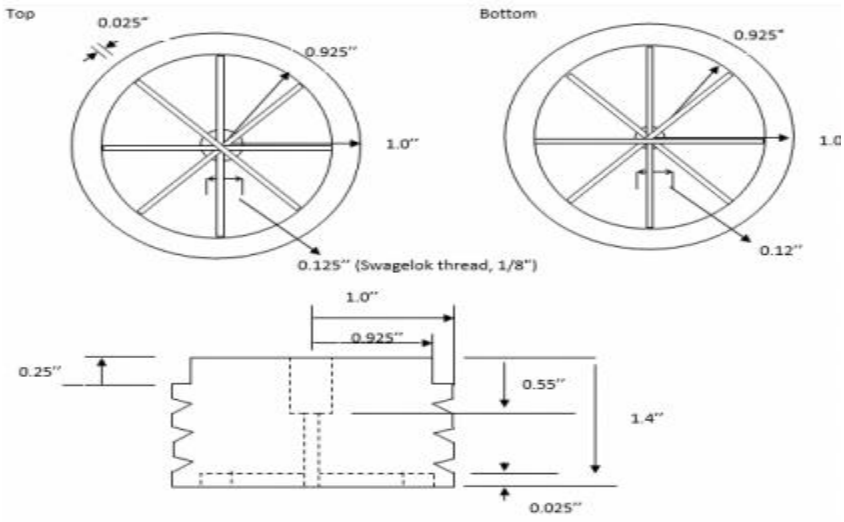

Figure 3.9: Custom polycarbonate end cap pieces (Jin, 2019)

v. Additional 5-minute epoxy was then coated all over the side of the core, which was used to seal the core surface face. The quicker curing epoxy created a protective coat that will prevent the imbibition of the slow curing epoxy into the sandstone.

vi. Once the quick 5-minute curing epoxy has set, the Benthemier core was placed in the middle of a larger polycarbonate tube (2.-inch diameter and 15-inch length). The inlet and outlet of the end pieces should be protected with tape to prevent the epoxy from leaking in and blocking the inlet or outlet of the core.

vii. The slow curing, 24-hour epoxy was prepared by mixing the epoxy base (EPON Resin 828) with the curing agent (Versamid 125) in a 2:1 ratio by weight. The epoxy was mixed in a disposable plastic container until it becomes a homogenous mixture. This slow curing

epoxy was poured into the annular space between the core and the polycarbonate tube. The epoxy was poured slowly to prevent the formation of large air bubbles.

viii. The core was left to cure overnight, at minimum. The epoxy must have solidified completely before moving on to drilling the pressure taps as shown in figure 3.10 below.

Figure 3.10 shows two Bentheimer sandstone cores filled with slow-setting epoxy

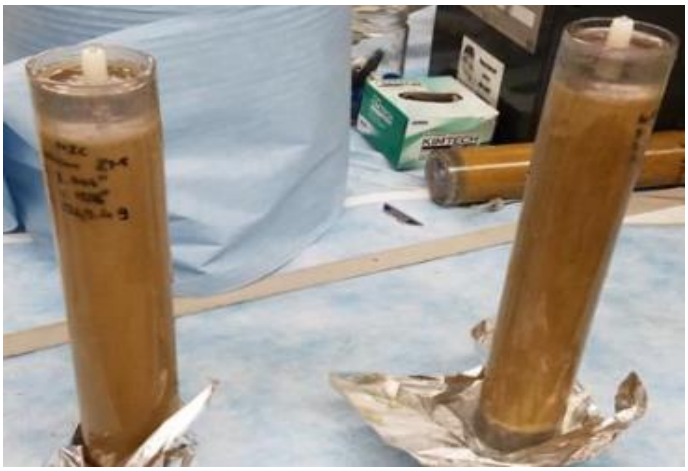

Figure 3.10: Two Bentheimer sandstone cores filled with slow-setting epoxy.

ix. The cores were then drilled in three evenly spaced out holes for pressure taps. The pressure taps should be on the same vertical line. The taps were secured with more epoxy and connected to 3-way Swagelok valves.

x. To make sure the taps have been drilled properly, high pressure (100psi) air was injected into the core and used to make sure all taps are flowing properly.

xi. The cores were submerged in a water bath while the air was being injected into the core as shown in figure 3.11. If there were any leaks or points of weakness in the epoxy, bubbles would appear in the water. The integrity of the core must be confirmed before moving on to any next steps.

Figure 3.11 shows a pictorial view of a leaking observation scenario from the middle tap of an epoxied Bentheimer sandstone core which is tested inside a container filled with water

Figure 3.11: Leaking observation from the middle tap of an epoxied Bentheimer sandstone core which is tested inside a container filled with water

3.5.3.2. Core saturation

After the core was potted in epoxy and passed the leak test, it is ready to determine its pore volume (PV) by both the mass method and the volume method. The pore volume (PV) of the core was estimated by the volume of brine that was imbibed into a vacuumed core. PV is defined as the total volume of the pores in a rock or, equivalently, the aqueous volume when the core is 100% saturated with brine (Lee, 2015). The dry core was first vacuumed with a vacuum pump for at 2-3 hours at minimum and then it is weighed and recorded to obtain its initial mass.

An initial volume (Vi) of waterflood brine was recorded in a graduated cylinder. The core inlet was connected to the graduated cylinder and the waterflood brine was allowed to be imbibed into the vacuumed core. When no change in volume of the graduated cylinder was observed, a final volume (Vf) was recorded and the core is weighed to record the final mass.

PV calculation based on mass was calculated by equation 3.3.:

$$PV = \frac{M_{final} - M_{initial}}{\rho_{brine}} - V_{dead} \quad (3.3)$$

where PV is pore volume of the core in ml; M_{final} and $M_{initial}$ are final mass and initial mass in grams respectively; ρ_{brine} is brine density in grams/cm^3, and Vdead is the dead volume in ml and

assumed to be 2 ml. V_{dead} is the total volume (~2 ml) of the fluid inside the nylon tubings (~1 ml; capacity ~0.03 ml/in) which connect the valves with the end-taps on the inlet, outlet, and the core face; and inside the end-taps (~1 ml; capacity ~0.85 ml/in) of the inlet and outlet.

PV is also calculated by the volume method using equation 3.4:

$$PV = V_{initial} - V_{final} - V_{dead} \quad (3.4)$$

where $V_{initial}$ and V_{final} are initial volume and final volume (ml), respectively.

PV determination with the mass method and volume method is used to estimate porosity. Porosity(ϕ) is defined as the ratio of the pore volume to the bulk volume (V_b) of the rock

$$\phi = \frac{PV}{V_b} \quad (3.5)$$

It should be noted that the value of the pore volume, PV obtained from the mass method and volume method is only an estimate and it should be confirmed and verified by conducting salinity tracer test which will be discussed in the following section.

3.5.3.3. Salinity tracer test

After saturating the core with brine and then injecting a few PVs of that high salinity brine, a salinity tracer test was performed to determine the heterogeneity of the core and to measure the aqueous pore volume. The salinity tracer test was conducted by injecting a lower salinity fluid (e.g. 1000 ppm NaCl aqueous solution) at 5 ml/min to displace the higher salinity fluid (5000ppm NaCl aqueous solution) until the effluent concentration is observed to have the same salinity as the injected brine. In this work, effluent samples were collected in volumes of 6 ml/tube.

By using a refractometer, the refractive index (salinity index) of each effluent was read and then normalized by using the initial and final salinity index. Initial salinity index is the salinity index at the beginning of the tracer test, while final salinity index is the salinity index at the end of the tracer test. The salinity index is referred to as the refractive index (RI).

The refractive index (RI) values were read from the refractometer were normalized in Equation 3.6 as

$$RI_{normalized} = \frac{RI_{effluent} - RI_{minimum}}{RI_{maximum} - RI_{minimum}} \quad (3.6)$$

For example, if the effluent refractive index shows 40 ppt, the initial refractive index shows 47 ppt, and the final refractive index shows 16 ppt, then the normalized refractive or salinity index is 0.23

The normalized salinity was plotted against the effluent volume. A typical salinity tracer test plot is shown in Figure 3.12. Aqueous volume is the summation of the area above the curve which is a determination based on the mass balance. Since the horizontal axis (x) is in ml, and the vertical axis (y) is normalized dimensionless value, the product of the x and y gives a volume.

Figure 3.12 shows the tracer test of a core. The tracer test in the core is going from low salinity brine to high salinity brine. The PV of the core is then calculated as the area above the curve

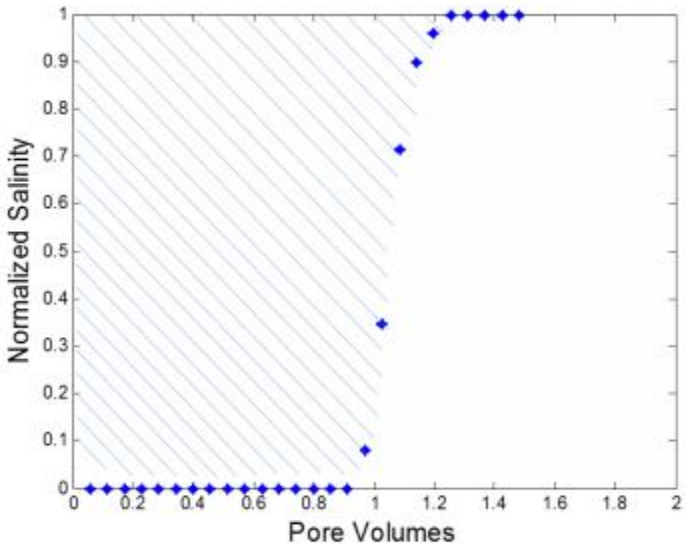

Figure 3.12: Sample tracer test of a core ((Jin, 2019)

Since Benthemier cores are usually relatively homogeneous, a sharp salinity gradient was observed. The displacement of the brine was stable, and the volume of the displaced brine was considered equal to the total core PV. This PV is compared to the PV estimated during the saturation of the core, and the porosity of the core was confirmed and verified.

3.5.3.4. Brine permeability of the core

Waterflood brine (. 5000 ppm NaCl) was used to measure single phase brine permeability. Brine was injected into the core at different flow rates and the pressure drop was recorded. Permeabilities were calculated from the pressure gradients and flow rates at steady state. The average of these permeabilities was used and considered the brine permeability. The brine permeability was calculated from Darcy's Law in Equation 3.7

$$k = \frac{\mu q L}{A \Delta P} \tag{3.7}$$

where k is the brine permeability, L is the core length, A is the core cross-sectional area, ΔP is the change in pressure, q is the volumetric flow rate, and μ is the fluid viscosity.

Figure 3.13 shows an example of a typical plot of different pressure values using different brine injection rates during a tracer test to determine permeability measurement

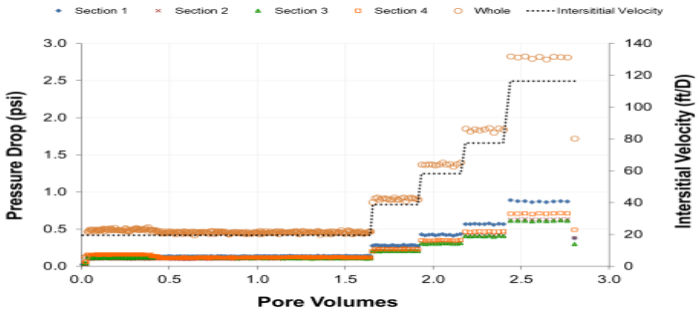

Figure 3.13: Pressure drop data using different brine injection rates during a tracer test to determine permeability measurement (Erincik, 2017)

3.5.3.5. Iron reduction in the core

The Bentheimer sandstones used in these experiments contain significant amounts of iron ions, which can degrade the silicate solution chemically. Ferric ions can crosslink silicate solution to form microgels, increase the retention of the silicate solution, prevent good transport, and degrade the silicate solution in the presence of oxygen. Therefore, it is a good practice to reduce the cores before injecting silicate solutions.

The following materials were used for the reduction step: deionized water, sodium chloride (NaCl), sodium bicarbonate ($NaHCO_3$), sodium dithionite ($Na_2S_2O_4$), tetrasodium EDTA (EDTA-Na^{4+}), 0.45μm Millipore filter paper, mineral oil, and Iron test strips. Core reduction is conducted to remove amorphous oxidized iron from the core.

In this research, the procedure explained by Lee (2015) was followed to reduce the core. The core was flooded with an aqueous solution of 4% $NaHCO_3$,1% EDTA-Na^{4+}, and 1% $Na_2S_2O_4$, at 23 ℃ and 0.5 ml/min (4.74 ft/D) to reduce the core and to remove amorphous oxidized iron from the core. Flooding was continued until the steady-state iron concentration reached 3 ppm. Once the effluent was measured to be below 3 ppm, the core was flushed with brine (4% $NaHCO_3$ + 1% $Na_2S_2O_4$) to clear the core of EDTA, and the iron concentration measured on the strip was 0 ppm.

3.5.4. Acetic acid (HAc) flood

After the core has been reduced of ferric ions, cleared of EDTA, and saturated with waterflood brine, the core can be flooded with acetic acid (HAc). The acetic acid (HAc) floods were prepared as previously described in section 3.2.3. Stock solutions were diluted to target concentrations and salinities. All solutions were filtered in the method previously mentioned and

degassed in argon for at least an hour. Solutions were transferred into the accumulator columns through a vacuum to prevent additional gasses from being trapped in the solution. This is performed by injecting the filtered acetic acid at a constant flow rate of 0.5 ml/min until steady-state pressure was observed for all four sections and effluents were collected in the fractional collector.

Once a steady-state was reached, the acetic acid (HAc) flood was continued for an additional 2 - 3 PVs. Tracer test measurements using the refractometer were carried out on the effluents to ensure that the core was fully saturated with the acetic acid flood.

3.5.5. Silica gel flood

All acetic acid (HAc) floods were followed by the silica gel flood. The silica gel floods were prepared as previously described in 3.2.4. Stock solutions were diluted to target concentrations. All solutions were filtered in the method previously mentioned and degassed in argon for at least an hour. Solutions were transferred into the accumulator columns through a vacuum to prevent additional gasses from being trapped in the solution. All solutions were injected at a constant flow rate and effluents were collected. Effluents were collected and analyzed similarly to the brine flood effluent samples.

The objectives of the silica gel flood were as follows

- Monitoring ΔP change and determine gelation time in core
- Monitoring ΔP in sections and determine gel location in the core
- Calculate permeability reduction using Darcy's law
- Test gel strength by continuously injecting fluid and monitoring ΔP after the gel is produced

3.6. HIGH-PRESSURE HIGH TEMPERATURE (HPHT) WITH CO_2 CORE FLOOD

In this section, the core flood experiments are conducted at High-Pressure High Temperature (HPHT) with CO_2 . The operating conditions are 1500 psi and 60℃ and 35,000 ppm salinity. Two sets of experiments are proposed. The first experiment is the initial pilot experiment run to investigate the gel's capability at sealing and permeability reduction whereas additional experiments will verify the results of the first experiment and perform sensitivity analysis.

3.6.1. Materials

The core used was a Benthemier sandstone. Cores used in these experiments were all 1.38 inches in diameter and 12 inches (1 ft) in length. The CO_2 dissolved is saturated with brine (30,000 ppm salinity).

Figure 3.14 a and b show stainless steel accumulators and core holders as well as Benthemier sandstone core wrapped with aluminium and Teflon respectively.

Figure 3.14. (a) stainless steel accumulators and core holders (b) Benthemier sandstone core wrapped with aluminium and Teflon.

The objectives include:

- Inject silicate solution into core and field remediation scenario
- Monitoring ΔP change and determine gelation time in core
- Monitoring ΔP in sections and determine gel location in the core
- Calculate permeability reduction using Darcy's law
- Test gel strength by continuously injecting fluid and monitoring ΔP after the gel is produced.

The core is fully saturated with CO_2 saturated brine. The injecting fluid for the gelation process is a silicate solution (Betol K28T). Cores were drilled out from the original Benthemier sandstone blocks and dried in a high-temperature oven (at least 90°C) for at least 36 hrs.

3.6.2. Core flood setup and schematic representation for the High-Pressure High Temperature (HPHT) with CO_2 core flood

The core is divided into four sections. The pressure tap on each section is linked to a 0-35 psi differential pressure transducer; the inlet and outlet of the core are linked to a 0-300 psi. differential pressure transducer. Additionally, the inlet and outlet of the core are linked to two 0-150 psi absolute pressure transducers. The linkage/connection between the pressure taps and the pressure transducers are the Swagelok® three-way valves and the tubing filled with water.

Using this hydraulic connection and a National Instruments LabViewTM data acquisition system software, the pressure drops for each section and the entire core are measured, recorded and displayed instantly on a computer. The core has an inlet where the fluid is injected into the core and an outlet where the displaced fluid is produced (effluent) and goes to a Teledyne Isco Retriever™ 500 fraction collector.

In case the air gets in the core accidentally, a back-pressure regulator (BPR) is connected to the outlet line to remove the air from the core by setting the BPR at 50 psi and injecting the brine at 50 psi.

Figures 3.15 a,b and c show the schematic representation and a pictorial view of the core flood apparatus set up in the high-temperature high-pressure condition (CO_2 core flood).

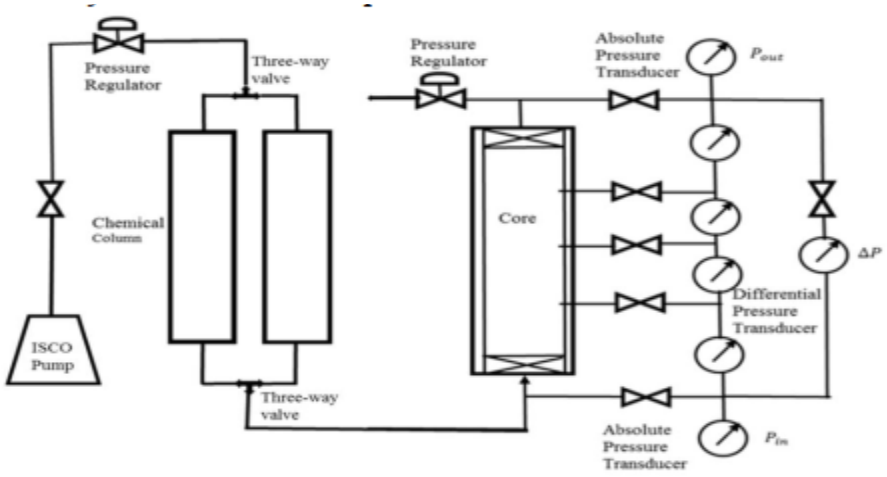

Figure 3.15. Schematic view of the CO_2 core flood

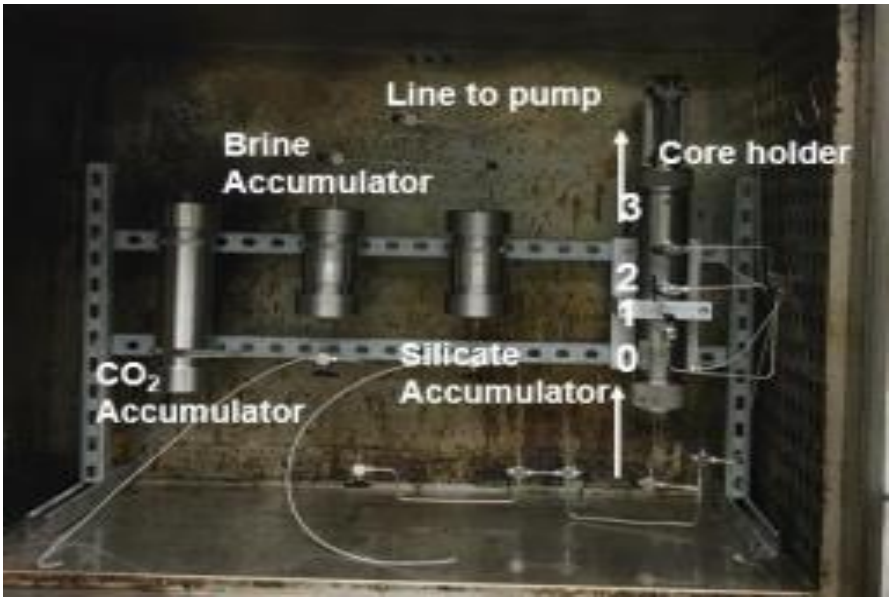

Figure 3.16. Core holder and accumulators in the oven

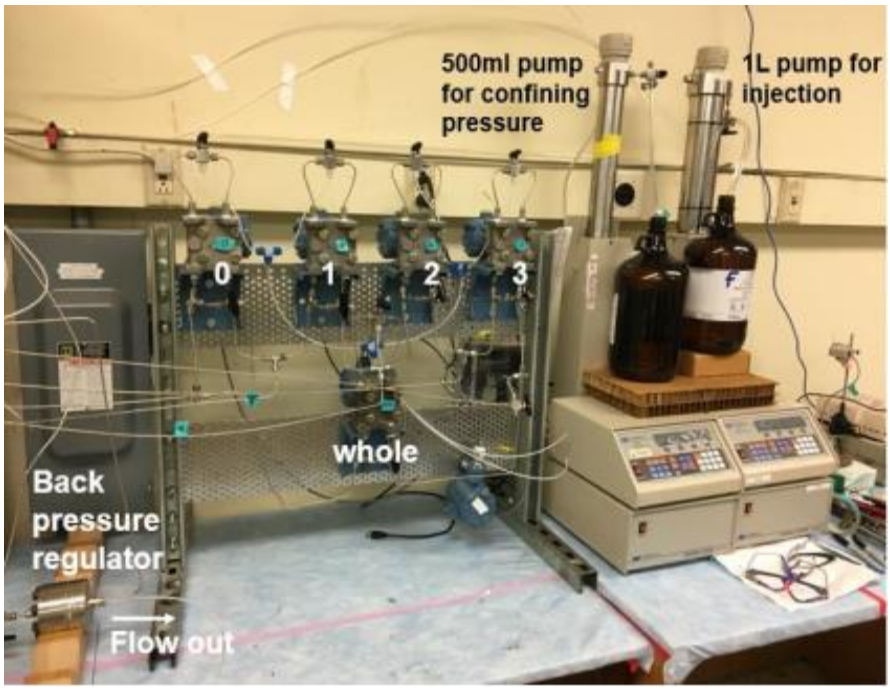

Figure 3.17. Pressure transducers, pumps, and backpressure regulator

3.6.3. Core preparation and experimental procedures

Here, the procedures for the HPHT with CO_2 core flood experiments such as the steps for core preparation and silicate solution injection are discussed.

3.6.3.1. Core Preparation

Materials used for core preparation include a core, aluminium foil, Teflon wrap, pressure taps, stainless steel piston accumulators, titanium core holder purchased from, Swagelok® metal fitting connectors, metal tubings, thread seal tape, CO_2 liquid tank, pressure gauges, back pressure regulator (BPR) and three-way valves were used.

The equipment used here includes a drill, drill bits, air system, and a water tub used for leaking test.

The core preparation procedure is described as follows:

i. The Benthemier sandstone cores were taken from the oven after being dried and left to cool to room temperature.

ii. The dimensions (length and mass) of the core were measured. The diameter was measured from three different spots and recorded bulk volume (V_B) of the core was determined using equation 3.8 and the average of the three measurements.

$$V_B = hA = h\pi\frac{D^2}{4} \quad (3.8)$$

where h is the core height, A is the area, and D is the diameter of the core.

iii. Weigh the core and calculate the bulk density of the core using equation 3.9

$$\rho_B = \frac{m}{V_B} \quad (3.9)$$

where ρ_B is the density of the core, and m is the mass of the core.

iv. The core is wrapped with heat-shrink Teflon tubing from Geophysical Supply Company that is 2 inches in diameter. The Teflon tubing is shrunk on the core using a Steinel HL 1810 S professional heat gun or kept in the oven at 100℃ for 48hrs.

v. Three layers of aluminium foil are then wrapped on the Teflon layer. The second layer of Teflon is then shrunk on the aluminium foil layers. The inner layer of Teflon acts as a water barrier to prevent brine from damaging the layers of aluminium foil. The four layers of aluminium foil act as a CO_2 barrier to prevent it from damaging the rubber sleeve inside the core holder. The outer Teflon layer holds the aluminium foil layers in place and acts as a physical barrier to prevent them from being damaged while the core is inserted into the core holder.

vi. The experimental fluids including sodium chloride brine, Silica gel solution, and liquid CO_2 are kept in stainless steel piston accumulators manufactured by Phoenix Instruments.

vii. The Teflon-aluminum wrapped core is inserted into the core holder and secured from both ends. A drill is used to drill through the Teflon and aluminium layers through each pressure tap. This allows pressure communication at the pressure tap locations so pressure drops can be measured. Then De-ionized water is used to apply a confining pressure of 10.34 megapascals (1,500 psi).

Figure 3.19 shows the core cross-section of the core holder after applying confining pressure

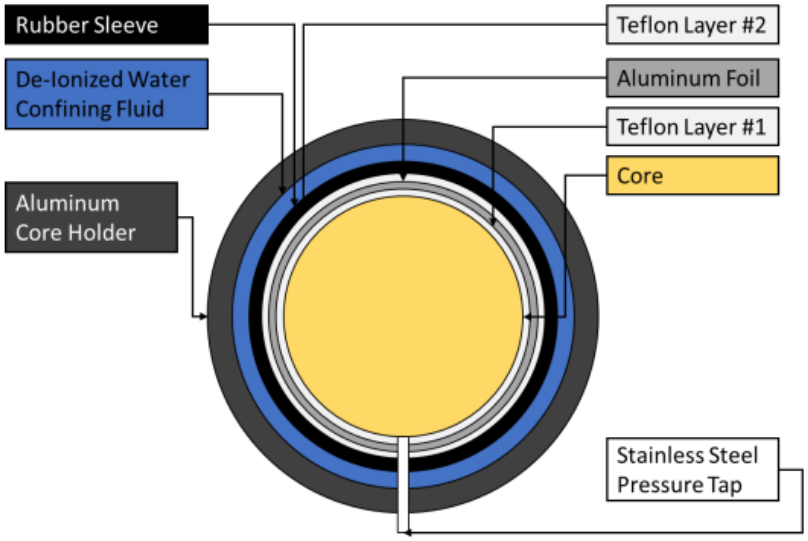

Figure 3.19: Core cross-section after applying confining pressure (Alfakher, 2019)

viii. The core is then connected to the tubing lines needed for the experiment. Each transducer has two ports and reads the difference in pressure between these two ports. Note that each pressure tap is shared by two transducers.

ix. The core is vacuumed to -29 inches of Mercury for 3 hours.

3.6.3.2. Core saturation

This follows the same procedure used in the ambient core flood as described in 3.5.3.2. However, the Brine is pumped to the vacuumed core until it is saturated and is at experimental pressure of 1,500 psi.

3.6.3.3. Salinity tracer test

This follows the same procedure used in the ambient core flood as described in 3.5.3.3. However, the salinity tracer test is conducted by injecting a lower salinity fluid (e.g. 10000 ppm NaCl aqueous solution) at 5 ml/min to displace the higher salinity fluid (50000ppm NaCl aqueous solution) until the effluent concentration is observed to have the same salinity as the injected brine.

3.6.3.4. Brine permeability of the core

This follows the same procedure used in the ambient core flood as described in 3.5.3.4. However, Waterflood brine (i.e. 50000 ppm NaCl) instead of 5000ppm NaCl was used to measure single phase brine permeability.

3.6.4. CO_2 flood

The experimental procedures for the CO_2 flood is given as follows;

i. The stainless accumulator is filled with 35,000 ppm brine and pressurized to 1500 psi
ii. Connect the CO_2 tank line to the low salinity brine accumulator and perform a withdrawal scenario with the pump which allows the CO_2 to slowly "bubble' (or breakthrough) into the brine, thus forming the CO_2 saturated brine needed for the HPHT experiment.
iii. The first CO_2 -saturated brine flood is then conducted to acquire a baseline. Liquid CO_2 -saturated brine is pumped to the core to displace high salinity brine from the tracer test.

iv. After the CO_2 -saturated brine flood is complete, CO_2 is vented out of the core until it is completely depressurized. The outlet is then closed, and the core is pressurized to experimental pressure.

v. Pressure drops are recorded, and permeability is measured.

vi. A second CO_2 -saturated brine flood is then conducted and compared to the previous flood to show repeatability.

3.6.5. Silica gel flood

All CO_2 -saturated brine floods were followed by the silica gel flood. The silica gel floods were prepared as previously described in 3.2.4. Stock solutions were diluted to target concentrations. All solutions were filtered in the method previously mentioned and degassed in argon for at least an hour. Solutions were transferred into the accumulator columns through a vacuum to prevent additional gasses from being trapped in the solution. All solutions were injected at a constant flow rate and effluents were collected. Effluents were collected and analyzed similarly to the brine flood effluent samples.

The objectives of the silica gel flood were as follows

- Monitoring ΔP change and determine gelation time in core
- Monitoring ΔP in sections and determine gel location in the core
- Calculate permeability reduction using Darcy's law
- Test gel strength by continuously injecting fluid and monitoring ΔP after the gel is produced

Chapter 4: Results and Discussion

4.1. INTRODUCTION

In this chapter, the results and analysis of the batch gelation experiments, and core flood experiments are discussed. From the core flood experiments, it is shown that using potassium silicate reagents (Betol K28T) to form a silica gel barrier is an applicable strategy for mitigating the risk of CO_2 leakage Reduction in the core permeability (up to 90%) of the Benthemier sandstone core was observed during the core flood experiments.

The main aim of this thesis is to evaluate the potential of conformance control agents such as silica gel as leakage prevention and remediation measure to improve carbon dioxide(CO_2) capture and sequestration. The objectives of conducting the core flood experiments are to predict and understand the reactive transport of silicate gel in porous media, compare the results obtained from gelation in porous media to the gelation results from the earlier bulk experiments, and finally investigate the capability of the gel for permeability reduction and sealing of the core within small- and medium-scale porous media under reservoir conditions. These core flood experiments are conducted under two conditions: ambient with an acetic acid solution as a CO_2 substitute and the high-pressure high-temperature condition with CO_2 saturated brine.

4.2. BULK GELATION EXPERIMENTS

In the bulk gelation phase, the gelation process of the silicate solution was inspected. The gel time at different silicate content, acid type, acid content, salinity and temperature were measured and analysed. Acetic (HAc) and hydrochloric (HCl) acid were used as two different gelation initiators. The purpose of this phase is to determine and quantify how the gelation process is affected by weak (HAc) and strong (HCl) acid solutions.

4.2.1. Gelation activated by acetic acid (HAC)

The mother solution used in these experiments is Betol K28T diluted with deionized water (50wt%). Following the methodology of Tognonvi (2009), we tested several mixtures of diluted Betol K28T and acetic acid (1M) with varying salinities and at different temperatures.

Figure.4.1 shows the change of the gel system from clear fluid to white gel during the gelation process. From left to right: a clear fluid; cloudy fluid; solid gel; expelled water separated from the solid gel. After the gel is formed, water is slowly expelled from the gel phase.

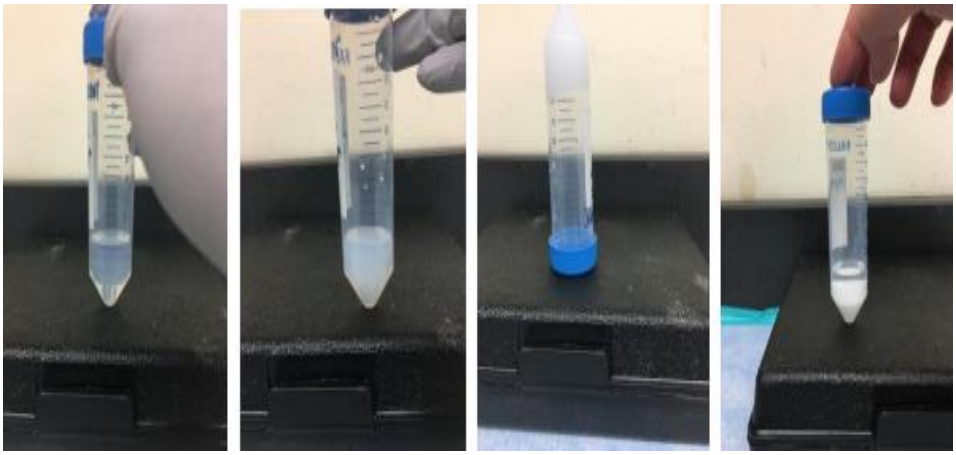

Figure 4.1. Photos showing phase change of a gel system.

4.2.1.1. Effect of acid concentration

To investigate the effect of acid and silicate concentrations on the gelation process (i.e. gel time), precipitation was qualitatively observed at 40°C for various fractions of the diluted stock potassium silicate solution (6.12 wt.%, 8.11 wt.%, 10.1 wt.% and 12.1 wt.%) and acetic acid concentrations (0.6 wt.%, 0.7 wt.%, 0.8 wt.% and 0.9 wt.%).

Figure. 4.2 shows the plots for the gelation time versus acetic acid (HAc). The gelation times were measured at 40°C. The results clearly show a shorter gelation time with increasing acetic acid content regardless of the amount of silicate present.

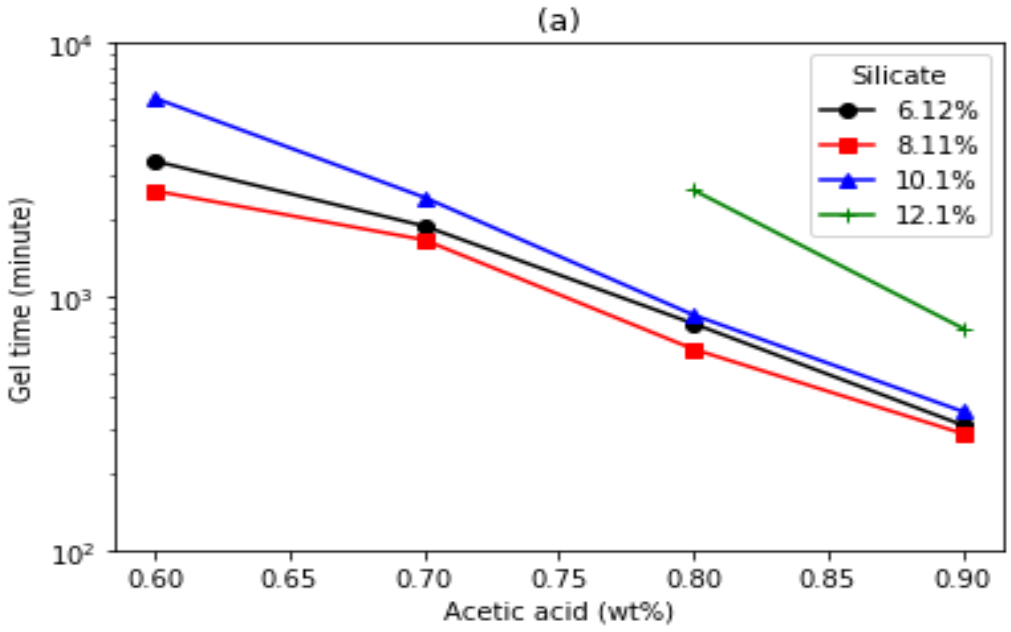

Figure 4.2: Gelation time vs acetic acid content at 1000 ppm salinity and silicate concentration from 6.12 to 12.1 wt%

4.2.1.2. Effect of silicate content

To investigate the effect of acid and silicate concentrations on the gelation process (i.e. gel time), precipitation was qualitatively observed at 40°C for various fractions of the diluted stock potassium silicate solution (6.12 wt.%, 8.11 wt.%, 10.1 wt.% and 12.1 wt.%) and acetic acid concentrations (0.6 wt.%, 0.7 wt.%, 0.8 wt.% and 0.9 wt.%).

Figure. 4.3 shows the plot of gelation time against silicate content. The gelation time decreases then increases with more silicate in the solution.

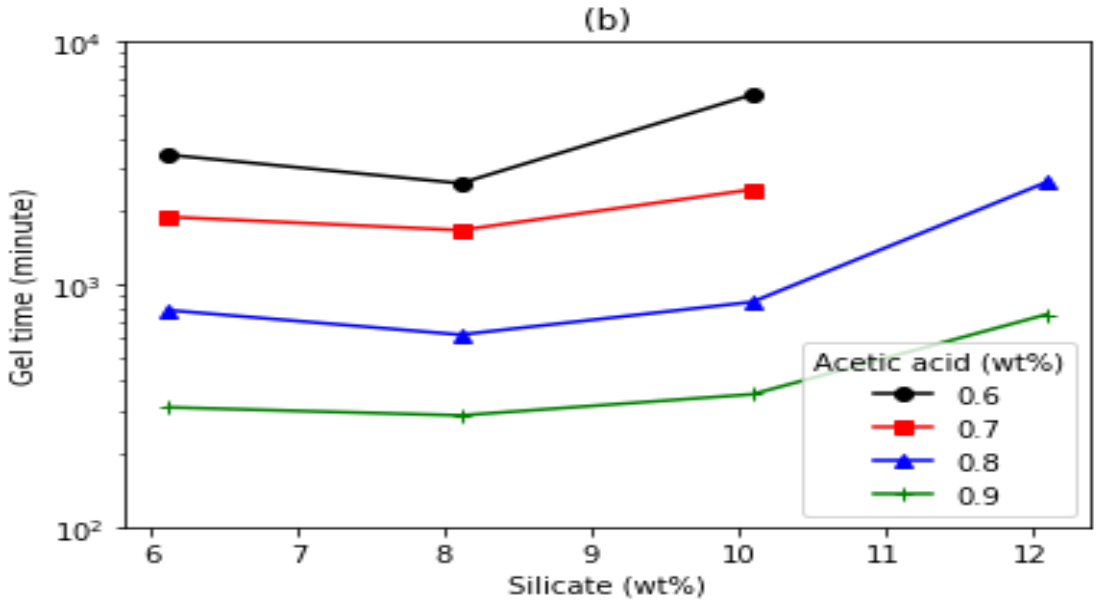

Figure 4.3: Gelation time vs silicate solution content at 1000 ppm salinity and acetic concentrations from 0.6 to 0.9 wt.%

4.2.1.3. Effect of salinity

To investigate the effect of salinity on the gelation process (i.e. gel time), precipitation was qualitatively observed using a constant silicate content of 8.64 wt.% and acetic acid (HAc) content of 0.94 wt.%. at varying salinities (500, 1000, 2500 and 5000 ppm respectively).

The gelation time is shorter at higher salinity. This can be explained by DLVO theory which gives the classical explanation of the stability of colloids in suspension that high salinity leads to stronger electrostatic attraction around silicate particles. Therefore, the silicate particles are more likely to come together and form a gel phase.

Figure. 4.4a shows the effect of salinity at different gelation temperatures.

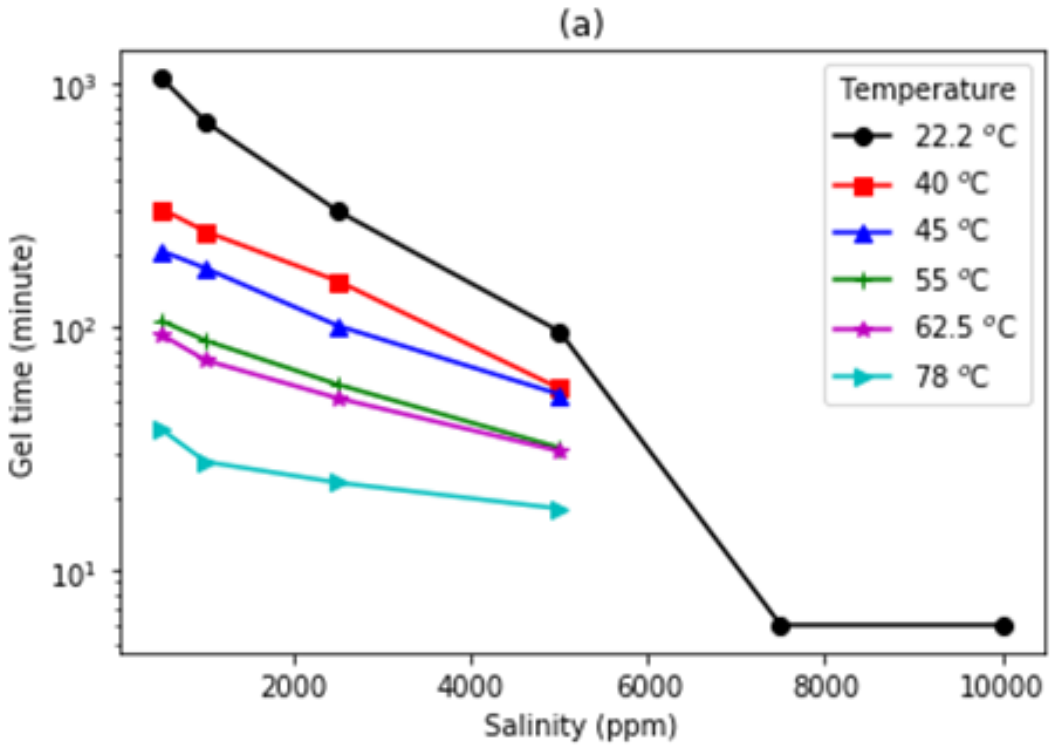

Figure 4.4a: Gelation time vs salinity at a silicate content of 8.64 wt.% and HAc content of 0.94 wt.%

4.2.1.4. Effect of temperature

To investigate the effect of temperature on the gelation process (i.e. gel time), precipitation was qualitatively observed using a constant silicate content of 8.64 wt.% and acetic acid (HAc) content of 0.94 wt.%. at varying temperatures (22.2°C, 40°C, 45°C, 55°C, 62.5°C, and 78°C respectively).

Figure 4.4 b shows the plot of gelation time against temperature at constant silicate content of 8.64 wt.% and HAc content of 0.94 wt.%. The graph shows a linear relationship in a semi-log plot, showing that the gel reaction follows an Arrhenius law.

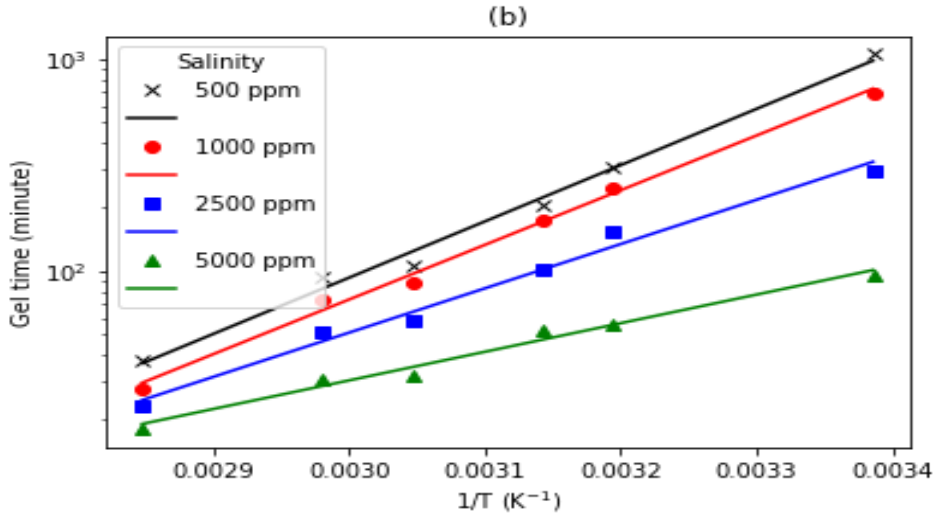

Figure. 4.4 b: The plot of gelation time against temperature at constant silicate content of 8.64 wt.% and HAc content of 0.94 wt.%

4.2.2. Gelation activated by hydrochloric acid (HCl)

The mother solution used in these experiments is Betol K28T diluted with deionized water (50wt%). Following the methodology of Tognonvi (2009), we tested several mixtures of diluted Betol K28T and hydrochloric acid (1M) with varying salinities and at different temperatures. Figure 4.5 shows the morphology of the samples at HCl from 0.6 to 1.0 wt.%. The silicate concentration is fixed at 8.11 wt.%

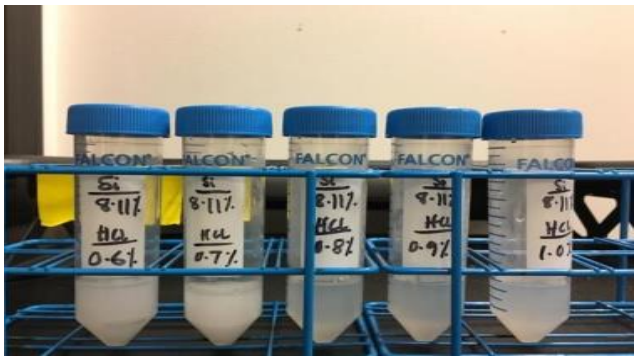

Figure 4.5: A photo showing the morphology of the samples at HCl from 0.6 to 1.0 wt.%.

4.2.2.1. Effect of acid and silicate solution concentration

The samples in this set of experiments have HCl from 0.6 to 1 wt.%, zero salinity and silicate from 6.12 to 12.1 wt.%. The gelation time was measured at 40°C.

The plot of gelation time vs. HCl (Figure. 4.6) is more complicated compared to the experiments conducted in acetic acid. At high silicate content (10.1 wt.% and 12.1 wt.%), the gelation time is longer with higher HCl concentration. However, at low K-silicate content (6.12 wt.% and 8.11 wt.%) the gelation time first decreases then increase with HCl.

Figure 4.6 shows the plot of gelation time against HCl concentration at different silicate content.

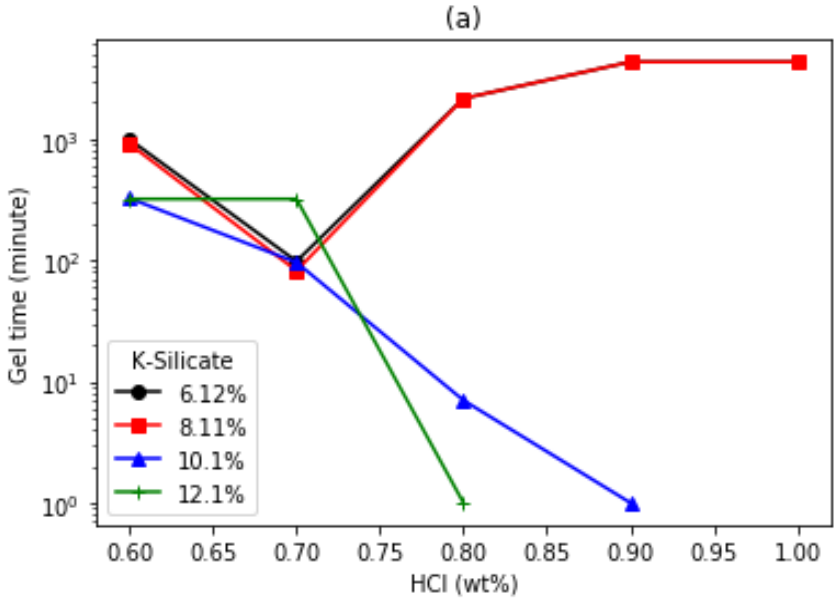

Figure 4.6: Gelation time vs. HCl concentration at different silicate content.

The gelation behaviour at low silicate content can be explained from the gelation mechanism. During the gelation process, the silicate first forms oligomers. The oligomers then aggregate and form covalent bonds to produce a 3D, gel-network. At low acid concentration, the

oligomers are mostly negatively charged on the surface. The negative charge is contributed by the Si-O group. With the increase of acid content (more H+), some of the negative-charge sites are neutralized and become Si-OH which results in less repulsive force between oligomers and faster gelation process (shorter gelation time).

When the acid content is high enough, all the Si-O- group on the oligomer surface will be neutralized. The gelation should have the fastest kinetics at this point. Further increase of acid content can produce Si-OH2+ group and flip the surface charge of oligomers from negative to positive. The oligomers become repulsive again beyond this point so slower gelation process was observed.

Since HCl is a much stronger acid than HAc, it can alter the surface charge of silicate oligomers at high enough concentration (about 0.7wt.% for 6.12 and 8.11 wt.% silicate content in these experiments). As the HCl concentration increases, the gel changes from white and opaque to transparent, indicating a transition of gelation mechanism from negative-charged aggregation to positive-charged aggregation as explained above.

4.2.2.2. Effect of salinity

The effect of salinity on gelation time in an HCl environment was also measured for constant silicate concentration 8.11 wt.% and HCl concentration 0.7% (Figure. 4.7). Gelation time increases then decrease with increasing salinity. As discussed in section 4.2.1.1, the chosen silicate and HCl composition may lead to positive-charged oligomers.

Some mechanism for the explanations of the observation in Figure 4.7 includes hydration effect and steric effect of the silicate-oxyl group (Gorrepati et al., Lagmuir 2010). However, the silicate gelation kinetics is still not fully understood and there is no clear explanation so far.

Figure 4.7 shows a plot of the gelation time against salinity in HCl environment. The chosen silicate content is 8.11 wt.% and HCl content is 0.7 wt.%.

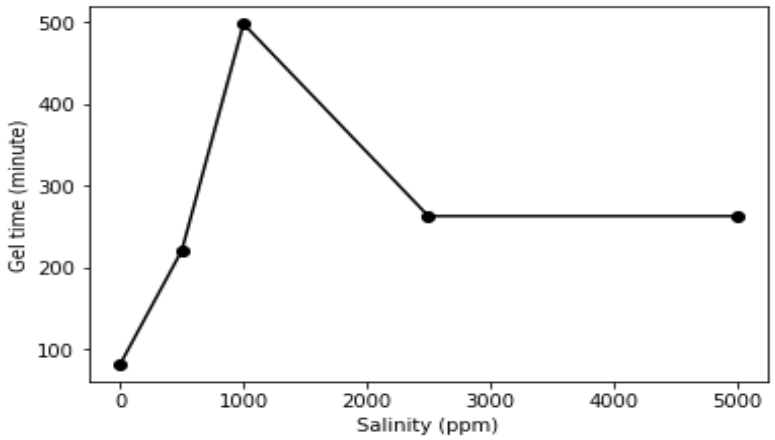

Figure 4.7: Gelation time vs. salinity in HCl environment. The chosen silicate content is 8.11 wt.% and HCl content is 0.7 wt.%.

4.2.2.3. Effect of temperature

Figure.4.8 shows a linear relationship in a semi-log plot of gelation time vs. 1/T for selected K-silicate and HCl concentration. The indication is that the gelation kinetics follows Arrhenius law.

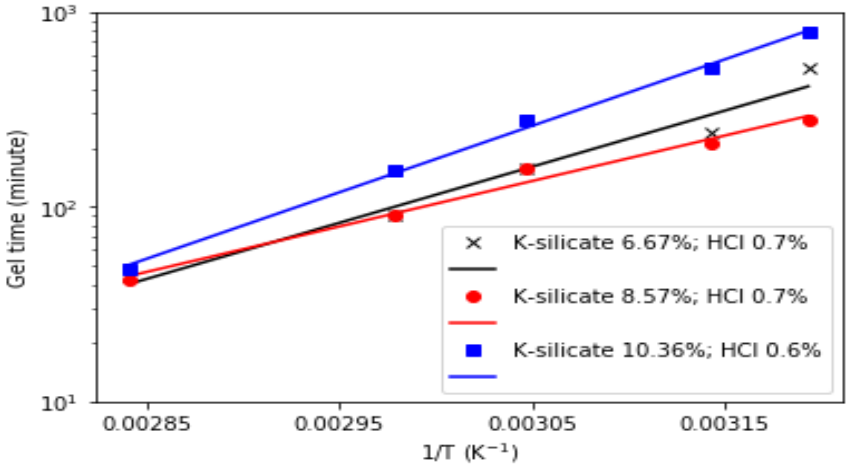

Figure 4.8: Gelation time vs. temperature in HCl environment for 3 samples with different silicate and HCl content. The experiments were conducted at 40 to 78.8 °C.

4.2.3. Gel model

A gel model was proposed by Stavland et al. (2011) to predict gelation time with given silicate content, acid concentration, salinity, and temperature. According to Stavland et al. (2011), the gelation time for our systems in HAc should have the following form:

$$\ln(t_{gel}) = M + a[\mathrm{Si}] + b[\mathrm{HAc}] + c[\mathrm{NaCl}] + E_a/RT \quad (4.1)$$

where t_{gel} is the gelation time in minutes, [Si], [HAc], [NaCl] are silicate, acetic acid and NaCl concentration in wt.%, T is the temperature in kelvin, M, a, b, c, and Ea are fitting parameters, and R=8.314 J·mol−1·K−1. In particular, Ea is the activation energy.

By fitting our data, we found M=-2.48, a=4.53, b=-903.22, c=-324.94 and Ea=42.6 kJ/mol for acetic acid.

4.2.4. Batch Gel time experiments at Higher Salinities and Acetic acid Concentrations

To mimic reservoir conditions and ensure accurate results, it is necessary to perform experiments near reservoir conditions of high salinity and a corresponding acetic acid(HAc) concentration that would match the CO_2 concentration in the reservoir.

Therefore, a new set of batch experiments were performed using higher salinities and acetic acid concentrations. The samples in this set of experiments have HAc from 0.001 to 1 wt%, 9 wt% silicate solution and salinity from 5000 to 50,000 ppm. The gelation time was measured at 60^0C.

The plot of gelation time vs. HAc shows that salinity has a major impact on the gelation time. The gelation time becomes shorter with increasing salinity. This can be explained by the classical DLVO theory. High salinity leads to stronger electrostatic attraction around silicate particles. Therefore, the silicate particles are more likely to come together and form a gel phase.

Figure 4.9 shows a plot of gel time against salinity at the various HAc concentrations while Figure 4.10 shows a plot of the gel time against HAc concentrations at various salinities

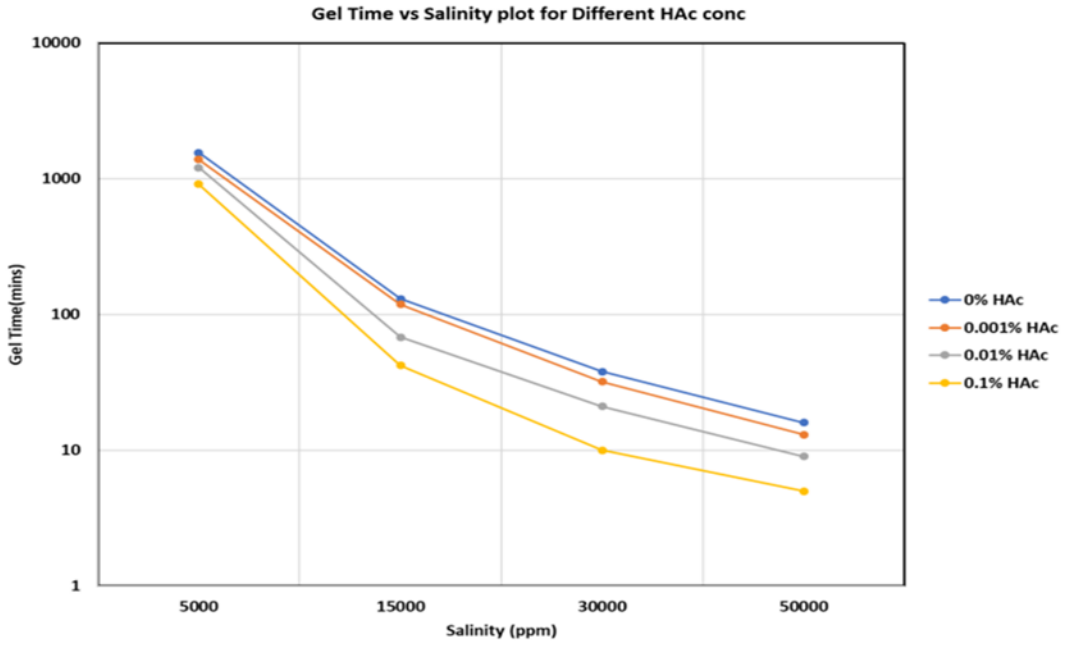

Figure 4.9: Gel time vs salinity at various HAc concentrations

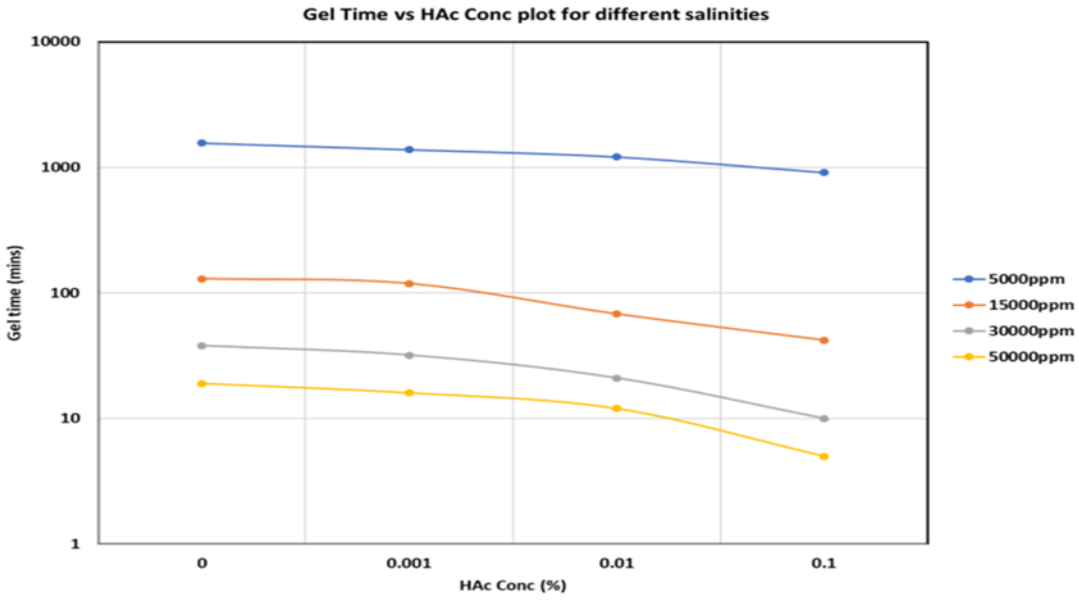

Figure 4.10: Gel time vs HAc concentrations at various salinities

4.2.5. Gelation activated by CO_2

To conduct the High-Pressure High Temperature (HPHT) with CO_2 , the results obtained from the bulk gelation experiments using acetic acid were used to determine the concentration of CO_2 that matches acetic acid (HAc) pH at a given concentration by matching the number of free hydrogen ions (H+).

4.2.5.1 pH conversion

The calculations for this pH conversion is shown as follows;

Acetic acid dissociates by the following chemical reaction,

$$\boldsymbol{HAc \rightleftarrows H^+ + Ac^-} \tag{4.2}$$

The equilibrium constant is given by

$$\boldsymbol{K_{HAc} = \frac{[H^+][Ac^-]}{[HAc]} = \frac{y_{HAc}c_{HAc} \cdot y_{HAc}c_{HAc}}{(1-y_{HAc})c_{HAc}} = \frac{y_{HAc}^2 c_{HAc}}{(1-y_{HAc})}} \tag{4.3}$$

where, [H+],[Ac-], and [HAc] are the molality (mol/Kg) of the respective species, c_{HAc} is the total acetic acid concentration/molality (associated and dissociated) in mol/Kg water, and y_{HAc} is the dissociation mole fraction.

Equation 4.3 can be written as a quadratic equation and solved for y_{HAc}.

$$y_{HAc} = \frac{-K_{HAc} + \sqrt{K_{HAc}^2 + 4K_{HAc}c_{HAc}}}{2c_{HAc}} \tag{4.4}$$

And the pH is the negative(-ve) logarithm of the H^+ concentration

$$p\mathrm{H} = -\log[\mathrm{H}^+] = -\log[\mathrm{y_{HAc}c_{HAc}}] = -\log\left(\frac{-\mathrm{K_{HAc}} + \sqrt{\mathrm{K_{HAc}^2 + 4K_{HAc}c_{HAc}}}}{2}\right) \tag{4.5}$$

For CO_2, it dissociates by the following chemical reaction,

$$\mathrm{CO_2 + H_20 \rightleftarrows H^+ + HCO_3^-} \tag{4.6}$$

The equilibrium constant, K_{CO_2} is given by

$$K_{CO_2} = \frac{[H^+][HCO_3^-]}{[CO_2]} = \frac{y_{CO_2} c_{CO_2} \cdot y_{CO_2} c_{CO_2}}{(1-y_{CO_2}) c_{CO_2}} = \frac{y_{CO_2}^2 c_{CO_2}}{(1-y_{CO_2})} \quad (4.7)$$

Where, $[H^+]$, $[HCO_3^-]$, and [HAc] are the molality (mol/Kg) of the respective species, c_{HAc} is the total acetic acid concentration/molality (associated and dissociated) in mol/Kg water, and y_{HAc} is the dissociation mole fraction.

Equation 4.3 can be written as a quadratic equation and solved for y_{HAc}.

$$y_{CO_2} = \frac{-K_{CO_2} + \sqrt{K_{CO_2}^2 + 4K_{CO_2} c_{CO_2}}}{2c_{CO_2}} \quad (4.8)$$

And the pH is the -logarithm of the H^+ concentration

$$pH = -\log[H^+] = -\log\left[y_{CO_2} c_{CO_2}\right] = -\log\left(\frac{-K_{CO_2} + \sqrt{K_{CO_2}^2 + 4K_{CO_2} c_{CO_2}}}{2}\right) \quad (4.9)$$

The objective is to determine the concentration of CO2 that would have the same pH (H^+ concentration) as an acetic acid solution,

$$[H^+] = y_{HAc} c_{HAc} = y_{CO_2} c_{CO_2} \quad (4.10)$$

From equations 4.3 and 4.7

$$\frac{K_{HAc}}{K_{CO_2}} = \frac{y_{HAc}^2 c_{HAc}}{(1-y_{HAc})} \frac{(1-y_{CO_2})}{y_{CO_2}^2 c_{CO_2}} = \frac{y_{HAc}}{(1-y_{HAc})} \frac{(1-y_{CO_2})}{y_{CO_2}} \quad (4.11)$$

Where the rightmost equality is only true for equivalent pH (4.10).

Solving for the mole fraction of CO2,

$$\frac{1}{y_{CO_2}} = \frac{K_{HAc}}{K_{CO_2}} \frac{(1-y_{HAc})}{y_{HAc}} + 1 \quad (4.12)$$

Finally, using 4.10 and 4.12, the concentration of CO_2 can be obtained.

$$c_{CO_2} = \frac{y_{HAc}}{y_{CO_2}} c_{HAc} = \left[\frac{K_{HAc}}{K_{CO_2}} \frac{(1-y_{HAc})}{y_{HAc}} + 1\right] y_{HAc} c_{HAc} \quad (4.13)$$

Where, K_{HAc} is 1.51×10^{-4} mol/kg at 60C and 8.71e-6 mol/kg at 20C and the equilibrium constant of CO2, K_{CO2}, is a function of temperature, pressure, and salinity and can be found from the mini-program: (https://doi.org/10.1016/j.chemgeo.2013.03.010).

Therefore, the mole fraction of acetic acid can be computed using the mini program above. For example, K_{CO2} =0.89 mol/Kg at 60C, 1500 psi and 15,000ppm salinity. The mole fraction of acetic acid, y_{Hac}, can be calculated using equation 4.4. Figure 4.11 shows the plot of the molality of HAC vs CO_2 at the same pH

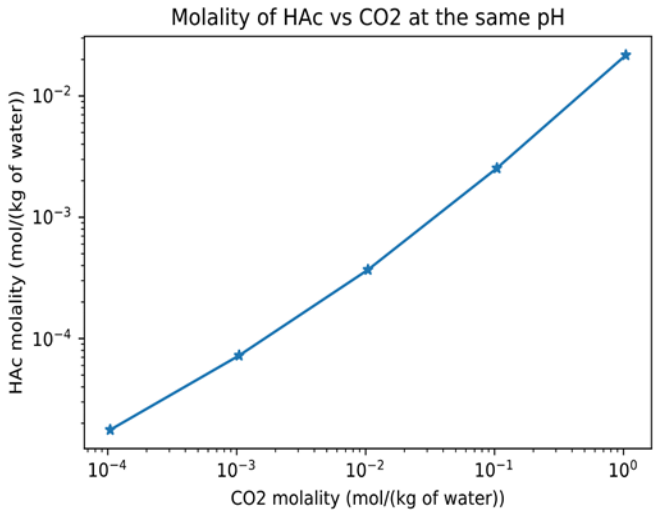

Figure 4.11: The molality of HAC vs CO_2 at the same pH

Table 4.1: A sample pH conversion table from HAc to CO_2 at 60C, 1500 psi and 15000ppm

T = 60 C, P = 1500 psi, Salinity 15,000 ppm

HAc (wt%)	0.001	0.01	0.1
mHAc (mol/Kg)	1.9e-4	1.86e-3	0.0186
pH	3.96	3.34	2.79
mCO2 (mol/Kg)	4.28e-3	0.073	0.889

4.2.5.2. Determination of silicate- CO_2 gelation time from the fitted empirical equation

The gelation time is determined using the correlation by Stavland (2011) and the coefficients were determined using acetic acid.

$$\ln t_{\text{gel}} = M + A \cdot c_{\text{Si}} + B \cdot c_{\text{HAc}} + C \cdot c_{\text{NaCl}} + \frac{E_a}{RT} \qquad 4.12$$

To use the equation for a CO2 system, the concentration of CO2 must be converted to acetic acid concentration,

$$c_{\text{HAc}} = y_{\text{CO}_2} \cdot c_{\text{CO}_2} \cdot \left[\frac{K_{\text{CO}_2}}{K_{\text{HAc}}}\left(\frac{1}{y_{\text{CO}_2}} - 1\right) + 1\right] \qquad (4.13)$$

where

$$y_{\text{CO}_2} = \frac{-K_{\text{CO}_2} + \sqrt{K_{\text{CO}_2}^2 + 4\,K_{\text{CO}_2}\,c_{\text{CO}_2}}}{2c_{\text{CO}_2}} \qquad (4.14)$$

4.2.6. Analysis of bulk gelation experiments

When the gelation was initiated by acetic acid, the results show that increasing acid content consistently accelerates the gelation kinetics (shorter gelation time) regardless of silicate content, while adding more silicate to the gelation system initially retards, then accelerates the gelation. Higher salinity in the system and higher temperature both lead to faster gelation time. Overall, the effects of silicate content, acid content, salinity, and temperature on the gelation kinetics in weak acid are as expected.

A literature model for gelation time prediction was adopted and the parameters were tuned to match the experimental results. The effect of acid content and salinity on gelation kinetics is much more complicated when a strong acid (HCl) was used as the initiator. In particular, more acid accelerates gelation at high silicate content. However, at low silicate content, increasing acid in the solution first accelerates then deaccelerates gelation. The effect of increasing salinity decreases gelation time at high salt concentration but slows down the kinetics at low salt

concentration. Based on the bulk gelation experiments, the acetic acid behaves similarly to CO_2 and is thus chosen as the substitute for CO_2 in the ambient phase core flood.

4.3. AMBIENT PHASE CORE FLOOD EXPERIMENT

Two sets of experiments were conducted at ambient conditions. The first experiment was the initial pilot experiment performed to investigate the gel's capability at sealing and permeability reduction whereas the second experiment was conducted to verify the results of the first experiment.

Ambient Phase Experiment 1

The ambient experiment was conducted using 1000 ppm salinity to understand the reaction transport of silicate gel in porous media, compare the results obtained from gelation in porous media to the gelation results from the earlier bulk experiments and finally, investigate the capability of the gel in permeability reduction and sealing of the core. Table 4.2 shows the core properties and fluid properties data for ambient phase experiment 1

Table 4.2. Core properties and Fluid properties data for Ambient phase experiment 1

Core Properties	Value
Core rock type	Benthemier Sandstone
Core length	1 ft
Core diameter	1.5 inch
Core pore volume	82 ml
Core porosity	23.68 %
Core permeability	1469 md

Fluid Properties	Value
Concentration of acetic acid	1 wt %
Concentration of brine	1000 ppm
Concentration of silicate solution	8.64 wt %
Viscosity of silicate solution	3 cp

Ambient Phase Experiment 2

In the second ambient experiment, all procedures from experiment 1 were repeated. However, it was conducted to determine the effect of higher salinity (that is, increasing the salinity

from 1000 ppm in experiment 1 to 2500 ppm) on gelation time, gel strength and also to verify the results obtained from the earlier experiment. Table 4.3 shows the core properties and fluid properties data for Ambient phase experiment 2

Table 4.3. Core Properties and Fluid Properties data for Ambient phase experiment 2

Core Properties	Value
Core rock type	Benthemier Sandstone
Core length	1 ft
Core diameter	1.5 inch
Core pore volume	83.13 ml
Core porosity	23.92%
Core permeability	2566 md

Fluid Properties	Value
Concentration of acetic acid	1 wt %
Concentration of brine (NaCl)	2500 ppm
Concentration of silicate solution	8.64 wt %
Viscosity of silicate solution	3 cp

4.3.1. Tracer, pore volume and permeability test results

Tracer tests were performed for both ambient phase experiments to measure the pore volume, porosity, and permeability of the core sample. The tracer test is done to measure the pore volume and determine the measured porosity of the core while the permeability test determines the measured permeability of the core. Results and plots from the tracer and permeability tests are shown below.

4.3.1.1. Ambient Phase Experiment 1

Figure 4.12 shows the tracer test plot for ambient experiment 1 whereas Figure 4.14 shows the sectional permeability measurement plot for ambient experiment 1

In Figure 4.13, a uniform pressure breakthrough is observed through the homogenous core. This was done to show the pressure trace in the sections of the core over 5 different flow rates.

Slightly different permeabilities were found in different sections of the core but all were linear as expected from Darcy's law.

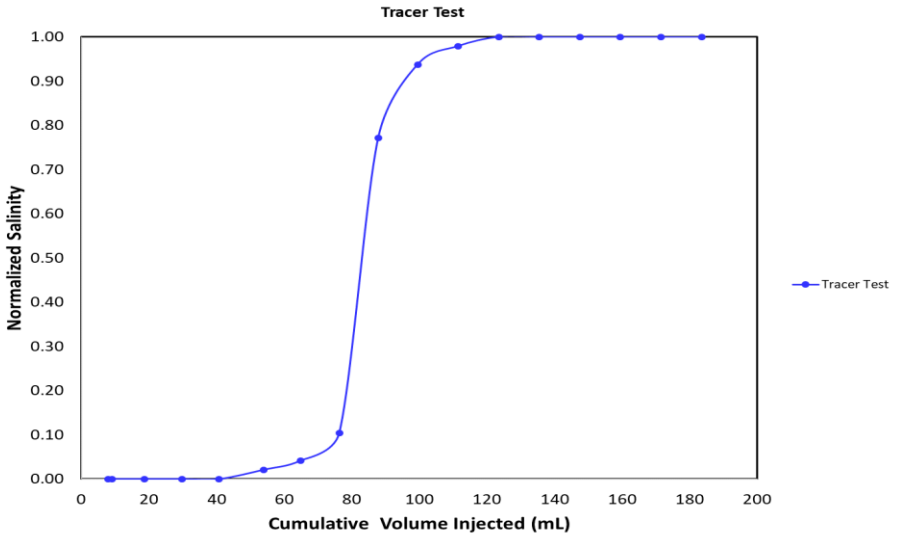

Figure 4.12. Tracer test plot for ambient experiment 1

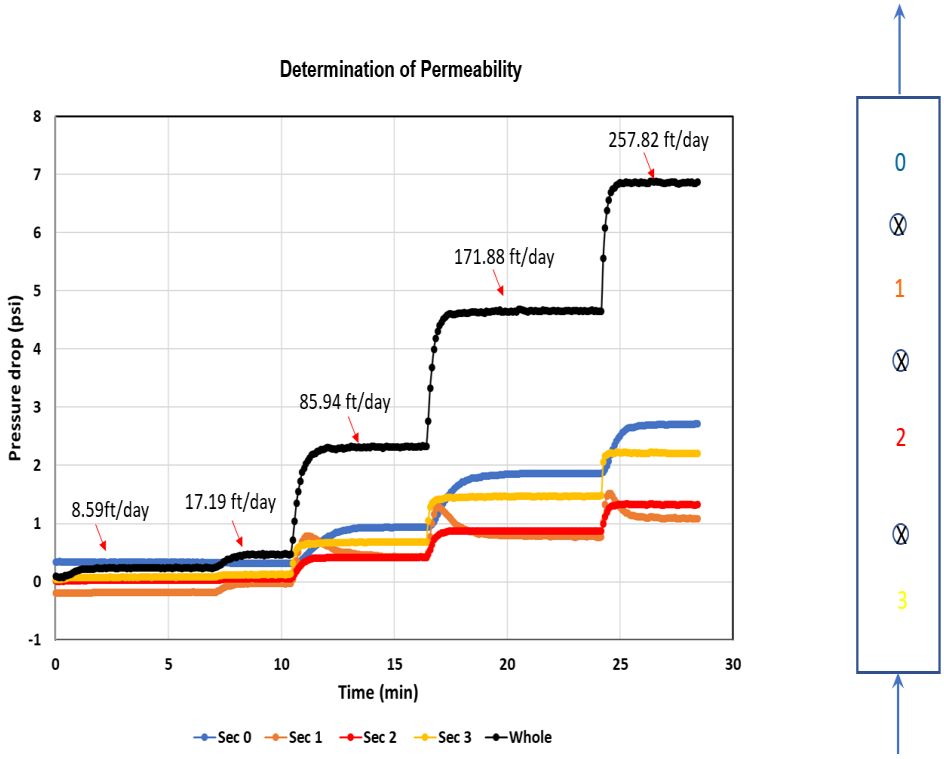

Figure 4.13. Sectional permeability measurement plot for ambient experiment 1

4.3.1.2. Ambient Phase Experiment 2

Figure 4.14 shows the tracer test plot for ambient experiment 1 whereas Figure 4.16 shows the sectional permeability measurement plot for ambient experiment 1

In Figure 4.15, a uniform pressure breakthrough is observed through the homogenous core. This was done to show the pressure trace in the sections of the core over 5 different flow rates. Slightly different permeabilities were found in different sections of the core but all were linear as expected from Darcy's law.

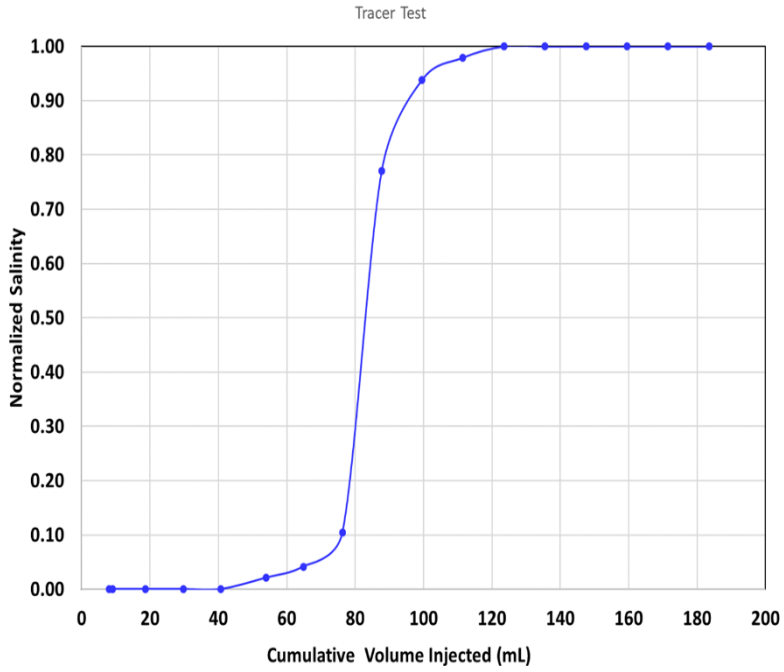

Figure 4.14. Tracer test plot for ambient experiment 2

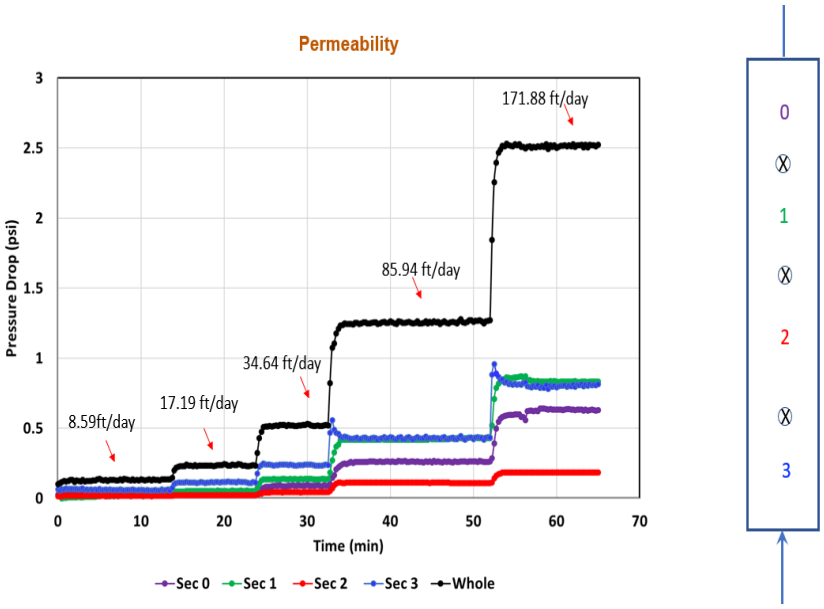

Figure 4.15. Sectional permeability measurement plot for ambient experiment 2

4.3.2. Pressure vs time/ pore volume injected plots

This discusses the plot of pressure drop against time or injected pore volume for the two ambient phase core floods.

4.3.2.1. Ambient Phase Experiment 1

For the ambient experiment 1, the Benthemier sandstone is initially saturated with 1wt% acetic acid and 1000 ppm brine. From the sectional permeability plot using brine of 0.95 cp and extrapolating for a 3 cp Newtonian fluid, it is determined that the reference pressure drop (ΔP) for 3 cp Newtonian fluid (silicate solution) is 0.075 psi.

Also, from earlier bulk gelation experiments, the gelation time duration is determined to be 12 hrs. The silicate residence time is estimated to be 24 hrs. The pressure build-up is expected to occur mostly at the bottom section.

An 8.64 wt.% silicate solution is initially injected (t=0) into the core at a 1 ft/day frontal velocity for 16 hrs.

Figure 4.16 shows the pressure drop against pore volume injected plot for the ambient phase experiment 1 within the initial 22 hrs

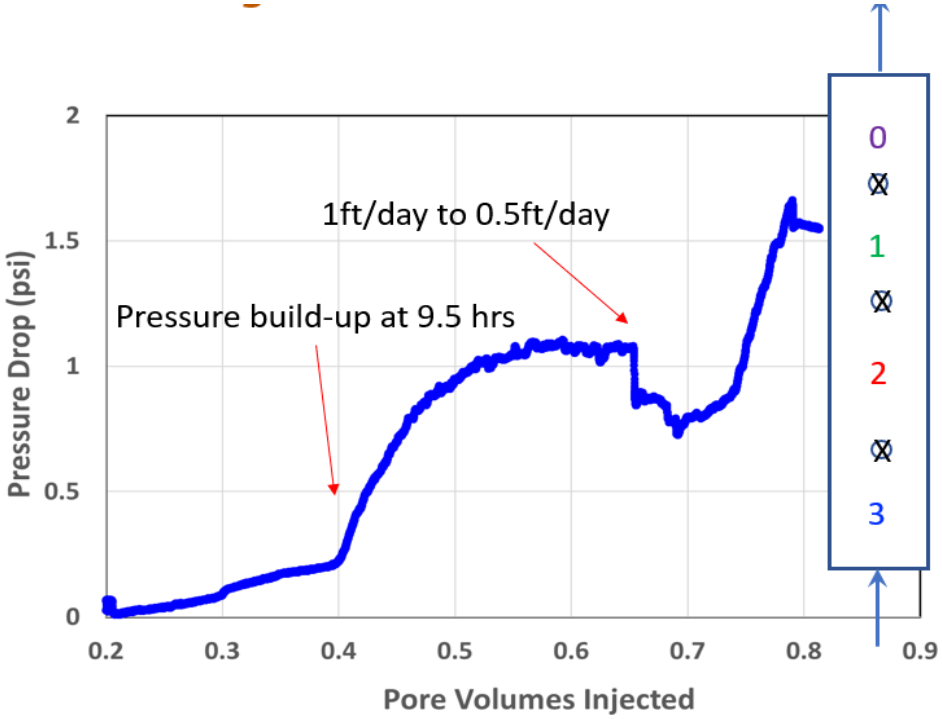

Figure 4.16. Pressure drop vs pore volume injected plot for Ambient phase experiment 1 within the initial 22 hrs.

A rapid and continuous increase in the pressure drop occurs after 0.4 PV of the silicate solution has been injected into the core within the initial 10 hrs. which is earlier than the 12 hrs predicted by the bulk gelation experiment. After 16 hrs., the frontal velocity was then reduced to 0.5 ft/day with a corresponding reference pressure drop of 0.038 psi to increase the silicate residence time for gelation. This increases the silicate residence time from 24 hrs to 32 hrs. However, the silicate breakthrough occurs at 22 hrs after the initial gelation (t=0). The maximum pressure drop observed after the initial 22 hrs is 1.55 psi and the experiment is then shut-in for 5 days.

After 5 days, more silicate was injected at varying frontal velocities of 0.5 and 1 ft/day to investigate the strength of the gel and its corresponding maximum pressure drop. The total injection time is 24 hours at a constant frontal velocity of 0.5 ft/day. The reference pressure drop at 0.5 ft/day is 0.038 psi. A total of 1.32PV was injected into the core and a pressure drop of 3.64 psi was observed before shut-in.

. Figure 4.17 shows a plot of the observed pressure drop versus the pore volume injected plot for the second silicate injection in the ambient experiment 1.

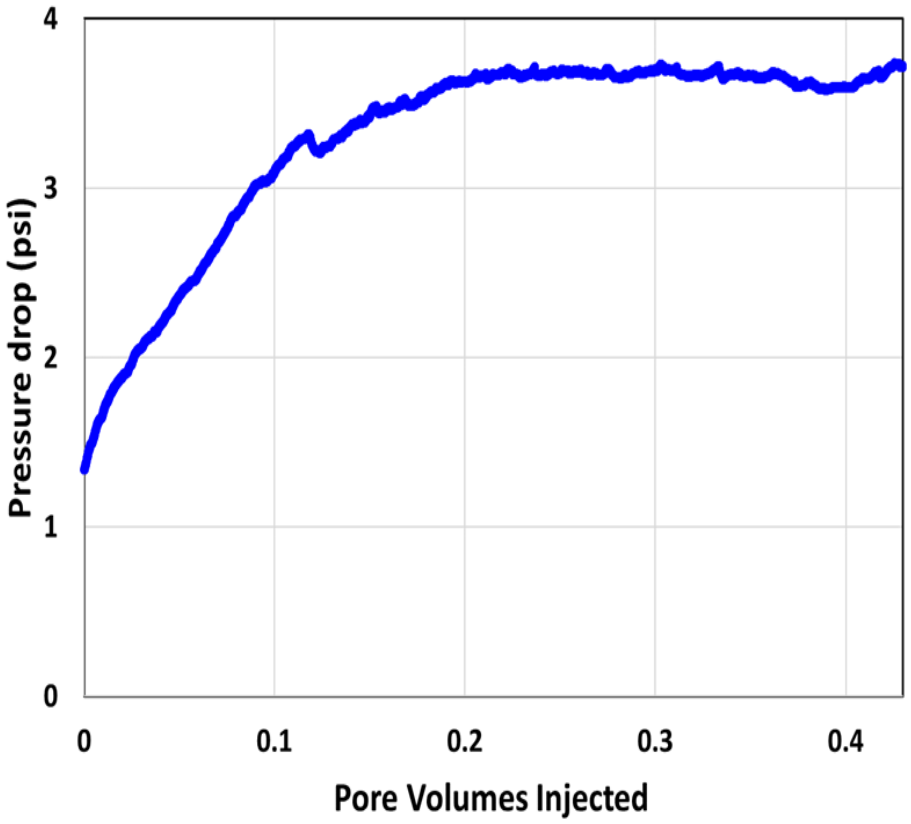

Figure 4.17: Pressure drop versus pore volume injected plot for the second silicate injection in the ambient experiment 1

4.3.2.2. Ambient Phase Experiment 2

For ambient experiment 2, the brine salinity was increased from 1000 ppm to 2500 ppm and the same steps in the ambient experiment 1 were repeated. For this given salinity, it is determined that the reference pressure drop (ΔP) for 3 cp Newtonian fluid (silicate solution) is 0.050 psi.

Also, from earlier bulk gelation experiments, the gelation time duration is determined to be between 5 to 6 hrs. The silicate residence time is estimated to be 12 hrs. The pressure build-up is expected to occur mostly at the bottom section. The total injection time is 14 hours at a constant frontal velocity of 0.5 ft/day. Also, a total pressure drop of 2.4 psi was observed before shut-in.

Figure 4.18 shows the pressure drop versus time plot for the second silicate injection in the ambient experiment 2

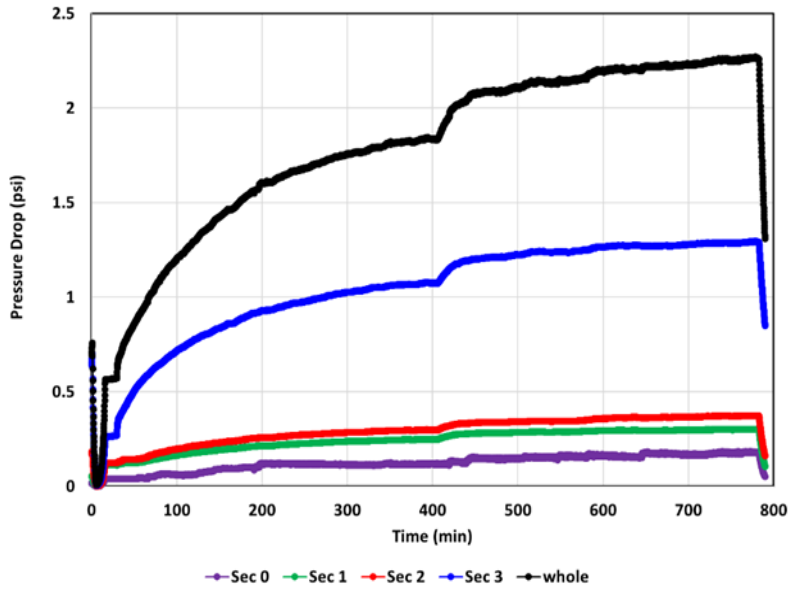

Figure 4.18: Pressure drop versus time plot for the second silicate injection in the ambient experiment 2

4.3.3. Permeability reduction plots

Experiments were conducted at standard temperature and pressure with acetic acid (acetic acid is used as a substitute for CO_2 at ambient conditions).

4.3.3.1. Key findings from the permeability reduction in the Ambient phase experiment 1

The following observations were made:

- Permeability reduction in the core by ~100 times.
- Delay of 0.4 PVs (9.5 hrs) before permeability reduction occurred but sooner than bulk (12 hrs).
- Permeability reduction mostly occurred in the first part of the core (i.e. section 3).
- Reduction in the latter part of the core in section 1 after multiple injections.
- Perm reduction continues as more pore volumes of silicate solution is injected.

Figure 4.19 shows the permeability reduction(K/Ki) plots for ambient phase experiment 1

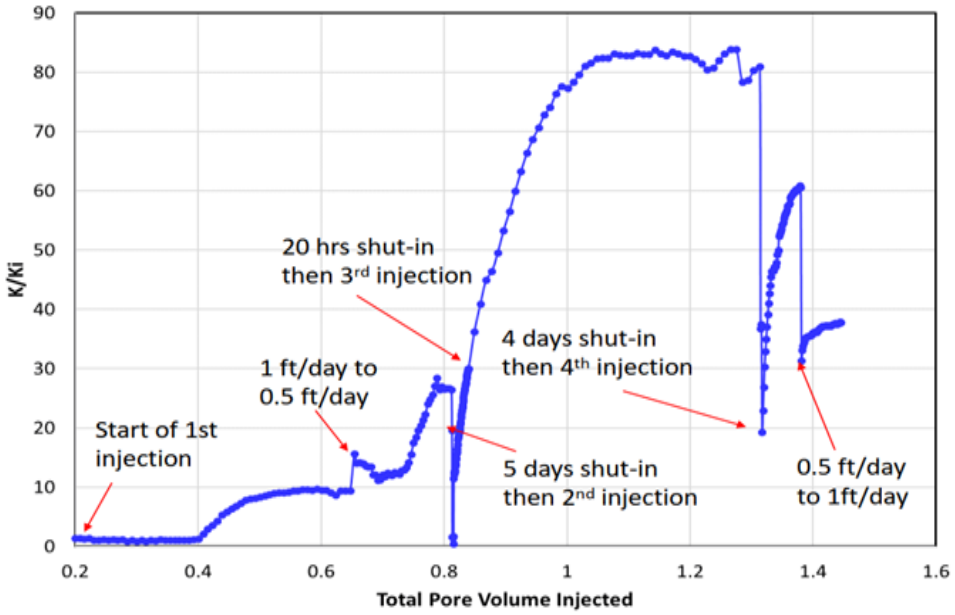

Figure 4.19: Permeability reduction(K/Ki) plots for ambient phase experiment 1

4.3.3.2. Key findings from the permeability reduction in the Ambient phase experiment 2

The following observations were made:

- Permeability reduction in the core by ~80 times.
- Permeability reduction mainly occurred in the first part of the core (i.e. section 3)
- Reduction in the latter part of the core (sections 0 -2) after multiple injections.
- Perm reduction continues as more pore volumes of silicate solution are injected.

Figure 4.20 shows the permeability reduction(K/Ki) plots for ambient phase experiment 2

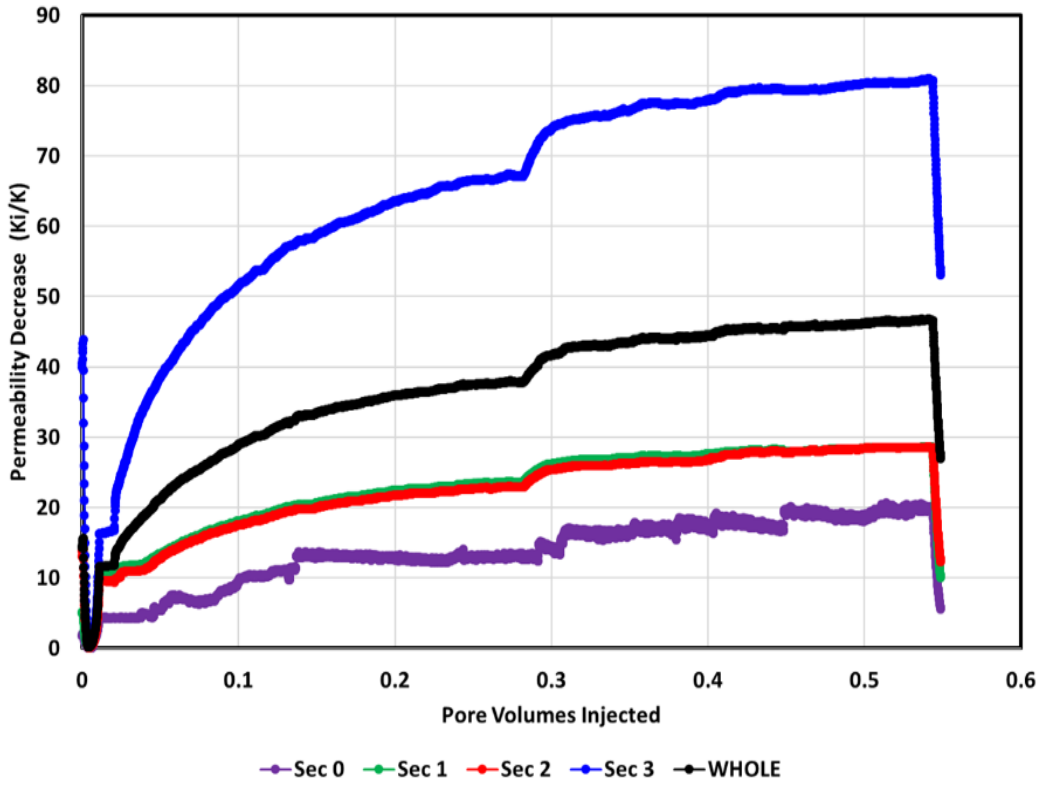

Figure 4.20: Permeability reduction(K/K_i) plots for ambient phase experiment 2

4.3.4. Analysis of ambient phase core flood experiment

In the ambient core flood, two sets of experiments were conducted. The first experiment was the initial pilot experiment run at a salinity of 1000 ppm to investigate the gel's capability at sealing and permeability reduction whereas the second experiment was conducted at a salinity of 2500 ppm.

The plots show that salinity has a major impact on the gelation times as the gelation time became shorter with increasing salinity. An 80 times reduction in the permeability of the core was found. Permeability reduction, however, occurred mostly in the first part of the core. The latter part of the core exhibited permeability reduction tendencies after multiple pore volume injections of silicate solution were performed. The core was also found to be permeable even after gel produced.

It was also observed that the total volume of fluid leaving the core at the end of the experiment was less than the total volume of fluid injected into the core at the state of the experiment. A possible explanation for this observation is the syneresis effect (shrinkage and water expulsion) found in silicate gel, which induces a potentially a time-dependent blocking effect. Therefore, some of the injected fluid could be lost to shrinkage and water expulsion.

4.4. HIGH-PRESSURE HIGH TEMPERATURE (HPHT) WITH CO_2 CORE FLOOD

In the CO_2 core flood, experiments were performed at High-Pressure High Temperature (1500 psi, 60C). The dissolved CO_2 is saturated with brine (30,000ppm salinity).

Table 4.3 shows the core and fluid properties data for the HPHT phase experiment(CO_2 core flood).

Table 4.4: Core and fluid properties data for the HPHT phase experiment

Core Properties	Value
Core rock type	Benthemier Sandstone
Core length	1 ft
Core diameter	1.38 inch
Core pore volume	83 ml
Core porosity	24.53%
Core permeability	1662 md

Fluid Properties	Value
Estimated CO2 saturation at operating condition	0.7555 mol/kg
Concentration of brine (NaCl)	30000 ppm
Concentration of silicate solution	15 wt %
Viscosity of silicate solution	3 cp

4.4.1. Tracer, pore volume and permeability test results

Tracer tests were performed for both High-Pressure High Temperature (HPHT) phase experiments to measure the pore volume, porosity, and permeability of the core sample. The tracer test is done to measure the pore volume and determine the measured porosity of the core while the permeability test determines the measured permeability of the core. Results and plots from the tracer and permeability tests are shown below.

Figure 4.21. Tracer test plot for the HPHT experiment (CO2 core flood)

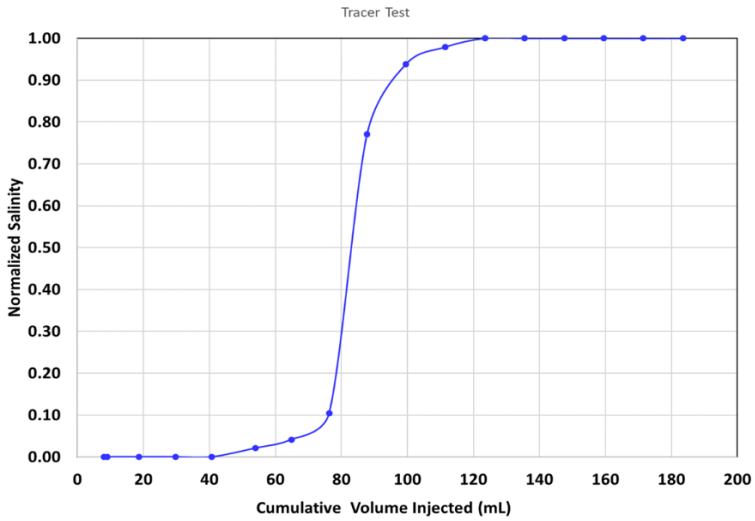

Figure 4.21. Tracer test plot for the HPHT experiment (CO_2 core flood)

Figure 4.22 shows the sectional permeability measurement plot for HPHT experiment 1. A uniform pressure breakthrough is observed through the homogenous core. This was done to show the pressure trace in the sections of the core over 5 different flow rates. Slightly different permeabilities were found in different sections of the core but all were linear as expected from Darcy's law.

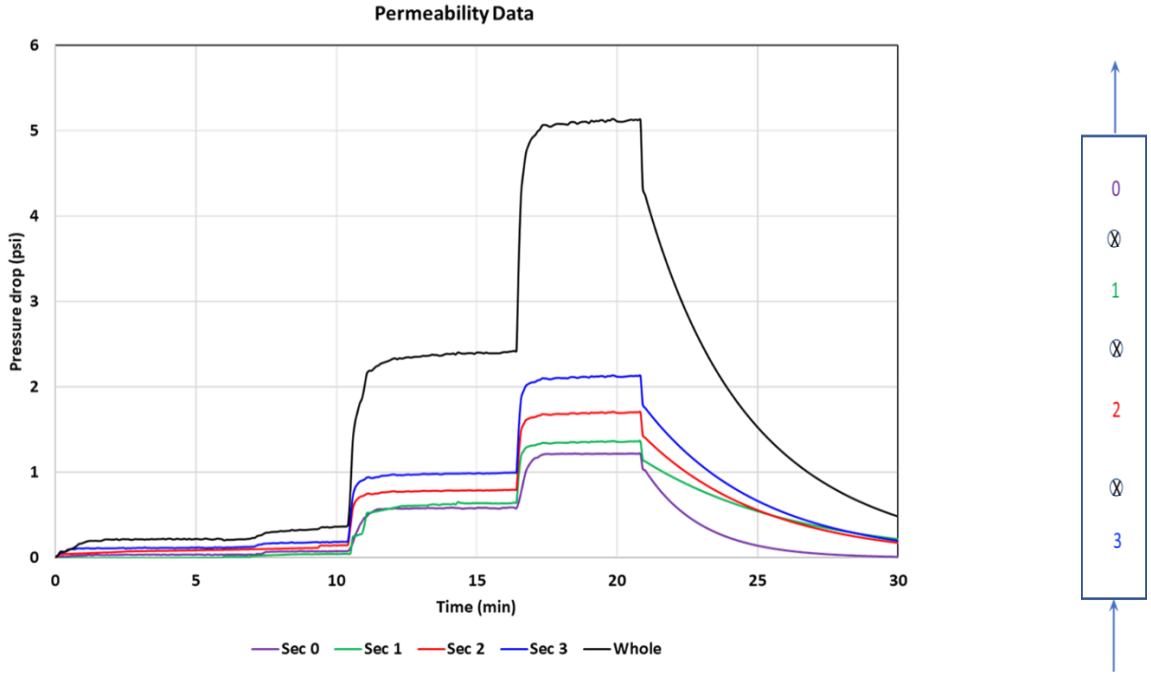

Figure 4.22. Sectional permeability measurement plot for the HPHT experiment (CO_2 core flood)

The results of the tracer test showed that the Benthemier core used in the HPHT experiment has a pore volume of 83 ml. This implies that it would require at least 83ml to pass through the core to achieve saturation. Using the pore volume gotten from the tracer test, the porosity of the Benthemier core was calculated to be 24.53%

From the permeability results, it was determined that the Benthemier core used in the HPHT experiment had a permeability of 1662 md. It should be noted that the 1662 md is the

permeability of the whole core and not the individual sections of the core where the pressure taps were placed.

Table 4.5 shows the permeability values of the individual sections of the core where the pressure taps were placed.

Table 4.5: Permeability values of the individual sections of the core

Core Sections	0	1	2	3	whole
Permeability(mD)	1770	1582	1184	1035	1662

4.4.2. CO_2 saturated brine plot

Figure 4.23 shows the pressure drop versus pore volumes injected of CO2-saturated brine. The pressure drop quickly reached steady state in all sections of the core.

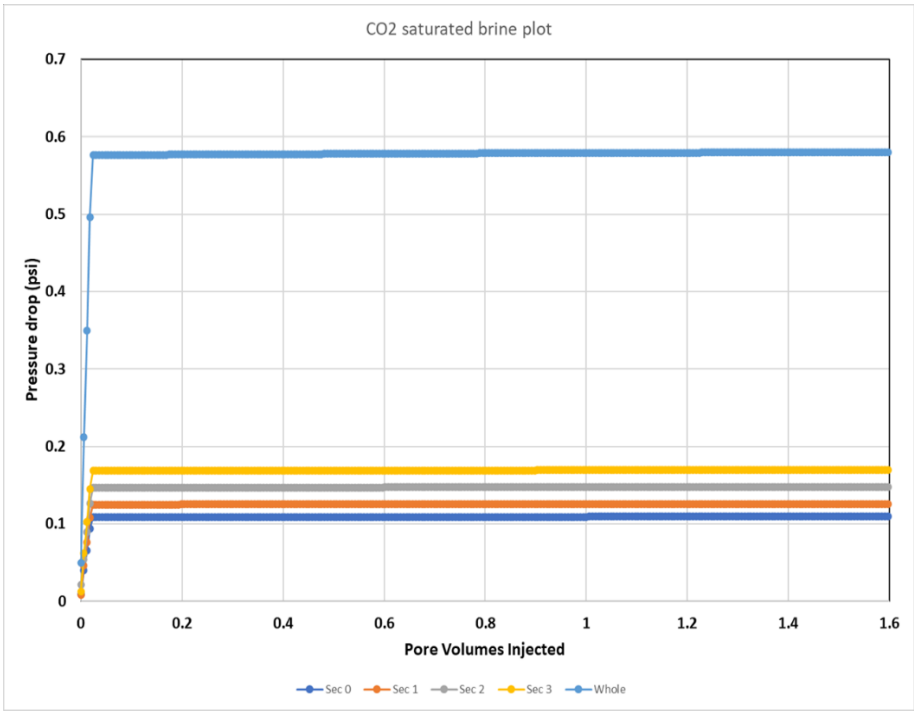

Figure 4.23: CO_2 saturated brine plot

The plot (Figure 4.24) above is another form of tracer test that was run using CO_2 saturated brine instead of only brine. This was done to eliminate error and ensure that the core achieved saturation and stability at a constant flow rate of 1 ml/min. It was also used to create a baseline for the HPHT experiment

CO_2 saturated brine was injected into the core at a constant flow rate of 1 ml/min until equilibration was achieved. A steady baseline and pressure line on the LabVIEW screen indicated that equilibration had occurred in the core. The whole core achieved equilibration at 0.58 psi. Two additional pore volumes were injected to ensure that there were no fluctuations in the baseline plots as shown in the plot above.

4.4.3. Pressure plots

For the HPHT experiment (CO_2 core flood), the Benthemier sandstone is initially saturated with 0.755 mol/kg of CO_2 saturated brine at 1 ml/min. The baseline pressure for the experiment is then achieved and the reference pressure drop for each section is then recorded. This was determined to be 0.21 psi for the whole core while the individual four sections of the core (sections 0-3) with the pressure taps had values ranging from 0.049 psi to 0.069 psi respectively

Also, from earlier bulk gelation experiments, the gelation time duration at 30,000 ppm, 60^0C and the acetic acid equivalent of 0.755 mol/kg CO_2 saturated brine was determined to be 40 mins. The silicate residence time is estimated to be at least 1.2 -1.5 times the bulk gelation time i.e. 48 -60 mins. The pressure build-up is expected to occur mostly at the bottom section.

A 15 wt.% silicate solution is then injected (t=0) into the core at a flow rate of 1 ml/min to initiate the gelation process with the CO_2 saturated brine core. The pressure drops of each section are automatically monitored and recorded by the LabVIEW software.

Figure 4.24 shows the pressure plots showing the silicate gelation at the HPHT experiment (CO_2 core flood). A rapid and continuous increase in the pressure drop was observed as more pore volumes of the silicate solution is injected.

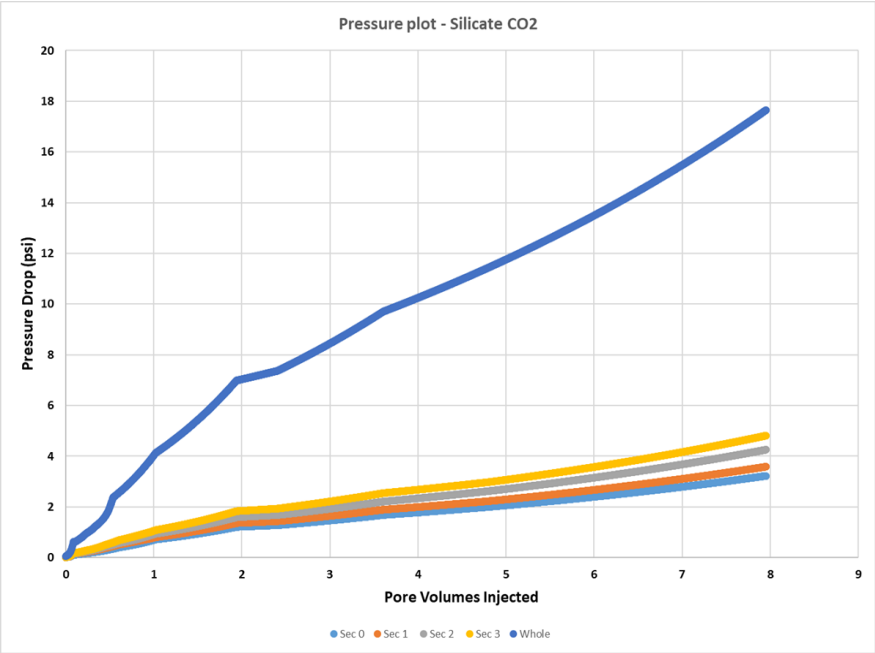

Figure 4.24: Pressure plots showing the silicate gelation at the HPHT experiment (CO_2 core flood)

After 10 hrs (8 PVs), the experiment was then shut-in for 5 days. The maximum pressure drop observed after the initial 10 hrs is 17.65 psi for the whole core. The individual four sections of the core (sections 0-3) with the pressure taps had values ranging from 3.2 psi to 4.8 psi respectively after 10 hrs.

4.4.3. Permeability reduction plots

Since the injection rate was kept constant before and after the gel treatment in this thesis, equation 2.1 above can be expressed as the flowing equation based on the relation of permeability with flow rate and pressure difference:

$$KR = \frac{\Delta P2 - \Delta P1}{\Delta P1} * 100\% \qquad (4.15)$$

where KR is also a measure of the water flow resistance with the formation of gels in the simulated leakage zone, ΔP1 is the pressure difference for CO_2 before gel treatment i.e. the CO_2 saturated brine pressure plot, and ΔP2 is the pressure difference for CO_2 after gel treatment.

Figure 4.25 shows the permeability reduction plots at the HPHT experiment (CO2 core flood) (CO2 core flood)

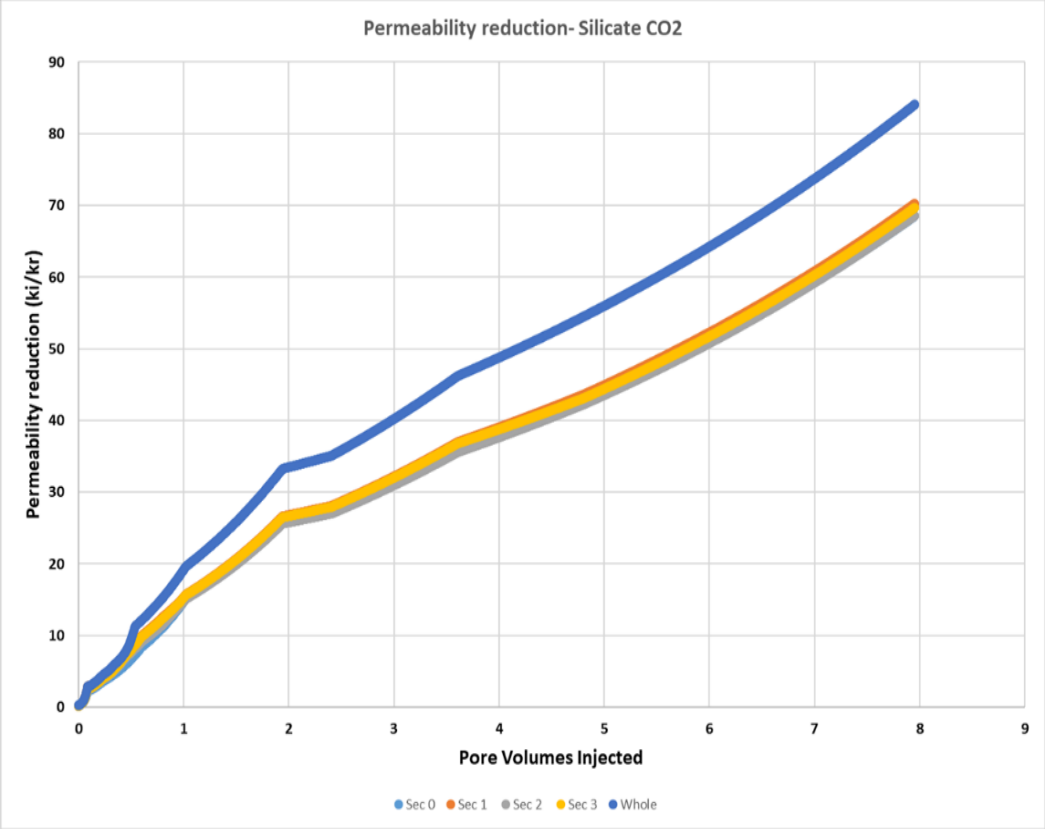

Figure 4.25: Permeability reduction plots at the HPHT experiment (CO_2 core flood)

From the results of the CO_2 HPHT core flood, it is seen that the permeability reduction capability of the gel continues to increase as more pore volumes of the silicate solution is injected. It achieved almost a 90% permeability reduction in the whole core after 10 hrs. The individual sectional pressure drops are oddly the same and add up to a value much greater than the whole pressure drop. It was also observed that each section of the core achieved a corresponding

reduction in their permeabilities as they had an approximately 70% reduction in permeability, respectively.

It was also observed that the total volume of fluid leaving the core at the end of the experiment was less than the total volume of fluid injected into the core at the state of the experiment. A possible explanation for this observation is the syneresis effect (shrinkage and water expulsion) found in silicate gel, which induces a potentially a time-dependent blocking effect. Therefore, some of the injected fluid could be lost to shrinkage and water expulsion.

Chapter 5: CONCLUSIONS AND FUTURE WORK

5.1 CONCLUSIONS

The experimental work was conducted in two major phases: bulk gelation and core floods. The mother solution used in these experiments is Betol K28T diluted with deionized water (50 wt.%) which acts as the silicate gel being investigated. Bulk gelation experiments were initially performed to measure the gel time at different silicate content, acid concentrations, salinities, and temperatures. The results were then fit to an existing model for gelation time and then used as a predictive tool for the core flood experiments. Core flood experiments (using acetic acid at ambient conditions and CO_2-saturated brine at HPHT conditions) were then performed to investigate the reactive transport of silicate gel in porous media, compare the results obtained from gelation in porous media to the gelation results from the earlier bulk experiments and finally, investigate the capability of the gel in permeability reduction and sealing of the core.

The main conclusions from the experiments are summarized below:

- In the bulk gelation phase, acetic (HAc) and hydrochloric (HCl) acid were used as two different gelation initiators with the silicate gel to observe the gelation process and determine their respective gel time. The purpose was to determine and quantify how the gelation process is affected by weak and strong acid solutions. When the gelation was initiated by acetic acid, the results show that increasing acid content consistently accelerates the gelation kinetics (shorter gelation time) regardless of silicate content, while adding more silicate to the gelation system initially retards, then accelerates the gelation. Higher salinity in the system and higher temperature both lead to faster gelation time. The effect of acid content and salinity on gelation kinetics is much more complicated when a strong acid was used as the initiator. In particular, more acid accelerates gelation at high silicate content. However, at low silicate content, increasing acid in the solution first accelerates then deaccelerates gelation. The effect of increasing salinity decreases gelation time at high salt concentration but slows down the kinetics at low salt concentration. These

observations suggest different kinetic process between weak acid initiated and strong acid-initiated gelation. Overall, the effects of silicate content, acid content, salinity, and temperature on the gelation kinetics in weak acid are as expected. A literature model for gelation time prediction was adopted and the parameters were tuned to match the experimental results. The results were then fit to an existing model for gelation time and then used as a predictive tool for the core flood experiments.

- The core flood experiments were conducted in two conditions: ambient condition with an acetic acid solution as a CO_2 substitute and the High-Pressure High-Temperature (1500 psi, 600C, 30,000 ppm NaCl) condition with CO_2 saturated brine. Two sets of experiments were conducted at ambient conditions. The first experiment was performed using 1000 ppm NaCl brine to investigate the gel's capability at sealing and permeability reduction whereas the second experiment was conducted at 2500 ppm NaCl. The plots show that salinity has a major impact on the gelation times as the gelation time became shorter with increasing salinity. Up to 80 times reduction in the permeability of the core was found. Permeability reduction, however, occurred mainly in the first part of the core. The downstream sections of the core showed permeability reduction after multiple pore volume injections of silicate solution.
- In the CO_2 core flood, experiments were conducted at High-Pressure High Temperature (1500 psi, 60C). The dissolved CO_2 was saturated with brine (30,000 ppm salinity). The first experiment is the initial pilot experiment performed to investigate the gel's capability at sealing and permeability reduction; subsequent experiments are proposed to confirm the results of the first experiment and investigate the effect of variables such as salinity, concentration, and injection rate.
- From both ambient and HPHT (CO_2) core floods, It was observed that the total volume of fluid leaving the core at the end of the experiment was less than the total volume of fluid injected into the core at the state of the experiment. A possible explanation for this observation is the syneresis effect (shrinkage and water expulsion) found in silicate gel,

which induces a potentially a time-dependent blocking effect. Therefore, some of the injected fluid could be lost to shrinkage and water expulsion.

- From the core flood experiments, it was shown that using potassium silicate reagents (Betol K28T) to form a silica gel barrier could be a feasible strategy for mitigating the risk of CO_2 leakage. Reduction in the core permeability (up to 90%) of the Benthemier sandstone core was observed during barrier formation. However, to further validate the use of the silica gel to form a chemical barrier under CO2 storage conditions, additional field-scale modeling and experiments using micromodel chips are recommended.

5.2 FUTURE WORK

Further future work can be done to validate the use of the silica gel to form a chemical barrier under CO2 storage conditions. While it has been observed in the Benthemier sandstone core for this thesis, the process has not been fully optimized as it involved injecting many pore volumes of silicate solutions in the core flood. Therefore, additional core flood experiments will be useful to understand and optimize the use of silicate gel in the future.

Some proposed future core flood experiments include;

- Additional experiments to investigate the sealing capability and performance as well as the effects of salinity and silicate concentrations in other rock types such as other sandstone and carbonate cores are recommended. It is known that the Benthemier core is homogenous, thus having a uniform porosity and permeability, therefore, observing the performance of the silicate gel in heterogeneous cores is important.
- Experiments using a CT scanner in situ can help clarify the gelation mechanisms during a core flood. The fluid gelation mechanisms and a visualization of the changes in silicate gel formation during the core flood can be observed via CT imaging.
- Experiments using a chip micromodel are recommended. Micromodels are microfluidic devices that mimic the geometry of porous media; they are typically small (mm to cm), two-dimensional, and often homogeneous but allow for visualization. Our core flood

experiments have demonstrated the success of using silica gels as a conformance control agent and the reduction of permeability. This, however, cannot be confirmed from the data, observation of the core, or CT scans (density of gel is not significantly different than silica solution that has not gelled). Furthermore, it is unknown if the gel forms uniformly or if only some pores are blocked. Direct visualization of the gelation would indicate the location of gel, flow paths of CO2, and allow for optimization of the gelation process. Micromodel experiments help visualize more pore-scale behaviors that might not be seen when doing core floods. Therefore, the micromodels might be able to give a closer look at how the silicate gel behaves in smaller pore spaces.

Appendix A

Summary of the properties of rock and fluids for core flood experiment

Coreflood Experiment	Condition	Porosity	Permeability (mD)	Acid	Acid conc (wt%)	Salinity(ppm)	Silicate conc (wt%)	Viscosity of silicate	Pressure(psi)	Temperature ©
1	Ambient	23.68	1469	Acetic	1	1000	8.64	3	room	room
2	Ambient	23.92	2566	Acetic	1	2500	8.64	3	room	room
3	HPHT	24.53	1662	CO2	saturated	30000	15	3	1500	60

Appendix B

Summary of bulk gelation experiment plots to determine the effect of acetic acid, salinity and silicate concentration on gel time

Exp	Acid	Acid Conc. (wt%)	Salinity (wt%)	Silicate Conc. (wt%)	T (K)	Gel time (meas) (min)	Gel time predict (min)
1	Acetic	0.60%	0.10%	6.12%	313	3421	4551.55
2	Acetic	0.60%	0.10%	8.11%	313	2610	4980.92
3	Acetic	0.60%	0.10%	10.11%	313	6789	5453.27
4	Acetic	0.70%	0.10%	6.12%	313	1898	1844.57
5	Acetic	0.70%	0.10%	8.11%	313	1673	2018.58
6	Acetic	0.70%	0.10%	10.11%	313	2462	2210.01
7	Acetic	0.80%	0.10%	6.12%	313	782	747.54
8	Acetic	0.80%	0.10%	8.11%	313	620	818.06
9	Acetic	0.80%	0.10%	10.11%	313	846	895.63
10	Acetic	0.90%	0.10%	6.12%	313	311	302.95
11	Acetic	0.90%	0.10%	8.11%	313	288	331.53
12	Acetic	0.90%	0.10%	10.11%	313	352	362.97

$$\ln(t_{gel}) = M + a[\mathrm{Si}] + b[\mathrm{HAc}] + c[\mathrm{NaCl}] + E_a/RT$$

M	-2.48
a	4.53
b	-903.22
c	-324.94
Ea	42600
R	8.314

Appendix C

A plot of measured gel time vs predicted gel time using data presented in Appendix B for acetic acid

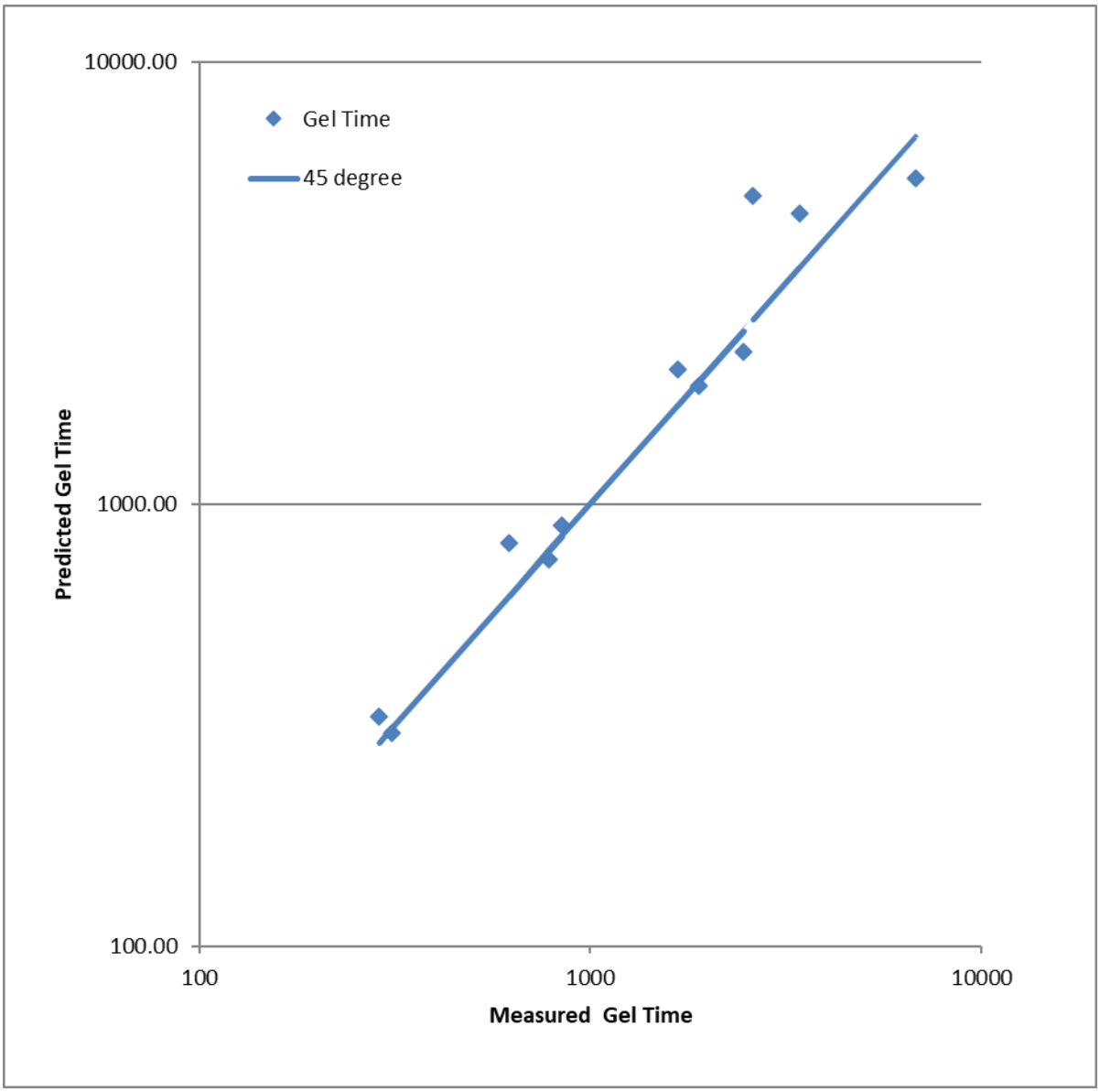

Appendix D

Silicate gelation process during the bulk experiment

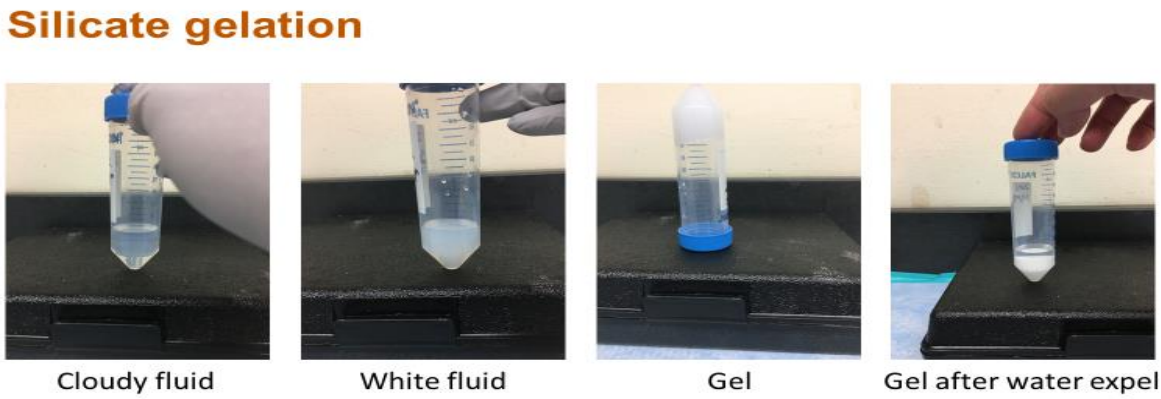

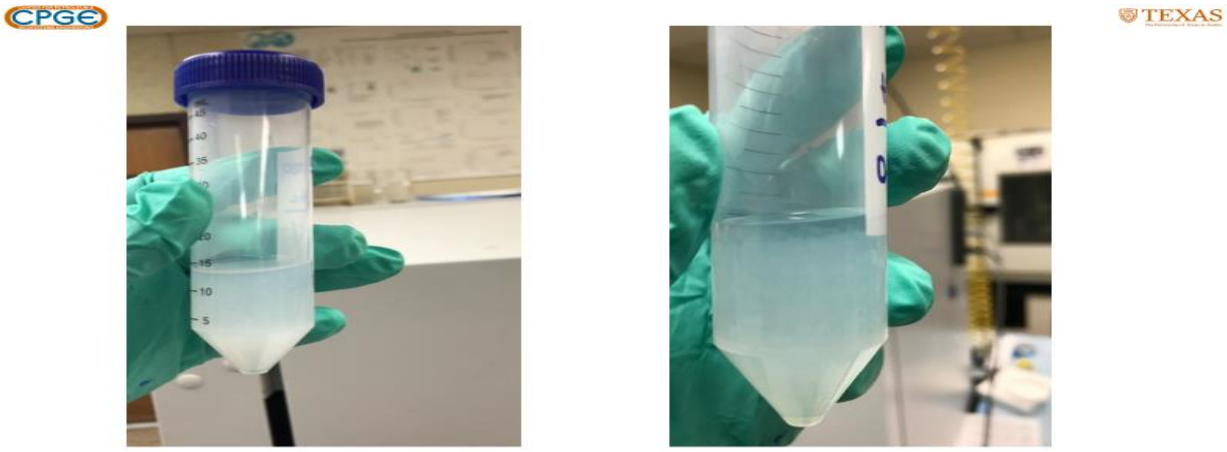

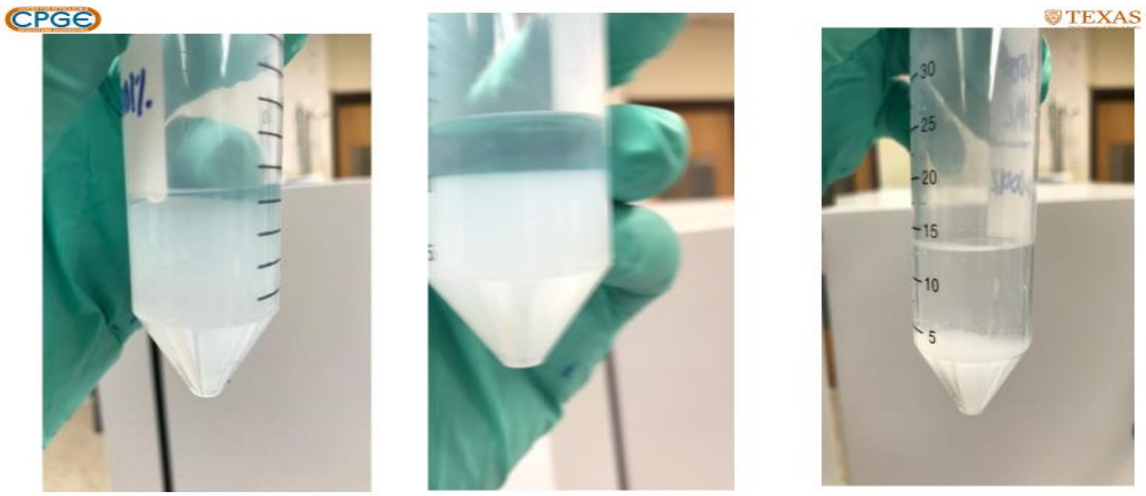

References

1. Andrew C. Mitchell, Adrienne J. Phillips, Randy Hiebert, Robin Gerlach, Lee H. Spangler, Alfred B. Cunningham, Biofilm enhanced geologic sequestration of supercritical CO2, International Journal of Greenhouse Gas Control, Volume 3, Issue 1,2009, Pages 90-99, ISSN 1750-5836, https://doi.org/10.1016/j.ijggc.2008.05.002.
2. Ajayi, T., Gomes, J.S. & Bera, A. A review of CO2 storage in geological formations emphasizing modeling, monitoring and capacity estimation approaches. Pet. Sci. 16, 1028–1063 (2019). https://doi.org/10.1007/s12182-019-0340-8
3. Amiri, H.A., Hamouda, A., Roostaei, A., 2014. Sodium Silicate Behavior in Porous Media Applied for In-Depth Profile Modifications. Energies 2014, Vol. 7, Pages 2004-2026 7, 2004–2026. doi:10.3390/en7042004
4. Axford, S.D.T., 1997. Aggregation of colloidal silica: Reaction-limited kernel, stability ratio and distribution moments. J. Chem. Soc., Faraday Trans. 93, 303–311. doi:10.1039/A606195H
5. Batôt, G.; Fleury, M.; Nabzar, L. Reducing CO2 Flow using Foams. Energy Procedia 2017, 114, 4129−4139.
6. Benson SM, Cole DR (2008) CO2 sequestration in deep sedimentary formations. Elements 4(5):305-310
7. Benson SM, Cook P (2005) Underground Geological Storage. In: Carbon Dioxide Capture and Storage: Special Report of the Intergovernmental Panel on Climate Change (IPCC). Cambridge University Press, Interlachen, Switzerland, p 5-1 to 5-134
8. Bergna, H. E., Roberts, W. O., Colloidal Silica: Fundamentals and Applications, Taylor & Francis, 2006

9. Blue, Aaron Jeffrey, "Experimental evaluations of selected sealants to remediate CO_2 leakage" (2016). Masters Theses. 7497. https://scholarsmine.mst.edu/masters_theses/7497
10. C.A. Castañeda-Herrera, J.R. Black, E.M. Llanos, G.W. Stevens, R.R. Haese, Formation of an amorphous silica gel barrier under CO2 storage conditions, International Journal of Greenhouse Gas Control, Volume 78, 2018, Pages 27-36, ISSN 1750-5836, https://doi.org/10.1016/j.ijggc.2018.07.013.
11. CMG. STARS User Guide; Computer Modelling Group Ltd.: Calgary, 2015.
12. Donald J. DePaolo, Alexandra Navrotsky, David R. Cole, Ian C. Bourg; PREFACE. Reviews in Mineralogy and Geochemistry; 77 (1): iii-iv.
13. El-Maghraby, R.M., Pentland, C.H., Iglauer, S., Blunt, M.J., A fast method to equilibrate carbon dioxide with brine at high pressure and elevated temperature including solubility measurements, The Journal of Supercritical Fluids (2010), doi:10.1016/j.supflu.2011.11.002
14. Fortenberry, R., Kim, D. H., Nizamidin, N., Adkins, S., Arachchilage, G. W. P. P., Koh, H. S., Weerasooriya, U., Pope, G. A. (2015). Use of Cosolvents to Improve Alkaline/Polymer Flooding. SPE Journal, 20(02), 255–266. https://doi.org/10.2118/166478-PA
15. Hadi Mosleh, M., Govindan, R., Shi, J.-Q., Durucan, S., Korre, A., 2016. Application of Polymer-Gel Solutions in Remediating Leakage in CO₂ Storage Reservoirs, SPE Europe featured at 78th EAGE Conference and Exhibition. Society of Petroleum Engineers. doi:10.2118/180135-MS

16. Hatzignatiou, D.G., Helleren, J., Stavland, A., 2014. Numerical Evaluation of Dynamic Core-Scale Experiments of Silicate Gels for Fluid Diversion and Flow-Zone Isolation. SPE Production & Operations 29, 122–138. doi:10.2118/170240-PA
17. Hild, G.P., Wackowski, R.K., 1999. Reservoir Polymer Gel Treatments To Improve Miscible CO2 Flood. SPEREE 2, 196–204. doi:10.2118/56008-PA
18. Hiorth, A., Sagen, J., Lohne, A., Nossen, J., Vinningland, J.L., Jettestuen, E., Sira, T., 2016. IORSim - A Simulator for Fast and Accurate Simulation of Multi-phase Geochemical Interactions at the Field Scale. Amsterdam2016. doi:10.3997/2214-4609.201601882
19. Ho, J. F.; Tavassoli, S.; Patterson, J. W.; Shafiei, M.; Huh, C.; Bommer, P. M.; Bryant, S. L.; Balhoff, M. T. The Use of a pH Triggered Polymer Gelant to Seal Cement Fractures in Wells. SPE Drill. Completion 2016, 31 (3), 225−235.
20. Huang, J., Al-Mohsin, A., Bataweel, M., Karadkar, P., Li, W., Shaikh, A., 2017. Systematic Approach to Develop a Colloidal Silica Based Gel System for Water Shut-Off, SPE Middle East Oil & Gas Show and Conference. Society of Petroleum Engineers. doi:10.2118/183942-MS
21. Iler, R.K., 1979. Chemistry of Silica--Solubility, Polymerization, Colloid and Surface Properties, and Biochemistry.
22. IPCC, 2005: IPCC Special Report on Carbon Dioxide Capture and Storage. Prepared by Working Group III of the Intergovernmental Panel on Climate Change [Metz, B., O. Davidson, H. C. de Coninck, M. Loos, and L. A. Meyer (eds.)]. Cambridge University Press, Cambridge, United Kingdom and New York, NY, USA, 442 pp.
23. IPCC (Intergovernmental Panel on Climate Change), (2014). Summary for policymakers. In: Edenhofer, O., Pichs-Madruga, R., Sokona, Y., Farahani, E., Kadner, S., Seyboth, K.,

Adler, A., Baum, I., Brunner, S., Eickemeier, P., Kriemann, B., Savolainen, J., Sclömer, S., von Stechow, C., Zwickel, T., Minx, J.C. (Eds.), Contribution of Working Group III to the Fifth Assessment Report of the Intergovernmental Panel on Climate Change. Cambridge University Press, Cambridge, UK, New York, NY, USA

24. IPCC A. Intergovernmental panel on climate change. IPCC Secretariat Geneva; 2007
25. Ito, T.; Xu, T.; Tanaka, H.; Taniuchi, Y.; Okamoto, A. Possibility to Remedy CO2 Leakage from Geological Reservoir using CO2 Reactive Grout. Int. J. Greenhouse Gas Control 2014, 20, 310− 323.
26. Jordan, D.S., Green, D.W., Terry, R.E., Willhite, G.P., 1982. The Effect of Temperature on Gelation Time for Polyacrylamide/Chromium (III) Systems. Society of Petroleum Engineers Journal 22, 463–471. doi:10.2118/10059-PA
27. Jurinak, J.J., Summers, L.E., 1991a. Oilfield Applications of Colloidal Silica Gel. SPE Production Engineering 6, 406–412. doi:10.2118/18505-PA
28. Jurinak, J.J., Summers, L.E., 1991b. SPE 18505 Supplement: Laboratory Testing of Colloidal Silica Gel for Oilfield Applications.
29. Kaldi JG, Gibson-Poole CM, Payenberg TH. Geological input to selection and evaluation of CO2 geosequestration sites; 2009
30. Kim, M., Corapcioglu, M.Y., Park, J.-W., 2007. Numerical investigation of the gel barrier formation with vertical injection pipe. Environ Geol 53, 635–642. doi:10.1007/s00254-007-0678-x
31. Lakatos, I., Lakatos-Szabo, J., 2012. Reservoir Conformance Control in Oilfields Using of Silicates: State-of-the-Arts and Perspectives, SPE Annual Technical Conference and Exhibition. Society of Petroleum Engineers. doi:10.2118/159640-MS

32. Lee, V. B. (2015). The Development and Evaluation of Polymers for Enhanced Oil Recovery. MS Thesis. The University of Texas at Austin.
33. Leung, D. Y., Caramanna, G., & Maroto-Valer, M. M. (2014). An overview of the current status of carbon dioxide capture and storage technologies. Renewable and Sustainable Energy Reviews, 39, 426-443
34. Li, D. X.; Zhang, L.; Liu, Y. M.; Kang, W. L.; Ren, S. R. CO2- Triggered Gelation for Mobility Control and Channeling Blocking during CO2 Flooding Processes. Pet. Sci. 2016, 13 (2), 247−258
35. M. Fleury, O. Sissmann, E. Brosse, M. Chardin. A Silicate Based Process for Plugging the Near Well Bore Formation. Energy Procedia, Elsevier, 2017, 114, pp.4172 - 4187. 10.1016/j.egypro.2017.03.1558. hal-01740288
36. Manceau, J.C., Hatzignatiou, D.G., de Lary, L., Jensen, N.B., Réveillère, A., 2014. Mitigation and remediation technologies and practices in case of undesired migration of CO2 from a geological storage unit—Current status. International Journal of Greenhouse Gas Control 22, 272–290. doi:10.1016/j.ijggc.2014.01.007
37. McIntosh, G.J., 2012. A theoretical kinetic model of the temperature and pH-dependent dimerization of orthosilicic acid in aqueous solution. Physical Chemistry Chemical Physics 14, 996–1013. doi:10.1039/C1CP22273B
38. Metz, B, Davidson, O, de Coninck, H, Loos, M, Meyer, L. Carbon dioxide capture and storage, intergovernmental panel on climate change, Geneva (Switzerland). Working group III; 2005

39. Mitchell, A. C.; Phillips, A. J.; Hiebert, R.; Gerlach, R.; Spangler, L. H.; Cunningham, A. B. Biofilm Enhanced Geologic Sequestration of Supercritical CO2. Int. J. Greenhouse Gas Control 2009, 3 (1), 90−99.
40. Nasr-El-Din, H.A., Taylor, K.C., 2005. Evaluation of sodium silicate/urea gels used for water shut-off treatments 48, 141–160. doi:10.1016/j.petrol.2005.06.010
41. Oglesby, K.D., D'Souza, D., Roller, C., Logsdon, R., Burns, L.D., Felber, B.J., 2016. Field Test Results of a New Silicate Gel System that is Effective in Carbon Dioxide Enhanced Recovery and Waterfloods, SPE Improved Oil Recovery Conference. Society of Petroleum Engineers. doi:10.2118/179615-MS
42. Omekeh, A., Hiorth, A., Stavland, A., Lohne, A., 2017. Silicate Gel for In-depth Placement Gelation Kinetics and Pre-flush Design. Stavanger2017. doi:10.3997/2214-4609.201700282
43. Peng, Shudai, "Overview of CO_2 leakage problems and sealants for CO_2 leakage remediation"(2017).Masters Theses. 7723.
44. Phillips, A. J.; Lauchnor, E.; Eldring, J.; Esposito, R.; Mitchell, A. C.; Gerlach, R.; Cunningham, A. B.; Spangler, L. H. Potential CO2 Leakage Reduction through Biofilm-Induced Calcium Carbonate Precipitation. Environ. Sci. Technol. 2013, 47 (1), 142−149.
45. Pizzocolo, F., Hewson, C.W., Heege, ter, J.H., 2016. Polymer-Gel Remediation of CO₂ Migration through Faults and Caprock: Numerical Simulations Addressing Feasibility of Novel Approaches.
46. Remy, N., 2011. Applied Geostatistics with SGeMS: A User's Guide. Cambridge University Press

47. Reveille´ re, A.; Rohmer, J.; Manceau, J. C. Hydraulic barrier` design and applicability for managing the risk of CO2 leakage from deep saline aquifers. Int. J. Greenhouse Gas Control 2012, 9, 62−71.
48. Ricks, G.V.J., Portwood, J.T., 2000. Injection-side Application of MARCIT Polymer Gel Improves Waterflood Sweep Efficiency, Decreases Water-Oil Ratio, and Enhances Oil Recovery in the McElroy Field, Upton County, Texas, SPE Permian Basin Oil and Gas Recovery Conference. Society of Petroleum Engineers. doi:10.2118/59528-MS
49. RISCS,2014. A Guide to potential impacts of leakage from CO2 storage. Pearce, J, Blackford, J, Beaubien, S, Foekema, E, Gemeni, V, Gwosdz, S, Jones, D, Kirk, K, Lions, J, Metcalfe, R, Moni, C, Smith, K, Steven, M, West, J and Ziogou, F. British Geological Survey. Available from www.riscs-co2.eu 70 pages.
50. Schmitz, D.; Pich, A. Responsive microgels with supramolecular crosslinks: synthesis and triggered degradation in an aqueous medium. Polym. Chem. 2016, 7, 5687−5697.
51. Scott, T., Roberts, L.J., Sharp, S.R., Clifford, P.J., Sorbie, K.S., 1987. In-Situ Gel Calculations in Complex Reservoir Systems Using a New Chemical Flood Simulator. SPE Reservoir Engineering 2, 634–646. doi:10.2118/14234-PA
52. Skrettingland, K., Giske, N.H., Johnsen, J.-H., Stavland, A., 2012. Snorre In-depth Water Diversion Using Sodium Silicate - Single Well Injection Pilot, SPE Improved Oil Recovery Symposium. Society of Petroleum Engineers. doi:10.2118/154004-MS
53. Stangeland, A., & Laird, B., (2006). Energy Infrastructure with CO2 Capture and Storage (CCS).

54. Stavland, A., Jonsbråten, H., Vikane, O., Skrettingland, K., Fischer, H., 2011. In-depth Water Diversion Using Sodium Silicate – Preparation for Single Well Field Pilot on Snorre. Cambridge2011. doi:10.3997/2214-4609.201404788
55. Sydansk, R.D., 1988. A New Conformance-Improvement-Treatment Chromium(III) Gel Technology, SPE Enhanced Oil Recovery Symposium. Society of Petroleum Engineers. doi:10.2118/17329-MS
56. Thomson AM, Izaurralde RC, Smith SJ, Clarke LE. Integrated estimates of global terrestrial carbon sequestration.Glob Environ Change Hum Policy Dimens. 2008;18(1):192–203.
57. Tognonvi, M.T. (2009) Physico-chimie de la gélification du silicate de sodium en milieu basique. Ph.D Univ. Limoges, 166 p
58. Tongwa, P., Nygaard, R., Blue, A., Bai, B., 2013. Evaluation of potential fracture-sealing materials for remediating CO2 leakage pathways during CO2 sequestration. International Journal of Greenhouse Gas Control 18, 128–138. doi:10.1016/j.ijggc.2013.06.017
59. U.S Environmental Protection Agency, (2020)
60. UNFCCC. (2015a). Decision 1/CP.21, in a report of the conference of the parties on its twenty-first session, held in Paris from 30 November to 13 December 2015. Addendum Part two: Action taken by the Conference of the Parties at its twenty-first session (FCCC/CP/2015/10/Add.1)
61. Vargas-Vasquez, S.M., Romero-Zerón, L.B., 2008. A Review of the Partly Hydrolyzed Polyacrylamide Cr(III) Acetate Polymer Gels. Petroleum Science and Technology 26, 481–498. doi:10.1080/10916460701204594

62. Wright, I.W., Lee, A., Middleton, P., Lowe, C., Imbus, S.W. and Miracca, I., (2004), January. CO2 Capture Project: Initial Results. In SPE International Conference on Health, Safety, and Environment in Oil and Gas Exploration and Production. Society of Petroleum Engineers

Vita

Kenechukwu Moneke received his Bachelor of Science in Petroleum Engineering from the University of Lagos, Nigeria in November 2016. In August of 2018, Kene enrolled in the Petroleum Engineering Master degree at the University of Texas at Austin. He also served as a graduate research assistant under Professor Matthew Balhoff. Kene received his Master of Science in Petroleum Engineering from the University of Texas at Austin in August of 2020.

Permanent email: kene_moneke@utexas.edu

This dissertation was typed by Kenechukwu Moneke